University of Turin

Doctoral Thesis

Mechanisms for the persistence of rabies in multiple host species: the role of host spatial distribution, mobility and host-pathogen interaction

Author:
Davide Colombi

Supervisors:
Prof. Michele Caselle
Dr. Vittoria Colizza

A thesis submitted in fulfillment of the requirements for the degree of Doctor of Philosophy

in the

PhD Programme in Complex Systems for Life Sciences
Doctoral School in Life and Health Sciences

Declaration of Authorship

I, Davide Colombi, declare that this thesis titled, "Mechanisms for the persistence of rabies in multiple host species: the role of host spatial distribution, mobility and host-pathogen interaction" and the work presented in it are my own. I confirm that:

- This work was done wholly or mainly while in candidature for a research degree at this University.
- Where any part of this thesis has previously been submitted for a degree or any other qualification at this University or any other institution, this has been clearly stated.
- Where I have consulted the published work of others, this is always clearly attributed.
- Where I have quoted from the work of others, the source is always given. With the exception of such quotations, this thesis is entirely my own work.
- I have acknowledged all main sources of help.
- Where the thesis is based on work done by myself jointly with others, I have made clear exactly what was done by others and what I have contributed myself.

Signed:

Date:

University of Turin

Abstract

Faculty Name
Doctoral School in Life and Health Sciences

Doctor of Philosophy

Mechanisms for the persistence of rabies in multiple host species: the role of host spatial distribution, mobility and host-pathogen interaction

by Davide Colombi

The PhD thesis is focused on the analysis of the mechanisms for the rabies persistence in different hosts and in different ecological contexts. The first study concern the endemicity of European Bat Lyssavirus subtype 1 (EBLV-1) in two non-synanthropic bats, *Myotis myotis* and *Miniopterus schreibersii*, in the Catalonia region. Lyssaviruses, the agents of rabies, were probably originated in bats and progressively diverged from a common ancestor to infect other species. Knowledge about persistence remains incomplete, mainly due to the complex interplay of bats ecology and immune response to infection. Through an extensive ecological field survey on those two bat species, I developed a data-driven mathematical model to identify the mechanisms of persistence of EBLV-1 in that region. Different disease progressions were considered, accounting for lethal infection, immunity waning, along with potential cross-species transmission when the two populations share the same refuge. Comparison with serology suggests that EBLV-1 circulation is ensured by the spatial migration of *M. schreibersii* and the mixing with *M. myotis*, offering novel numerical evidence to support non-lethal infection in bats with a transient immunity of few months. Shelters hosting multi-species colonies are critical for virus exchange so they should be monitored for public health. Subsequently I analyzed the persistence of rabies virus (RABV) in domestic dogs, the most important rabies reservoirs for human exposure, in Central African Republic. The drivers of rabies in dogs are still largely unknown and this impairs the probability of success of vaccination campaigns. Dogs exhibit an unusually heterogeneous incubation period that is related to process of dissemination of the virus inside the body, in addition environmental heterogeneities and hosts distribution may have an impact on the persistence. To study the role and interplay of these factors I introduced a novel stochastic compartmental model with realistic data-driven distributions for incubation and infectious periods and I explored through numerical simulations the conditions that can lead the persistence in a network of geographical fragmented populations, taking the Central African Republic as a model. The inclusion of empirical distributions in the infection stages alters the epidemic scenario favoring the circulation even for low transmissibilities as observed empirically. In addition, our findings predict that spatially fragmented population and human mediated mobility represent key elements in the persistence. The model developed may help in the design of efficient control strategies not only in the Central African Republic, the country analyzed, but also in other countries where the disease is endemic.

Acknowledgements

Firstly, I would express my sincere and deepest gratitude to my supervisor, Dr. Vittoria Colizza, for the continuous support during my Ph.D, for her patience and motivation. Her guidance helped and stimulated me in all the time and I could not have imagined having a better advisor and mentor for my Ph.D study. Thank you, Vittoria, for teaching me how to do Science and for sharing your optimistic scientific attitude. I would like also to acknowledge Prof. Michele Caselle for his comments and encouragement, and for his supervision during this Ph.D.

I would like to thank Hervé Bourhy who hosted me in at the Institut Pasteur in Paris (France) for one month and for his supervision during that period. He encouraged me and he gave to me precious and illuminating suggestions sharing his multi-disciplinary knowledge.

I would also like to thank my collaborators: Chiara Poletto, Raphaelle Metras and Andrea Apolloni (Abu) for their invaluable assistance and for all the stimulating discussions. Doing research together has been simply great and your support was fundamental.

Then I would express my gratitude to the ISI Foundation, an amazing and unique place for doing Science. All the people that have been part of this "family" during my Ph.D firstly welcomed me warmly and then helped and supported me in the scientific research as in the all day life. ISI Foundation is a wonderful environment and a stimulating workplace composed by fantastic people which are also top scientists in their field. In particular, I warmly thank Giovanni, Michele, Daniela, Ciro, Fran, Ubi, Pietro, Lorenzo, Corrado, Kyriaki, Francesco and Laetitia for being much more than exceptional colleagues and/or guides. You have all been a tremendous inspiration, and I will always be grateful for all the fun (and Science) we have had together. The EC-Health contract no. 278433 (PREDEMICS) funded this work is gratefully acknowledged since it gave me many fantastic opportunities, enabling me to carry out my research. Lastly, I would like to acknowledge the valuable comments and suggestions of the reviewers, which have improved the quality of this thesis.

From a personal point of view, a big group of people made by friends have been for me a source of motivation and inspiration. I would like to thank all the friends of my Turin "family" in particular Lorenzo and Nicola for making the experience in this city something magic and unique. It would not have been the same without you guys. I want to thank all the old friends in Rome with whom I share a deep friendship and who remained so along these years. A big and loving thanks goes to my friends in Paris in particular to Laura who hosted me through these years and who welcomed me every time making me feel at home.

Finally, I want to thank my family. My parents for their continuous support during these years. Thanks also to Arianna for her presence, patience and love that she showed in all the beautiful and difficult moments that I had during this experience.

Contents

List of Figures

List of Tables

To my parents, for their unconditional support and for how they taught me to look at things from an unconventional perspective.

1 INTRODUCTION

Infectious diseases are those diseases caused by pathogenic microorganisms, such as bacteria, viruses, parasites or fungi, which can be spread from one host to another. Managing infectious diseases is one of the greatest challenge for mankind. During my doctoral research I focused on a particular disease, rabies. Rabies is a zoonosis, i.e. an infectious disease of animals that can be transmitted to humans, which causes a progressive encephalitis that is almost always fatal following the onset of clinical symptoms. The high mutation rate and the extreme adaptability of this pathogen allowed its colonization on all continents except to Antarctica. The susceptible hosts include all mammals and the primary reservoir resides in the Orders of Carnivora and Chiroptera. Globally, domestic dogs remain the most significant vector for human exposure in particular in the developing countries of Asia and Africa [1]. Differently in North America, Western Europe and Australia, where the disease in terrestrial mammals has been controlled, bats are the most prominent source of human rabies. Even if multiple attempts were made to eradicate rabies in these two species the mechanisms that lead to endemicity are unfortunately not completely clear due to the complex interplay among multiple biological, virological and ecological factors.

The main aim of this work is to unveil part of those mechanisms using a mathematical and computational approach. The application of mathematical methods has been crucial for infectious disease epidemiology since the first model on smallpox made by Daniel Bernoulli in 1760 [2]. Mathematics applied to infectious diseases is a fundamental tool that permits to compare and test theories, as well as to gauge uncertainties given that experimenting epidemics in the "real world" is not a viable option. From the end of the 20th century mathematical epidemiology has had an important boost since the availability of new computational resources created the perfect environment to perform numerical experiments. The possibility to implement huge calculations represents a substantial opportunity to analyze natural processes integrating realistic features and multiple interacting objects in a complex framework.

My doctoral thesis is deeply rooted in this multidisciplinary approach. I worked on two epidemiological problems, both concerning rabies and its persistence mechanisms but in two different host species such as bats and dogs. In this work, I show how analytical methods combined with proper biological, virological and ecological inputs may help to unravel mechanisms of disease spreading and maintenance. In chapters 2 and 3, I provide the ingredients used to develop my work and my methods. Chapter 2 deals with the epidemiology and pathogenicity of rabies disease and in general of lyssavirus infection. After introducing the disease starting from a brief historical presentation, I give an essential description of the structure of the pathogen and how transmission and pathogenesis take place. Even if those mechanisms are similar in the different hosts, certain peculiarities of

the host-pathogen interaction give rise to slightly different infection dynamics. However, the common features that characterize spread and endemicity are related to hosts' ecology in particular hosts' spatial distribution and mobility.
In chapter 3 I review the basic notions of mathematical epidemiology. Firstly, I describe the mathematical approach applied to epidemiology, then I illustrate how this approach can be modified in order to model rabies infection dynamics in bats and dogs. Special attention is devoted to spatial transmission models, in particular to the metapopulation approach, since in rabies the transmission is driven by host movements and by the spatial heterogeneities of the landscape where hosts live.
My novel contribution to the field can be found in chapters 4 and 5. In chapter 4 I apply my method integrating population, mobility and surveillance data to identify the mechanisms of persistence of European Bat Lyssavirus subtype 1 (EBLV-1) in two different and interacting bat species in a system of caves in the Catalonia region. Subsequently, in chapter 5, I analyze the interplay between multiple virological and ecological factors that can lead to rabies persistence in domestic dogs in Central African Republic using high resolution human demographic data as a proxy. These results compose two manuscripts that I wrote together with my doctoral supervisor Vittoria Colizza and other collaborators, one under submission in a peer-reviewed journal and the other one in finalization.
The work has also been presented in several international conferences on mathematical epidemiology and complex systems such as: CCS 2016, International Conference on Complex Systems, Amsterdam, The Netherlands; Complex Nets 2016, "Complex Networks from theory to interdisciplinary applications", Marseille, France; MathEpi 2015 Conference, "Mathematical and Computational Epidemiology of Infectious diseases – the interplay between models and public health policies", Erice, Italy; ECCS 2014, European Conference on Complex Systems, Lucca, Italy.
The work has been realized as part of a European consortium, named *Predemics*, composed by 23 internationally recognised teams from 17 institutions in 8 countries with cross-disciplinary expertise in veterinary, human medicine and modeling. I developed my doctoral work across two institutions: the Institute for Scientific Interchange of Turin (ISI Foundation), Italy and the EPIcx Lab in Paris, France. Moreover, I spent one month to collaborate with Hervé Bourhy, the head of the *Lyssavirus Dynamics and Host Adaptation Lab*, at the Institut Pasteur in Paris, France thanks to the *PREDEMICS exchange training program*.

2 RABIES

In this chapter I provide the characterization and theories about rabies disease with particular reference to those that I employ in the following chapters. In Section 2.1 I introduce rabies disease and its history. In Section 2.2 I give an essential description of the pathogen. Section 2.3 deals with rabies transmission and its interaction with the host. Section 2.5 deals with the epidemiology of rabies, focusing on the case of bat rabies in Europe and domestic dog rabies in Africa. Section 2.6 describes the landscape effects on rabies diffusion and persistence. Finally Section 2.7 presents the control strategies commonly used.

2.1 Introduction

Rabies is a zoonotic, fatal and progressive neurological infection with a long history that is lost in antiquity starting from the pre-mosaic Eshmuna code of Babylon in the twenty-third century BC. Rabies disease is caused by *lyssaviruses* where *lyssa* in Greek means madness. The infectious nature of saliva from infected dogs was firstly recognized by Zinke in 1804. No effective preventive or curative treatment was available before 1885 when Louis Pasteur discovered and administered the first rabies vaccine to Joseph Meister, who was attacked by rabies-affected animal. Only later, in 1903, Remlinger and Riffat-Bay finally identified the virus.
Even if rabies is a preventable disease, it still remains an important public health issue particularly in developing countries. Globally it is responsible for more than 60 000 human deaths annually and approximately 15 million people receive rabies post-exposure prophylaxis (PEP) [3]. Over 95% of deaths occur in Asia and Africa [4], where canine rabies is still enzootic despite of the strong attempt to eliminate it through implementation of extensive control strategies and public health awareness programs. Rabies in humans is one of the most severe diseases [5] and when it occurs it is fatal ($\sim 100\%$) even after advanced medical treatments [6].
Multiple different lyssavirus genotypes are present in several areas of the world and most of them can cause the disease in humans. Most rabies-free areas are islands (for example UK, Japan, Hawaii, Mauritius) or geographically isolated peninsulas (such as Norway and Sweden). In Asia and Africa, rabies is hard to control since human mortality is often underestimated because of under-reporting, cultural beliefs and poor or inadequate diagnostic units [7]. This resulted in the neglect of the disease leading to poor assistance from international community and donor agencies [7].
Rabies involves the nervous system (NS) causing an acute encephalomyelitis that can affect primarily carnivores and bats but with the capability to affect also warm-blooded

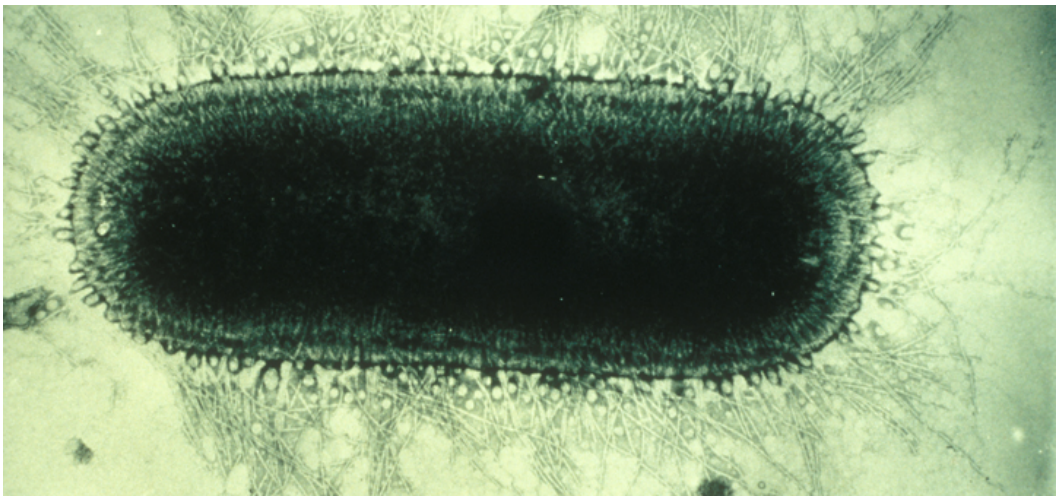

FIGURE 2.1: Electron microscope image of rabies virus. Photo by Norden, Smith-Kline Company

animals including humans as well as a wide variety of wildlife species [8]. The susceptibility varies greatly depending upon the animal species, genetic makeup, age, viral strain or dose of the virus and exposure route. Dogs are one of the major reservoir and also the major vector for human exposure causing the majority of human deaths each year [4]. Cats are very effective for transmission, but it seems that both domestic and wild can not act as reservoir. Foxes played an important role for rabies maintenance and spread through Europe after World War II but that species nowadays serves as reservoir only in Arctic areas and in some temperate and tropical latitudes. Other important canid reservoirs include coyotes in the America and raccoons in Eurasia.
In most European countries the virus is present in bats species. Bats are legally protected under certain international treaties and national nature conservation legislations. Bat rabies research is important because the virus has the potential to cross species barrier and infect domestic and wild mammals [9–11], therefore it is fundamental to gain insight into whether rabies in bats can be a real problem for public health or not.
Rabies has been the subject of many extensive reviews and texts (recent examples include [12–15]). This chapter focuses only on specific aspects of the disease relevant for my PhD work.

2.2 Lyssavirus

The causative agents of rabies disease are negative sense, non-segmented, single-stranded RNA viruses (Figure 2.1) with a helical nucleocapsid surrounded by a thin protein-studded membrane (Figure 2.2 panel a) that belongs to the *Lyssavirus* genus of the *Rhabdoviridae* family and *Mononegavirale* order. Based on sequencing and phylogenetic studies several genotypes have been identified [14] (see Figure 2.4), in particular: rabies virus (RABV), Lagos bat virus (LBV), West Caucasian bat virus (WCBV), Shimoni bat virus (SHIBV), Mokola virus (MOKV), Duvenhage virus (DUVV), European bat lyssavirus subtype 1 (EBLV-1), Irkut virus (IRKV), Australian bat lyssavirus (ABLV), European bat lyssavirus subtype 2 (EBLV-2), Bokeloh bat lyssavirus (BBLV), Khujand virus (KHUV), Aravan virus (ARAV), and Ikoma lyssavirus (IKOV).
The genome is approximatively 12 kb size, which carries five structural proteins namely, nucleoprotein (N), phosphoprotein (P), matrix protein (M), glycoprotein (G) and RNA-dependent RNA polymerase (L) [13, 16–18] (Figure 2.2 panel b). The N gene codes for

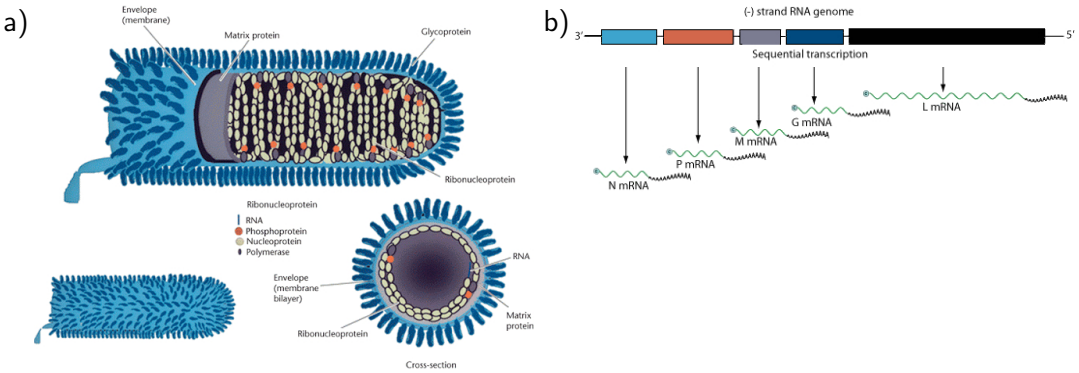

FIGURE 2.2: a) Lyssavirus structure, 180 nm long and 75 nm wide. b) Shape of RNA, about 11-15 kb in size, encodes for 5 to six proteins.

a nucleoprotein that encapsulates the viral RNA; the P gene produces a phosphoprotein, which is important not only in transcription and replication, but also for interactions with cellular protein components during axoplasmic transport; the M gene codes for a matrix protein; the G gene produces a single glycoprotein, a membrane-bound moiety that mediates reception and fusion at cell surfaces and serves as a target for the induction of virus neutralizing antibodies; and the L gene encodes a polymerase for RNA synthesis [13]. A representation of lyssavirus flow in a host cell is illustrated in schematic way in Figure 2.3.

2.3 Transmission

In infectious hosts the virus is present in a lot of different tissues and in particular in the salivary glands from where it can be excreted in saliva. Bites are the most common transmission route, other ways even if less common are however possible. The virus can enter into the body through wounds or cuts and also through intact mucous membranes [5, 19]. The risk of infection by bite is 5%–80%, which is approximately 50 times more than by licks or scratches whose occurrence is 0.1%–1% [20]. The severity of the infection depends on the location of the virus inoculation and on the amount of virus injected [20, 21].
Other non-bite exposure includes inhalation of aerosolized and oral route infection. In both cases the infection requires higher doses with respect to the direct contact infection although species vary considerably in their susceptibility [22]. Cases due to airborne exposure were documented in laboratories during vaccine production [23] and in caves occupied by many infected bats [24, 25].
Disease transmission through organ transplantation was reported in the United States in 2004 [26] and during 2005 into German patients [27] so it was then suggested that donors, mainly those with nervous signs, must be tested for rabies [28].
The virus may be also excreted through breast feeding milk [29] and also transplacental transmission has been reported in animals but it is extraordinarily rare.

2.4 Pathogenesis

The pathogenesis begins after the injection of the virus into the host and involves all the pathologic mechanisms occurring in the development of the disease. The virus after the

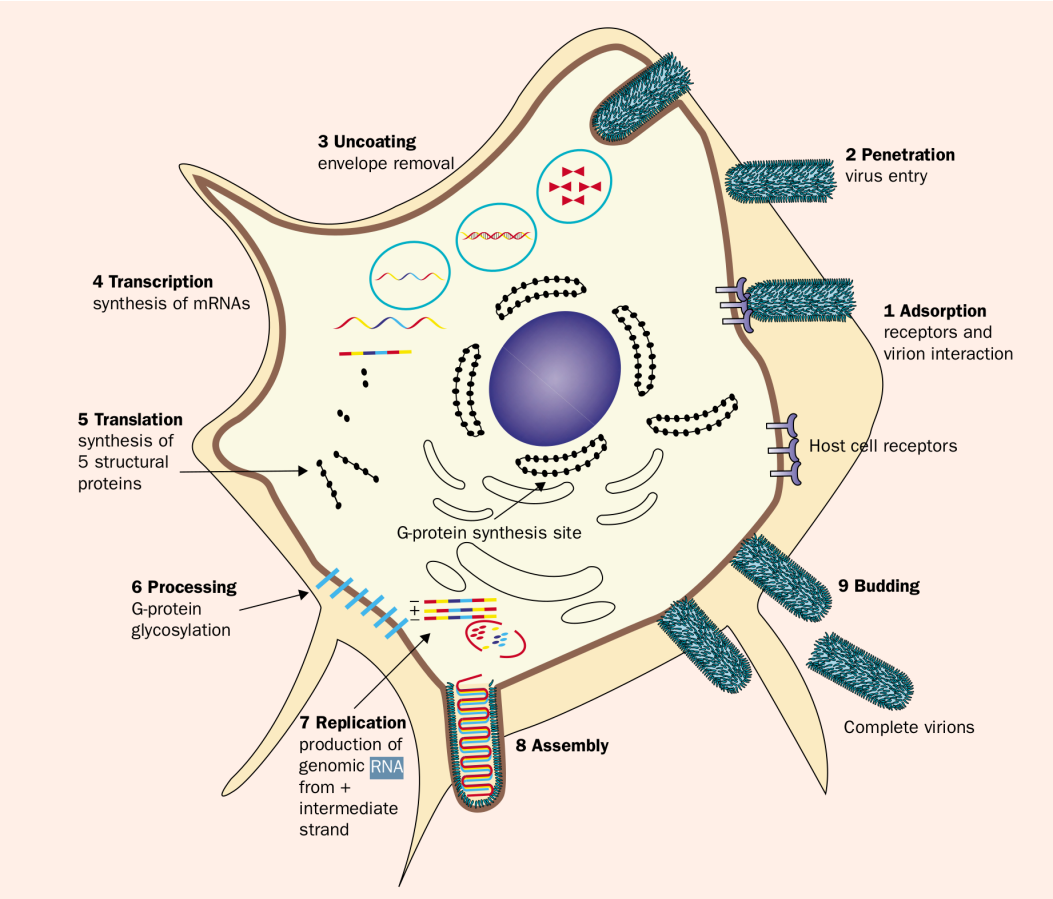

FIGURE 2.3: Conceptual flow of lyssavirus reception, entry, transcription, translation, replication, and exit from a generalized host cell (from *Rupprecht et al.* [12]).

injection gets attached through G-protein receptors to the target cells such as myocytes, local sensory and motor neurons and amplifies in muscle cells and in macrophages [30]. Then, through the muscle spindles of sensory nerves or neuromuscular junction of motor nerves the virus ascends centripetally along the nerves (3 mm/hr, experimental data) and reaches the central nervous system (CNS) to infect the nerve cells [14, 31–33]. This is the incubation period, which can vary from 2 weeks to 6 years (the longest period ever documented) with an average of 1 or 2 months. The length of incubation depends on the host, on the virus genotype, on the concentration of the virus inoculated, on the inoculation site and on the density of innervation in that site [34]. Finally, through the CNS the virus reaches the brain where it causes encephalitis and passes to the salivary glands via cranial nerves. The nearer the injection site is to the brain the faster can the virus reaches the brain and the salivary glands for the viral shedding. Bites on hands, neck, face and head lead to shorter incubation period.

The pattern just described represents the typical rabies pathogenesis. However, experimental studies [35–37] suggest that the pathogenesis of bat rabies infection may be slightly different, in particular in the early stages of the process. Given the small size of bats, the infection is caused by more superficial bites in respect to the terrestrial vectors like dogs, foxes, etc. Rabies isolates from silver-haired bats (*Lasionycteris noctivagans*) have been found to have much higher infectivity for fibroblast and epithelial cells lines than to neuroblast cell lines, in particular at low temperature (34°C). This suggests a better adaptation of the virus to replicate in the slightly cooler superficial dermis. The

genotypes that have been demonstrated to cause clinical signs and death in bats are the RABV and the Australian bat lyssavirus which are closely related [38, 39]. Differently, it seems that bats can survive either natural infection or experimental peripheral inoculation with bat-derived lyssaviruses [40] although the nature of this behaviour is controversial. In particular, the observation of a high prevalence of lyssavirus antibodies in bats colonies [41–44] has been interpreted either with the possibility of abortive infection that permits the development of antibodies but not the virus shedding or with the possibility of recovery from the disease (see Section 2.5.1).

2.5 Rabies epidemiology

All mammals are susceptible to rabies but not all mammals are capable to maintain the infection as reservoir hosts. Surveillance data, monoclonal antibody and genetic studies show that a single virus biotype is maintained by a single principal host species in a given geographical area [45–47]. Even if other species may sporadically acquire the infection from major host they seem unable to sustain the infection independently. There is also evidence that susceptibility depends on the host-pathogen interaction [48, 49].
Rabies circulates with interrelated epidemiological cycles named *urban* and *sylvatic*, which have mainly as vectors/reservoirs dogs, cats and wild mammals like bats, foxes, raccoons, etc., respectively [50]. Both cycles may overlap in some geographical areas. In developed countries rabies is maintained mostly in the sylvatic cycle, for example in Europe the main reservoirs are: the fox in central and eastern Europe, the raccoon dog in northeastern Europe and the insectivorous bat throughout the entire territory. Only in eastern Europe and on the borders with the Middle East dogs are reservoir. Differently, in developing countries of Africa and Asia both epidemiological cycles are present. The urban cycle is mainly maintained by domestic and stray dogs, and spill-over to pet dogs represents an important burden for humans [51–53].
In the following I focus on the two cases that are related to my work: the epidemiology of bat rabies in Europe and the epidemiology of domestic dog rabies in Africa.

2.5.1 Bat rabies in Europe

The lyssavirus species that are the causative agents of rabies in European bats are [55]: *European bat lyssavirus* subtypes 1 and 2 (EBLV-1 and EBLV-2, respectively), *Bokeloh bat lyssavirus* (BBLV), *West Caucasian bat virus* (WCBV) and one tentative species, *Lleida bat lyssavirus* [56–61]. In Europe bat rabies seems not so frequent, possibly as result of heterogeneous surveillance intensity in the different countries [55]. Only 1200 cases were reported to the WHO Rabies Bullettin Europe (RBE) in the period between 1977 and 2017 (Figure 2.6) with the vast majority characterized as EBLV-1, frequently isolated in the Netherlands, North Germany, Denmark, Poland and also in parts of France and Spain. Most EBLV-2 isolates originated from the United Kingdom (UK) and the Netherlands, and EBLV-2 was also detected in Germany, Finland and Switzerland. Only one isolate of BBLV was found in Germany. Circulation of RABV among bats in Europe was repeatedly suggested but never confirmed [62].
About 95% of EBLV-1 cases have been observed in *Eptesicus serotinus* [63, 64]. However, it was reported also in *Nyctalus noctula*, *Vespertilio murinus* [65], *Myotis myotis*, *Myotis dasycneme*, *Myotis daubentonii*, *Pipistrellus pipistrellus*, *Pipistrellus nathusii*, *Myotis natterreri*, *Rhinolophus ferrumequinum* and *Miniopterus schreibersii* [43, 56, 63]. Antibodies to EBLV-1 were found additionally in *Tadarida teniotis* [43]. EBLV-2 was diagnosed not as frequently as EBLV-1. This virus was isolated from *M. dasycneme* and *M. daubentonii*

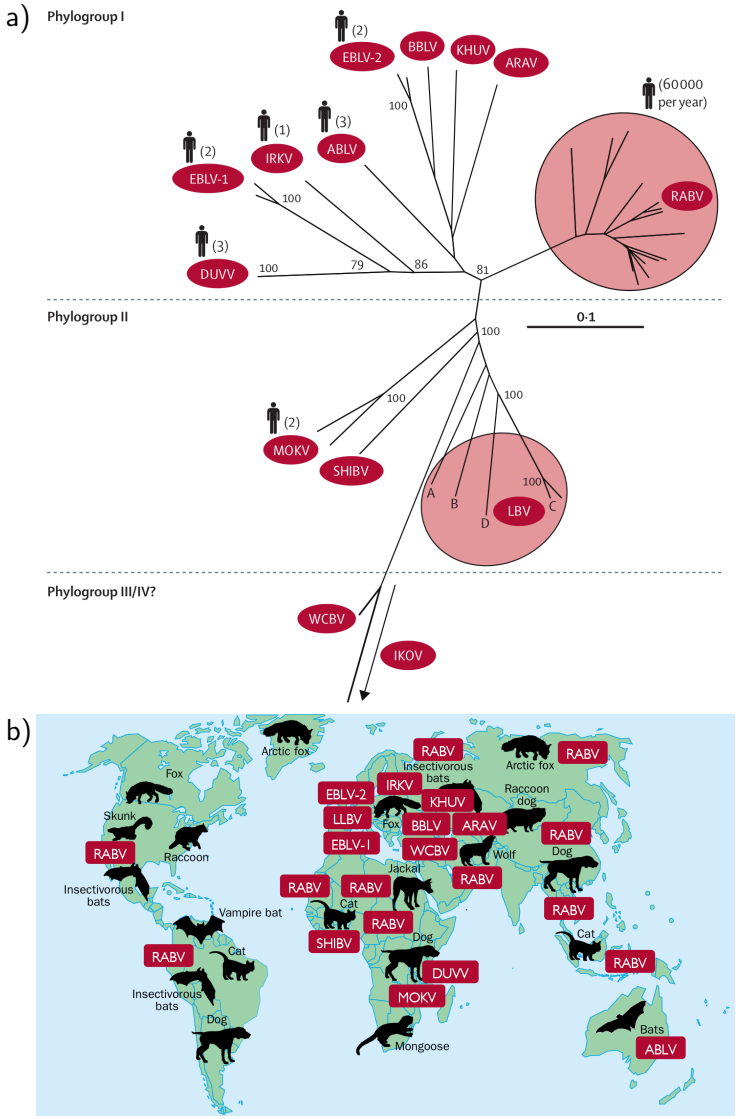

FIGURE 2.4: a) Lyssavirus genotypes: rabies virus (RABV), Lagos bat virus (LBV), West Caucasian bat virus (WCBV), Shimoni bat virus (SHIBV), Mokola virus (MOKV), Duvenhage virus (DUVV), European bat lyssavirus subtype 1 (EBLV-1), Irkut virus (IRKV), Australian bat lyssavirus (ABLV), European bat lyssavirus subtype 2 (EBLV-2), Bokeloh bat lyssavirus (BBLV), Khujand virus (KHUV), Aravan virus (ARAV), and Ikoma lyssavirus (IKOV). Several sequences within the phylogeny are unpublished and as such do not have accession numbers. The scale bar represents 0·1 substitutions per nucleotide site. The number of human cases are shown next to silhouettes where reported. (Figure adapted from *Fooks et al.* [14]). b) Geographic distribution of the genotypes and the corresponding reservoirs (Figure adapted from *Rupprecht et al.* [12]).

and found also in *N. noctula* or *V. murinus* from Ukraine.

The disease progression following lyssavirus infections in bats is largely debated and controversial. Natural observations [10, 60, 66] and controlled experiments [67–69] suggest that clinically infected bats may die, however there is an increasing body of evidence to suggest that bats tolerate EBLV natural infection. Non-lethal exposures or abortive infections with lyssavirus (i.e. developing a neutralizing antibody response in the absence of

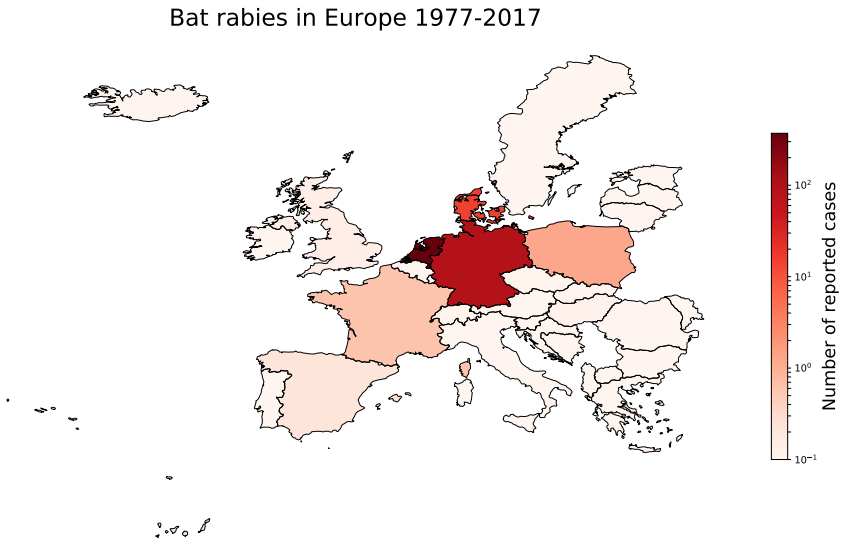

FIGURE 2.5: Bats rabies cases. Heatmap of the number of bat rabies cases detected in Europe between 1977 to 2017, data from WHO Rabies Bullettin Europe (RBE) [54].

disease) appear to be relatively common and have been documented in a number of studies [70–72]. The detection of healthy seropositive bats in different populations suggests that bats may be able to clear the infection surviving the disease. Further, longitudinal and serological surveys for EBLV-1 circulation in *M. myotis* in Europe [73] showed substantial temporal fluctuations, with individual waves of seroconversions and waning immunity.

The legal framework that protects European bat species has largely precluded meaningful assessment of virus infection in the European area (see Section 2.7). Where experiments have been undertaken, sample sizes have been small, and results have been difficult to interpret [60]. Passive surveillance of abnormal or dead bats submitted to veterinary laboratories often gives inappropriate results [56]. Active surveillance has been limited mostly to the screening of oral swabs for the presence of viral RNA and to serological tests. During one survey in Spain, 15 of 71 oral swabs obtained from apparently healthy *E. serotinus* bats were reported positive for EBLV-1 RNA. Additionally, viral RNA was detected in 13 oral swabs but only in five brains of the 34 bats from which simultaneous testing of brains and oral swabs was available [74]. In a study made by *Wellenberg et al* in 2002 [44] they found the presence of EBLV-1 RNA in tissues of apparently healthy zoo bats, *R. aegyptiacus*, which presumably acquired the infection from European insectivorous bats. Finally, a recent serological survey of EBLV-1 antibodies in serotine bat (*E. serotinus*) in the North-East of France revealed that survival and recapture probabilities were not affected by the serological status of individuals [42]. All these empirical observations confirm the capacity of those European bat species to survive at least to a EBLV-1 infection. However, the infection dynamics may depend on the rabies genotype and on the bat species considered.

Next to the host-pathogen interaction, host ecology may also drive the virus circulation in bats population [75]. This may include the interaction between different species, type of

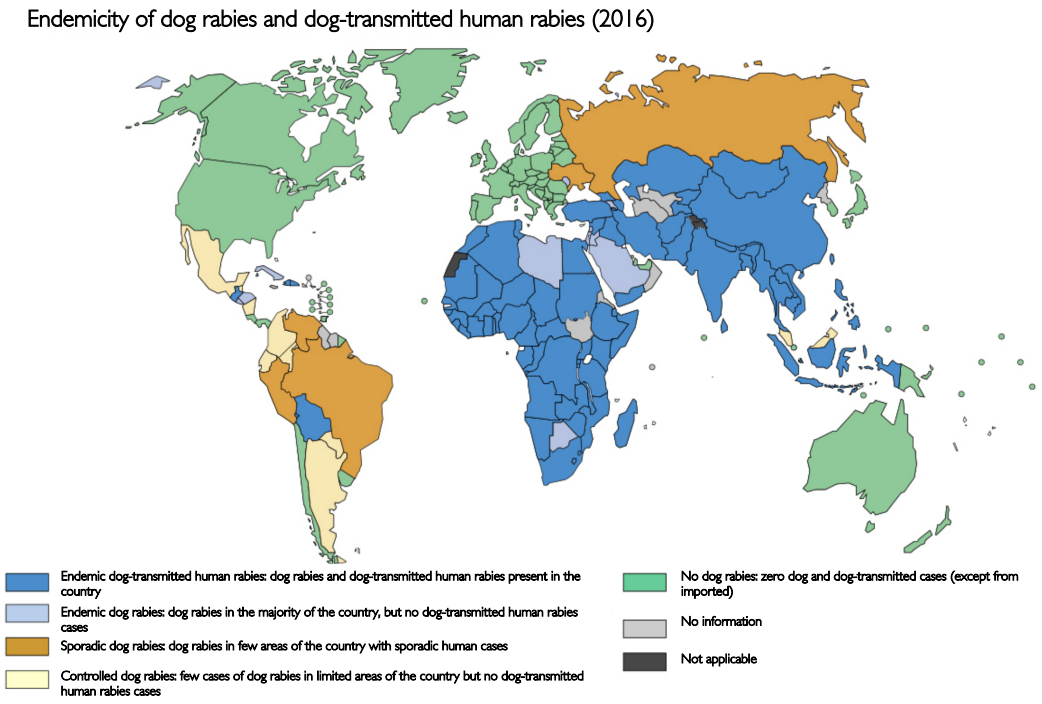

FIGURE 2.6: Dog rabies worldwide. Endemicity of dog rabies and dog-transmitted human rabies worldwide in the 2016 (Figure adapted from WHO).

habitat, synanthropic (i.e. living close to human population) vs. non-synantropic behavior, demographics parameters such as population size and structure, density of animals in their different roosting habitats, or behaviours such as overwintering [61, 75–79]. Finally, the presence of strong migratory bats species like *M. schreibersii* (longest recorded distance 833 km [80]), in which EBLV-1 genome was detected, can be risky for the virus diffusion since those species can lead to the dissemination of the pathogen on a wider geographical area [43].

2.5.2 Dog rabies in Africa

Domestic dog (*Canis familiaris*) remains the most important reservoir of rabies in overall case numbers and with regard to transmission to humans. Differently from bat rabies, in the case of domestic dogs the burden is mainly in Asia and Africa [81]. In most European countries and in other regions like Japan, USA and Canada where strict control of free-ranging dogs and mandatory parenteral rabies vaccination were enforced, canine rabies has been successfully eliminated.

In African domestic dogs, the circulating lyssavirus genotype is RABV [82–84], in particular four clades of this genotype are present: Africa 1 clade, adapted to dogs, which is similar to the Eurasian RABV lineages and was grouped in the 'Cosmopolitan' clade [84] with the Africa 4 clade [82, 83]; the Africa 2 clade includes RABV strains that circulate in dogs in central and western Africa; the Africa 3 clade is restricted to South Africa and is adapted to mongoose [82–84].

In Africa not only domestic dogs are involved in RABV life cycle, at least other five species of wild canids are part of it: the side-stiped jackal (*C. adustus*), the black-backed jackal (*C.*

mesomelas), the bat-eared fox (*Otocyon megalotis*) [85–87], the African wild dogs (*Lycaon pictus*) [88] and the Ethiopian wolves (*C. simensis*) [89]. Despite the predominance of domestic dog rabies, the role of wildlife as independent reservoir has been debated and sometimes seen as a possible barrier to canine rabies elimination in the African continent [90]. However, what is being observed in the Serengeti ecosystem (Tanzania), which is rich of wildlife, is that domestic dogs are the only population essential for maintenance [91–93] because: phylogenetic data showed only a single African canid-associated variant (Africa 1b) circulating among different hosts [93]; transmission networks suggested that, for wildlife hosts, within-species transmission cannot be sustained [93]; statistical inference indicated that cross-species transmission events from domestic dogs resulted in only relatively short-lived chains of transmission in wildlife with no evidence for persistence [94]. Also in other part of Africa the transmission is driven only by domestic dogs [95] concluding that they can be a fundamental reservoir for the disease [96].

Despite the importance of domestic dog rabies, surveillance data in Africa are in general scarce compared to the comprehensive datasets of wildlife rabies from Europe and North America, therefore the analyses of long-term patterns are consequently limited. However, in the last few years many interesting studies started to shed light on dogs ecology, rabies dynamics and control strategies in different African countries. For example a series of works analyzed domestic dogs ecology and RABV circulation both in rural and urban areas in Tanzania [81, 91, 97–99], Zambia [100], Zimbabwe [101, 102], Kenya [103, 104], Tunisia [105], Chad [53] and Central African Republic [106, 107]. Unfortunately, the dynamics of canine rabies and the principal mechanisms underlying the maintenance or the extinction of the virus are however not completely clear.

An interesting feature of dogs ecology is the strong relationship with humans including population distribution and movement patterns [102, 108]. Variations in human population can influence changes in domestic dog population and therefore the spread of rabies. During the 20th century the human African population increased enormously and the dog population expanded in parallel [109]. The subsequent social changes, i.e. massive urbanization and increasing human mobility, facilitated also dog movements and rabies diffusion in the whole continent [110]. In the beginning of the 20th century initial rabies outbreaks were temporally and spatially sporadic, whereas subsequently the outbreaks became more and more frequent until the disease started to be endemic in most of the countries (Figure 2.6). Different works highlighted the crucial role of human-mediated dog movements for RABV spatial diffusion in Africa [82, 111–113].

Another key aspect for the maintenance of domestic dog rabies in Africa is related to dogs demography. The African domestic dog population is composed by a very young population (around 2.2 years on average) with a short average life span [81, 99, 102, 103]. Even if this may suggest a suffering and decreasing population, the actual number of domestic dogs continues to increase reaching an estimated annual growth rate of 9% in Machakos region in Kenya [103] and a 2.6% and 3.8% respectively in Serengeti and Ngorongoro district in Tanzania [81]. The high growth rate is given by an extremely high turnover that represents an obstacle for control strategies such as vaccination and culling leading to a continuous renewal of naive population.

Finally the transmission dynamics, commonly evaluated with the *basic reproductive number* R_0 [114] (Chapter 3), is peculiar. Firstly because R_0 is low ($1.05 \leq R_0 < 2$) (see Table 3.1) [81] and near the threshold condition for an epidemic ($R_0 > 1$) (see Chapter 3). Since RABV is fatal this permits the virus circulation avoiding the elimination of the host population [81]. Secondly, R_0 seems insensitive to the host population density, which is anomalous for directly transmitted disease like rabies [81, 91, 115]. This last finding means that the virus can circulate in low-density rural areas contributing to the disease reintroduction in the neighbouring densely populated urban areas. For example

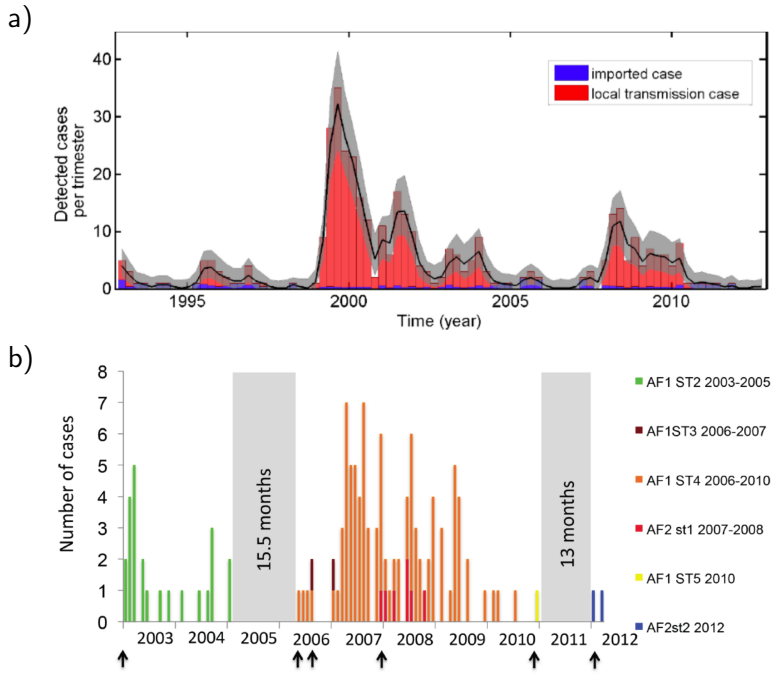

FIGURE 2.7: a) Dog rabies in Bangui. Estimation of the observed number of rabid dogs infected locally (red bar) or from outside the city (blue bar) and simulated number of rabid dogs from the model (black line: posterior median; grey area: 95% credible interval of the posterior distribution). b) RABV subtypes circulating Bangui. Temporal distribution of RABV subtypes in Bangui, black arrows indicates RABV introduction events in the city (first introduction of a new subtype circulating in Bangui). Grey areas indicated periods without any reported cases. (Figure adapted from *Bourhy et al.* [107]).

in Bangui [107], the capital city of the Central African Republic (CAR), it seems that RABV endemicity is maintained by the importation of different subtypes from outside the city (Figure 2.7). The dog population experiences the extinction of RABV transmission chains separating small outbreaks and reflecting a succession of epidemic waves, a pattern that is consistent with previous observations in Africa [81, 111]. This suggests that the maintenance at local geographic scales is driven by human-mediated dispersal of RABV among sparsely connected peri-urban and rural areas as opposed to dispersion in a relatively large homogeneous urban dog population.

2.6 Landscape effects on rabies spread

As observed in the previous sections, rabies transmission is related to host movements. In such context the landscape occupied by the hosts and the hosts spatial diffusion have a strong influence on the ability of the virus to spread and persist in a certain geographical area. The influence of spatial heterogeneities on rabies spread can be subdivided into three different categories: host movements, landscape features and population level effects [115].

Host movements can be classified in *natural* and *human-mediated*. In general the former case is more relevant for wildlife and bats while the latter for domestic dogs (as already discusses in Section 2.5.2). Natural movements can both facilitate the spread of

a pathogen as well as sustain the disease. Migratory bats species, which can migrate for hundreds of kilometers, are generally found to host more viruses in respect to the sedentary ones [116]. Migration increases the possibility to interact with other communities (or species) where a pathogen is present and then facilitates the diffusion and the persistence of the disease [76, 116–118]. Differently, for domestic dogs natural movements can be at maximum around 3 km per day [88, 119, 120] for an healthy domestic dog therefore the human-mediated dispersal is more relevant for rabies virus diffusion [82, 113, 121]. One of the most significant cases in regards to rabies epidemic started in 1997 on Flores Island, Indonesia, after the importation of three rabid dogs, causing more than one-hundred human death, massive reduction of the dog population and a significant economic cost [122].
The second category of spatial effects regard the spatial features of the landscape. Landscape attributes such as, mountains, water bodies and deserts as well as man made interventions such as roads, bridges, political borders or vaccine corridors, can impede or facilitate the hosts movements. All these features influence the spread of rabies both on wildlife and domestic animals, depending on the hosts' ecology and mobility. For example political borders have no evident impact on terrestrial wildlife [123] and bats [116] but they can restrict rabies spread on domestic dogs [113]. Differently natural features like rivers or lake have a strong impact on terrestrial wildlife [124] and domestic dogs [107] but not on bats [43, 116]. Phylogeography is an important tool to reveal the trace of the effects of these features on the gene flow and so on the rabies diffusion [115].
The third category of spatial effects is about the population level. Heterogeneities of the host population and spatial configuration are critical to understand the spread and persistence of pathogens [125]. Multi-species colonies, habitats sharing, fragmentation in the population structure, heterogeneous connectivity given by spatial features can have a complex interaction with the disease spread. To incorporate this kind of complexity in the study of the disease dynamics is particularly important in the case of direct host to host transmitted disease like rabies [126]. In general animal species that can be infected by rabies, both in wildlife and in domestic animals, can be subdivided in a certain number of defined and interacting communities such as colonies for bats and human settlements for domestic dogs. The contacts and the infectious disease dynamics in these cases can be described with a *metapopulation* approach [127–130] (see Section 3.3.2) that is structured on two levels: a inter-community dynamics, where the contacts among the individuals of the same community are more frequent and intense; a intra-communities dynamics, that consists in connections among communities given by less frequent interactions.

2.7 Control strategies

Multiple techniques to control rabies were adopted in the past such as habitat destruction, trapping, institution of boundaries, dens gassing, poisoning and culling [12]. Vaccination so far has been the only control method that worked properly.
The control of bat rabies represents a peculiar problem. Bats are protected in multiple countries since they are facing extinction. They have an important functions like pollination, seed dispersal and predation of insect. In the past a lot of different methods has been used to control bat rabies like the dynamiting of caves or gassing with cyanide [131].Those dramatic indiscriminate methods often kill other bat species that may be sharing the colony with rabies infected ones.
In Europe the guidelines for passive and active surveillance were established by a consortium named Med-Vet-Net [132]. Passive surveillance is the testing of sick or dead bats of all indigenous bat species for lyssavirus infections using standard antigen detection like

the fluorescent antibody test (FAT). Active surveillance regards the monitoring of bat population for lyssavirus infections by screening oral swab (detection of lyssavirus-specific RNA using different RT-PCRs or virus isolation) and/or sera (detection of virus neutralizing antibodies using virus neutralization assays, for example, modified RFFIT) [132]. The basic control strategy in Europe is the exclusion of commensal bats from human living quarters, then extension to bats of oral rabies vaccination or other novel techniques may occur in the future, particularly if rabies control in terrestrial carnivores is sustainable.
As for domestic dogs, all the advances obtained in developed countries are to be extended to less developed countries. Parental vaccination of dogs remains the most effective control strategy that can led to a significant decrease of dog-transmitted human rabies in many countries [133–137]. However, rabies control programs are often more directed to the culling of dog population, although this strategy has already proved to be ineffective [34, 138]. The actual recommendation of the WHO is to achieve at least the 70% of the canine population vaccinated [133, 136, 139, 140]. Important obstacles that hinder a proper implementation of a long term vaccination campaign are the high reproductive rate, the short life and the young skewed age distribution of the domestic dogs in developing countries [133, 141]. Thus, to have rabies eradication, also parallel strategies have to be implemented like sterilization of male and female dogs and the animal birth control to manage of dog population in the endemic areas [142–144].
An additional important factor is that the areas where the disease is endemic are in general developing or low-income countries where the accessibility in remote or risky areas represents a challenge for public health institutions, moreover dog rabies vaccination and animal birth control can represent an important economic burden. While achieving high vaccination coverage is critical for success, this alone will not ensure elimination because gaps in coverage drastically reduce the probability of elimination by creating refuges where disease can remain in circulation [145, 146]. Campaigns should, therefore, seek to achieve not just high coverage, but homogeneously high coverage because the reintroduction of infective animals by human-mediated transportation can render completely ineffective the campaign. Given the general lack of resources in the endemic areas a systematic approach can be achieved by a deeper understanding of the dog rabies dynamics.

2.8 Conclusions

In this Chapter I characterized the rabies disease. Since the subject is very wide this chapter will not be a comprehensive overview, but focuses only on specific aspects of the disease relevant to this study. In Section 2.1 I introduced the disease. In Section 2.2 I described the causative agents of rabies that belong to the lyssavirus family, in particular I listed the different genotypes and the general structure of the virus. In Section 2.3 I reported all the possible route transmission of rabies, remembering that bites are the most common and the more efficient one. Subsequently in Section 2.4 I illustrated rabies pathogenesis. I highlighted firstly the peculiar heterogeneity in the incubation period (in terrestrial mammals it can vary from 2 weeks to more than one year), and secondly the slightly different infection dynamics that occurs in bats respect to the terrestrial mammals. In Section 2.5 I introduced rabies epidemiology, listing the susceptible animals and the reservoirs in the two rabies epidemic cycles, urban and sylvatic. Subsequently I described the two cases that are related to my research: bat rabies in Europe and dog rabies in Africa. The presence of rabies in bats is wide diffused in Europe (Section 2.5.1) and the mechanisms underlying the persistence and the diffusion of the disease are not fully understood, in particular considering the interplay between host-pathogen interaction and

some aspects of bats ecology such as interaction between different species, the habitat, the demography and the role of migrations and seasonality. The problems to tackle in the analysis of rabies in African domestic dogs are different (Section 2.5.2). Firstly domestic dogs are strictly related to humans, so human demography and human migrations pattern can influence dog ecology and the circulation of the disease. Secondly rabies in dogs is invariably fatal so key aspects for maintenance can be also the rapid dogs population turnover and the low transmissibility of the disease. Finally sparse distribution of human settlement and the heterogeneous connectivity among them can help the persistence with the reintroduction of the pathogen in disease free areas.
In Section 2.6 I presented the landscape effects on rabies diffusion divided in: hosts movements, landscape features and population level effects. To conclude, in Section 2.7 I presented the common control strategies already used for bat rabies in Europe and for dog rabies in developing countries. In the following chapter, Chapter 3 I describe the analytical framework that I used to face the open questions on the disease maintenance presented in this chapter.

3 MATHEMATICAL MODELING OF RABIES

Here I introduce the main framework of my research, that is the contribution of statistical physics and mathematics methods to the investigation of spread and persistence of rabies disease in two different hosts. In Section 3.1 I give a basic introduction to mathematical epidemiology. In Section 3.2 and 3.3 I introduce the mathematical theory of infectious diseases and the spatial transmission models that will be applied to specific epidemic contexts in Chapters 4, 5.

3.1 Introduction

Mathematical epidemiology is based on deterministic and stochastic models and it is used to analyze the mechanisms of diseases spread and circulation. Since the first mathematical approach on the smallpox diffusion by Daniel Bernoulli (1766) [2], epidemic models have progressively increased their role in epidemiology, however we have to wait until the 20th century in order to have a further development in that field. In 1906 Hamer [147] hypothesized that the spread of an epidemic depends on the rate of contact between infectious and naive individuals. In 1927, Kermack and McKendrick [148] proposed a theoretical formulation of the *compartmental models* through a set of coupled differential equations to describe the dynamics of infectious diseases. Finally, the last significant boost in the field arrived in the late 20th century, thanks to the rapid improvement of the computational capability that allows the management of increasingly complex models and larger sources of data [149].
Rabies represents an interesting system for developing mathematical models as it is characterized by a complex epidemiological situation. As observed in the previous chapter (Chapter 2), this pathogen is widespread worldwide, it can infect a wide range of mammals in different ecological environments, the maintenance and the diffusion depend on the landscape features and on the host ecology, and finally the host-pathogen interaction may depend on the host and on the virus genotype.
A strong motivation in the analysis of the spread of rabies started after World War II when rabies in red foxes emerged in Europe (Section 2.1). At that time mathematical modeling started to be used to analyze the epidemiological characteristics and the transmission dynamics of rabies to design useful control measures. In particular, in three seminal works [150–152] deterministic models have been developed to explain epidemiological features such as the critical threshold for epidemic emergence and the transmissibility of the disease.
In this chapter, I introduce some key concepts in mathematical models in epidemiology,

especially those relevant for modeling rabies infection dynamics in bats and in domestic dogs. Then I analyze spatial transmission models with a special focus on spatial explicit models incorporating dynamics across heterogeneous landscapes, environmental stochasticity and multi-host interaction.

3.2 Compartmental models

The progress of an infectious disease is defined qualitatively in terms of the level of pathogen within the host, which depends on the growth rate of the pathogen and the interaction between the pathogen and the host's immune response. A simplified and general description of the real complex nature of the host-pathogen interaction can be given classifying each individual respect to its own health status. An individual before any contact with an infectious is susceptible, in this stage no pathogen and no (or a low-level) immunity are present. After the contact with an infectious the susceptible becomes infected. The abundance of the pathogen in the body grows over time and if during this stage it is too low to permit any transmission the host is exposed. When the pathogen abundance is sufficient to transmit the infection the host is infectious. Finally, if the immune system is able to clear the pathogen then the host becomes recovered otherwise the host dies and becomes removed.
The formulation of this dynamics into a mathematical model has been done by Kermack & McKendrick [148] with the compartmental model approach. The compartments are not static and a set of rules define the possible transitions from one compartment to the others; such transitions can be event-driven (like the infection) or spontaneous (like the recovery). This powerful framework becomes a milestone for the modern mathematical and computational epidemiology [114, 149, 153].

3.2.1 SIR

One of the most basic compartmental model is the SIR model where the possible health statuses are: *susceptible*, with size *S* and composed by naive healthy individuals; *infectious*, with size *I* and composed by individuals who have contracted the disease and can transmit it; *recover*, with size *R* and composed by individuals who have already contracted the disease and have recovered from it. In the simplest formulation, the total population size *N* remains constant even if the number of individuals in each class changes in time: $N = S(t) + I(t) + R(t)$, ignoring any demographic process (migration, births, deaths, etc.). In this assumption the time scale of the disease is much smaller than the average life time of the host. Such framework can be simply changed in: a SI model, if the disease gives a permanent and incurable infection; a SIS model, if the disease does not confer any immunity to the host; a SIRS model, if the immunity is temporal.
Despite the simple nature of the model, this formulation can help the understanding of some fundamental epidemiological questions like:

- in which condition a pathogen can cause an outbreak in a naive population?
- which is the rate of new infections in an epidemic?
- which is the proportion of population that suffered the infection during the epidemic?

To derive the differential equations from a general perspective lets start from a population of *N* individuals divided in m classes, which represent the different health statuses. The

number of individuals at time t in the class m is $X^m(t)$, to keep the population constant:

$$N = \sum_m X^m(t) \tag{3.1}$$

We can imagine the disease transmission as a reaction process where the rate of interaction of two different subsets of the population is proportional to the product of the numbers in each of the subset concerned, while the spontaneous recovery process occurs with a constant rate. Then:

- $S + I \to 2I$, transmission;
- $I \to R$, recover.

The transmission can be generally described as the variation of the number of hosts in m class as $N^{-1}\sum_{n,l}\nu^m_{n,l}a_{n,l}X^nX^l$, where $\nu^m_{n,l} = [-1, 0, 1]$, $a_{n,l}$ is the transition rate and N^{-1} comes from the *homogeneous mixing* approximation [114]. The homogeneous mixing approximation is the analogous of the mean-field approximation in physical models and assumes that all individuals can interact randomly with each other.
The recovery is a spontaneous process that happens after a certain amount of time, called infectious period, during which the host tries to recover from the infection. The spontaneous transition from a compartment m to a compartment n is given by $\sum_n \nu^m_n a_n X^n$, where $\nu^m_n = [-1, 0, 1]$ is the variation of the X^m individuals given the recovery and a_n is the transition rate.
The distribution of the infectious period can be obtained from clinical data. In general this period is distributed around a well-defined mean value so, in the modeling scheme, the transition probability is commonly assumed constant. The recovery process of individuals infected at time $T = 0$ is:

$$\frac{dI}{dT} = -\gamma I \tag{3.2}$$

Integrating such equation, the assumption of having a constant rate leads to an exponentially distributed infectious period:

$$\mathbb{P}(\text{infectious after time } T) = e^{-\gamma T} \tag{3.3}$$

Therefore the probability of leaving the infected state does not depend on how long an individual has been infectious. This is know as the "memoryless" property of the exponential distribution.
The general form for the deterministic reaction rate is then just the sum of the two contribution presented:

$$\partial X^m = N^{-1}\sum_{n,l}\nu^m_{n,l}a_{n,l}X^nX^l + \sum_n \nu^m_n a_n X^n \tag{3.4}$$

From this general expression (equation (3.4)) it is possible to obtain the differential equations for the SI, SIS and SIR models. In the following we will focus on the SIR model in order to introduce and explain in a simple way some critical quantities in mathematical epidemiology. Subsequently we will also generalize the analysis introducing the SEIR model, which represents the characteristic model for rabies infection.

Force of infection in homogeneous mixing assumption

The force of infection is a combination of: contact rate k, the probability to contact an infectious p and the probability that the contact with the infectious gives rise to a successful transmission v. Excluding any demographic process the incidence, i.e. the number of new infection per unit of time, can be written as:

$$\frac{dI}{dt} = \lambda S = kpvS \tag{3.5}$$

v is assumed to be constant. $p = I/N$ is the *prevalence* of infection within the population and it is given by the product of the number of infected I multiplied by N^{-1} that represents the homogeneous mixing approximation (each individual has the same probability to be in contact with all the other individuals in the population). k can lead to a density or frequency dependent of transmission.
For density dependent transmission, the contact rate depends on N/A, where A is the area occupied by the population commonly considered $A = 1$. Thus $k = \kappa N$, where κ is a constant and the transmission term becomes:

$$\frac{dI}{dt} = S\kappa(N)(I/N)v = \beta' SI \tag{3.6}$$

where $\beta' = \kappa v$ is the transmission rate and the force of infection is:

$$\lambda = \beta' I \tag{3.7}$$

Differently, for the frequency dependent transmission the rate of contact k is constant, giving a transmission term equal to:

$$\frac{dI}{dt} = Sk(I/N)v = \beta SI/N \tag{3.8}$$

where the transmission rate is $\beta = kv$ and the force of infection is:

$$\lambda = \beta I/N \tag{3.9}$$

With a frequency dependent transmission and considering densities ($s(t) = S(t)/N$, $i(t) = I(t)/N$ and $r(t) = R(t)/N$) the differential equations are:

$$\begin{aligned} \frac{ds(t)}{dt} &= -\beta s(t)i(t) \\ \frac{di(t)}{dt} &= \beta s(t)i(t) - \gamma i(t) \\ \frac{dr(t)}{dt} &= \gamma i(t) \end{aligned} \tag{3.10}$$

Let us analyze the system considering that a single infectious individual is introduced in a completely naive population at time $t = 0$. If N is large, at the early stage of the epidemic the three compartments will be $i(0) = 1/N$, $s(0) \simeq 1$ and $r(0) = 0$. Using a linear approximation the variation of the infected can be written neglecting $\propto i^2$:

$$\frac{di(t)}{dt} \simeq (\beta - \gamma)i(t) \tag{3.11}$$

Disease	Transmission	$\mathbf{R_0}$
SARS	Airborne droplet	2-5
2009 H1N1 Influenza	Airborne droplet	1.2-2
HIV/AIDS	Sexual contact	2-5
Mumps	Airborne droplet	4-7
Rubella	Airborne droplet	5-7
Polio	Fecal-oral	5-7
Smallpox	Social contact	5-7
Pertussis	Airborne droplet	12-17
Measles	Airborne droplet	12-18
Rabies	Bite and saliva contact (rarely transplant)	1.05 - 2

TABLE 3.1: Typical transmission route for different infectious diseases and the estimated values of the basic reproductive number R_0

which has a solution given by:

$$i(t) \simeq i(0)e^{\frac{t}{\tau}} \tag{3.12}$$

where τ is the typical outbreak time $\tau^{-1} = \beta - \gamma$ [114]. This result suggests that if the recovery rate is greater than the transmission rate, τ assumes negative values and the number of infected fades out on the τ timescale. This condition leads to a fundamental quantity named *basic reproductive number* given by:

$$R_0 = \frac{\beta}{\gamma} \tag{3.13}$$

The basic reproductive number is defined as *"the average number of secondary cases arising from an average primary case in an entirely susceptible population"* [149]. In a completely susceptible population ($s(0) = 1$) a pathogen can invade only if $R_0 > 1$, otherwise the infection dies out. Therefore the *epidemic threshold* of the system is when $\beta_c = \gamma$, below which the contagion is too low to permit the spread of the pathogen in an extensive fraction of the population. The value of R_0 and so of the epidemic threshold depends on the disease considered and also on the host population (contact structure, demography, etc.). In Table 3.1 some examples of R_0 are presented for different diseases and different conditions.

Finally, using this framework, it is also possible to evaluate the final size of an epidemic [114]. Starting from equation (3.10) and dividing the variation of the fraction of susceptibles to the variation of the fraction of recovered, we obtain:

$$\frac{ds}{dr} = \frac{-\beta s(t) i(t)}{\gamma i(t)} \quad = -R_0 s(t) \tag{3.14}$$

The result of the integration respect to dr is $s(t) = s(0)e^{-R_0 r(\infty)}$. When the epidemic is over, for $t \to \infty$, there are no more infectious so $i(\infty) = 0$ and $s(\infty) = 1 - r(\infty)$ and the *epidemic size* is defined as $r(\infty)$. Therefore it is possible to rewrite the solution of the equation (3.14) as:

$$r(\infty) = 1 - s(0)e^{-R_0 r(\infty)} \tag{3.15}$$

which is a transcendental equation (Figure 3.1). This result reveals that it is possible to compute numerically the basic reproductive number starting from the total number of

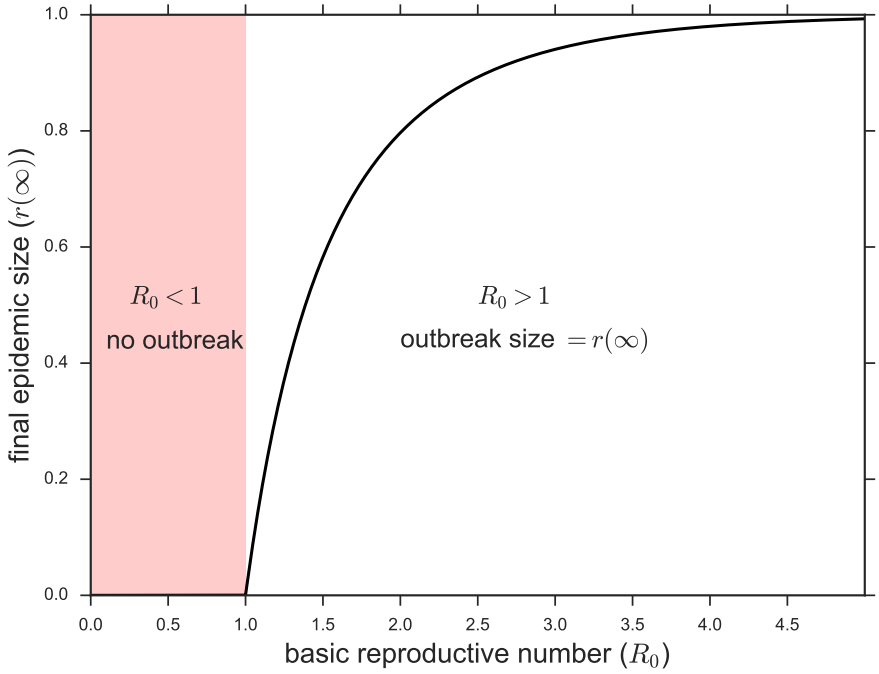

FIGURE 3.1: Epidemic size. The final outbreak size as a function of the basic reproductive number R_0. The curve is obtained considering the initial fraction of susceptible $s(0) = 1$, and the transcendental equation is solved numerically with the Newton-Raphson method.

individuals who have experienced the disease.

The deterministic continuous approach presented in this chapter is valid only in case of sufficiently large populations and in general a fully stochastic description represents a more realistic approach that is able to capture the natural chance effects of the epidemic transmission. To account for this variability the stochastic dynamics rely on an integer-based population and events occur at probabilistic rates. Initially, when few infected individuals are introduced in the population, we define a pre-outbreak stage in which the evolution is noisy and dominated by stochastic effects that are extremely relevant in the presence of few contagious events. This is a stage in which the epidemic may disappear from the population just because of stochastic effects. When the infected individuals are enough to make stochastic effects negligible, but still very few compared with the whole population, we observe an exponential take off of the infected cases as described by the equation (3.14). Finally, the decrease of susceptible individuals reduces the force of infection of each infected and the exponential growth cannot be sustained any longer in the population. Thus we observe the epidemic turn over and the outbreak will ultimately disappear. Stochastic fluctuations may lead to the extinction of the epidemics even well above the epidemic threshold. It has been shown [114] that the extinction probability of an epidemic starting with $I(0)$ infected individuals is equal to $R_0^{-I_0}$. For instance, in the case of a single infected individual, even for values of R_0 as high as 2 the outbreak probability is just 50%. The appropriate way to address the critical issue of the stochastic fluctuation in epidemic process is to employ computational models where it is possible to process and analyze a large number of random events, giving a more realistic description of the spreading process. In Section 3.3.3, there will be presented examples of stochastic models applied in epidemiology.

3.2.2 Demography

In the SIR model just presented we assumed that the epidemic spread is sufficiently fast that all the demographic processes are negligible. Since in this work we are interested in the analysis of the long-term persistence of a disease, also demographic processes have to be considered. A pathogen is endemic in a host population when a stable equilibrium is reached and it continues to circulate on a long temporal scale. One of the key ingredient for the endemicity is the renewal of the susceptible population given by the birth of naive individuals. The simplest and most commonly used way to introduce demography in compartmental models is to consider the average natural lifespan of the host population as l and assume that the probability of an individual to die is uniform through time. The resulting death rate is described by $\mu = 1/l$. It is important to stress that the natural lifespan and death rate are characteristic of the host population and are independent of the disease. It is also commonly assumed that the death rate is equal to the birth rate ($b = \mu$), in order to keep the population size constant. The resulting generalized SIR is then:

$$\begin{aligned} \frac{dS(t)}{dt} &= bN(t) - \beta\frac{S(t)I(t)}{N(t)} - \mu S(t) \\ \frac{dI(t)}{dt} &= \beta\frac{S(t)I(t)}{N(t)} - \gamma I(t) - \mu I(t) \\ \frac{dR(t)}{dt} &= \gamma I(t) - \mu R(t) \end{aligned} \tag{3.16}$$

where $N(t) = S(t) + I(t) + R(t)$, and all newborns are susceptible. In this model no vertical transmission and no maternal passive immunity are considered. Not always newborns enter directly in the susceptible compartment, for example in measles newborns can acquire passive immunity, which occurs when maternal antibodies are transferred to the fetus through the placenta or after the birth through breastfeeding. For other pathogens like HIV and zika the transmission may occurs directly from the mother to the embryo, fetus, or baby during pregnancy or childbirth (vertical transmission), so newborns enter directly in the infected class.
The expression of the basic reproductive number in this case can be obtained considering that the parameter β represents the transmission rate per infective, and the average time spent by an individual in the infectious class is $\frac{1}{\gamma+\mu}$ time units, therefore the number of secondary cases in a fully susceptible population is:

$$R_0 = \frac{\beta}{\gamma + \mu} \tag{3.17}$$

Since we have introduced the host demography, the disease can persist in a population, and this happens when it reaches the equilibrium ($\frac{dS(t)}{dt} = \frac{dI(t)}{dt} = \frac{dR(t)}{dt} = 0$). There are two possible kinds of equilibrium, one without any infection called *disease-free equilibrium* and one with infection circulating called *endemic equilibrium*. To obtain the equilibrium points, we can start from:

$$\beta\frac{S(t)I(t)}{N(t)} - (\gamma + \mu)I(t) = 0, \tag{3.18}$$

and factoring for I:

$$I(t)(\beta\frac{S(t)}{N(t)} - (\gamma + \mu)) = 0. \tag{3.19}$$

Considering densities (as in 3.10), the disease-free equilibrium is obtained for $i^* = 0$ in the point $(s^*, i^*, r^*) = (1, 0, 0)$, while the endemic state is obtained for $i^* \neq 0$ and $s^* = \frac{(\gamma+\mu)}{\beta}$ which is the inverse of R_0. This suggests that for a SIR model with demography the endemic equilibrium is the point in the phase space where the fraction of susceptible in the population is equal to the inverse of R_0. In particular the endemic equilibrium point is:

$$(s^*, i^*, r^*) = \left(\frac{1}{R_0}, \frac{\mu}{\beta}(R_0 - 1), 1 - \frac{1}{R_0} - \frac{\mu}{\beta}(R_0 - 1)\right). \tag{3.20}$$

This means that an endemic equilibrium is feasible only if $R_0 > 1$, the necessary condition to have an epidemic. This system is an excellent example of a "damped oscillator," which means the inherent dynamics contains a strong oscillatory component, but the amplitude of these fluctuations declines over time as the system equilibrates [149].

3.2.3 Latency period

In the model described in the previous sections (Sections 3.2.1 and 3.2.2) each infected is able to re-transmit the infection immediately after the exposure. On the biological point of view when the transmission occurs a small amount of pathogen is introduced inside the host then the pathogen starts to reproduce rapidly without any, or small, reaction of the immune system. This stage is called *incubation period* and by definition it represents the time, during the infection, when the amount of pathogen is too low to have an active transmission. Since for disease like rabies this stage is relevant, we consider another refinement of the SIR model that is obtained adding the *exposed* compartment indicated with E. The compartmental model obtained is the SEIR model:

$$\begin{aligned}
\frac{dS(t)}{dt} &= bN - \beta\frac{S(t)I(t)}{N} - \mu S(t) \\
\frac{dE(t)}{dt} &= \beta\frac{S(t)I(t)}{N} - (\sigma + \mu)E(t) \\
\frac{dI(t)}{dt} &= \sigma E(t) - (\gamma + \mu)I(t) \\
\frac{dR(t)}{dt} &= \gamma I(t) - \mu R(t)
\end{aligned} \tag{3.21}$$

Differently from the SIR, the infected are initially infected but not infectious yet, so they can not shed the pathogen. The functional form of the basic reproductive number R_0 can be obtained in different ways, the way adopted in this work is through the next generation matrix approach [154–156]. The system of ordinary differential equations (ODEs) that characterize the compartmental model can be rewritten as another set of ODEs, named *infection subsystem*, that describes the production of new cases and the changes in infected states. The *infection subsystem* can be linearized, decomposing the corresponding Jacobian matrix in two matrices named respectively: the *transmission* matrix $\mathbf{T}$, which contains the entries corresponding to transmission events; the *transitions* matrix $\mathbf{\Sigma}$, which contains the entries corresponding to all other changes of state (including death). The *next-generation matrix* NGM is then obtained as $\mathbf{K} = -\mathbf{T}\mathbf{\Sigma}^{-1}$. The basic reproductive number R_0 is defined by:

$$R_0 = \rho(\mathbf{K}) = \rho(-\mathbf{T}\mathbf{\Sigma}^{-1}) \tag{3.22}$$

where for the square matrix $\mathbf{K}$, $\rho(\mathbf{K})$ is the spectral radius of $\mathbf{K}$ defined as:

$$\rho(\mathbf{K}) := \mathbf{sup}\{|\lambda| : \lambda \in \alpha(\mathbf{K})\} \tag{3.23}$$

$\alpha(\mathbf{K})$ is the spectrum of $\mathbf{K}$, i.e. the corresponding set of eigenvalues. Summarizing R_0 is defined as the dominant eigenvalue of the NGM.
The system described in equation (3.21) has two infected classes represented by the compartment E and I and two uninfected state, S and R. The total population size is constant and given by $N = S + E + I + R$. To define the *infection subsystem* let us consider the system near the equilibrium (for small E and I), where the compartments are $E = I = R \simeq 0$ and $S \simeq N$:

$$\begin{aligned} \frac{dE(t)}{dt} &= \beta I(t) - (\sigma + \mu)E(t) \\ \frac{dI(t)}{dt} &= \sigma E(t) - (\gamma + \mu)I(t) \end{aligned} \tag{3.24}$$

where the term $\beta\frac{S(t)I(t)}{N} \simeq \beta I(t)$ for $S \simeq N$. To rewrite the equation (3.24) as linear system with the *transmission* $\mathbf{T}$ and *transitions* $\mathbf{\Sigma}$ matrices let us consider $\mathbf{x} = (E, I)'$ (the prime indicates transpose):

$$\dot{\mathbf{x}} = (\mathbf{T} + \mathbf{\Sigma})\mathbf{x} \tag{3.25}$$

For $\mathbf{T}$ the indices are $i, j \in 1, 2$ and $\mathbf{T}_{ij} = 0$ when no new cases produced by an individual in the infected state j can be in the state i immediately after the infection. Therefore the matrix has a form:

$$\mathbf{T} = \begin{pmatrix} 0 & \beta \\ 0 & 0 \end{pmatrix} \tag{3.26}$$

The other transitions are described by the matrix $\mathbf{\Sigma}$:

$$\mathbf{\Sigma} = \begin{pmatrix} -(\sigma + \mu) & 0 \\ \sigma & -(\gamma + \mu) \end{pmatrix} \tag{3.27}$$

The NGM is then:

$$\mathbf{K} = -\mathbf{T}\mathbf{\Sigma}^{-\mathbf{1}} = \begin{pmatrix} 0 & \beta \\ 0 & 0 \end{pmatrix} \times \begin{pmatrix} \frac{1}{\sigma+\mu} & 0 \\ \frac{\sigma}{(\sigma+\mu)(\gamma+\mu)} & \frac{1}{\gamma+\mu} \end{pmatrix} = \begin{pmatrix} \frac{\beta\sigma}{(\sigma+\mu)(\gamma+\mu)} & \frac{\beta}{\gamma+\mu} \\ 0 & 0 \end{pmatrix} \tag{3.28}$$

The dominant eigenvalue is then:

$$R_0 = \frac{\beta\sigma}{(\sigma + \mu)(\gamma + \mu)} \tag{3.29}$$

From the basic reproductive number it is possible to obtain the force of infection λ in function of R_0:

$$\lambda = \beta\frac{I}{N} = R_0\frac{(\sigma + \mu)(\gamma + \mu)}{\sigma}\frac{I}{N} \tag{3.30}$$

which represents the per capita rate at which susceptible individuals contract the infection [149].
Rabies disease is in general considered 100% lethal but, as already highlighted in chapter 2, the actual pathogenicity depends on virus genotype and on host species. In the following I describe some typical models used to study rabies infection dynamics considering different types of host-pathogen interactions.

Rabies infection in bats

As showed in Section 2.5.1, field and experimental studies provide different hypotheses for bat rabies infection dynamics. In particular the observation during field surveys of virus-neutralizing antibodies in captured bats has been interpreted in different ways. The first hypothesis is that exist two possible kinds of infections, a lethal infection and an abortive infection that consists in developing antibodies and recovery without any virus transmission. The second hypothesis suggests that bats tolerate lyssavirus natural infection and they can also recover from it developing a certain immunity. However, part of the scientific community assumes that both infection dynamics are possible and that the occurrence of one behaviour or the other depends on the rabies genotype and the bat species considered. Therefore, in this section I present different compartmental models that I use in my work to test different hypotheses on bat rabies infection dynamics.
The first model, introduced by *George et al.* in 2011 [76], considers that bats can experience nonlethal and lethal infection with lifelong immunity. The transmission dynamics can be described as following: susceptible (S) bats can be infected and they can experience a lethal infection with rate ρ (or a non-lethal infection with rate $1-\rho$); if lethally infected, bats become exposed (E_I), then infectious (I) and finally die with rate γ. With a non-lethal infection they become exposed (E_R) without developing symptoms and then become permanently immune to the virus (R). The disease progression is mathematically described by:

$$\begin{aligned}
\frac{dS(t)}{dt} &= bN - \beta\frac{S(t)I(t)}{N} - \kappa S(t)\\
\frac{dE_R(t)}{dt} &= (1-\rho)\beta\frac{S(t)I(t)}{N} - (\sigma_R+\kappa)E_R(t)\\
\frac{dE_I(t)}{dt} &= \rho\beta\frac{S(t)I(t)}{N} - (\sigma_I+\kappa)E_I(t)\\
\frac{dI(t)}{dt} &= \sigma_I E_I(t) - (\gamma+\kappa)I(t)\\
\frac{dR(t)}{dt} &= \sigma_R E_R(t) - \kappa R(t)
\end{aligned} \tag{3.31}$$

where $\kappa = \mu + (b-\mu)\frac{N}{K}$ is the density dependent death rate, N is the total population and K is the carrying capacity. The carrying capacity is an important quantity in ecology that represents the maximum number of individuals of a particular species that an environment can sustain [127]. It is commonly used in rabies modeling when lethal infection is considered [152, 157].
The second model is a variation of the previous one by adding loss of immunity with rate ω, while all the processes remain the same:

$$\begin{aligned}
\frac{dS(t)}{dt} &= bN - \beta\frac{S(t)I(t)}{N} - \kappa S(t) + \omega R(t)\\
\frac{dE_R(t)}{dt} &= (1-\rho)\beta\frac{S(t)I(t)}{N} - (\sigma_R+\kappa)E_R(t)\\
\frac{dE_I(t)}{dt} &= \rho\beta\frac{S(t)I(t)}{N} - (\sigma_I+\kappa)E_I(t)\\
\frac{dI(t)}{dt} &= \sigma_I E_I(t) - (\gamma+\kappa)I(t)\\
\frac{dR(t)}{dt} &= \sigma_R E_R(t) - (\kappa+\omega)R(t)
\end{aligned} \tag{3.32}$$

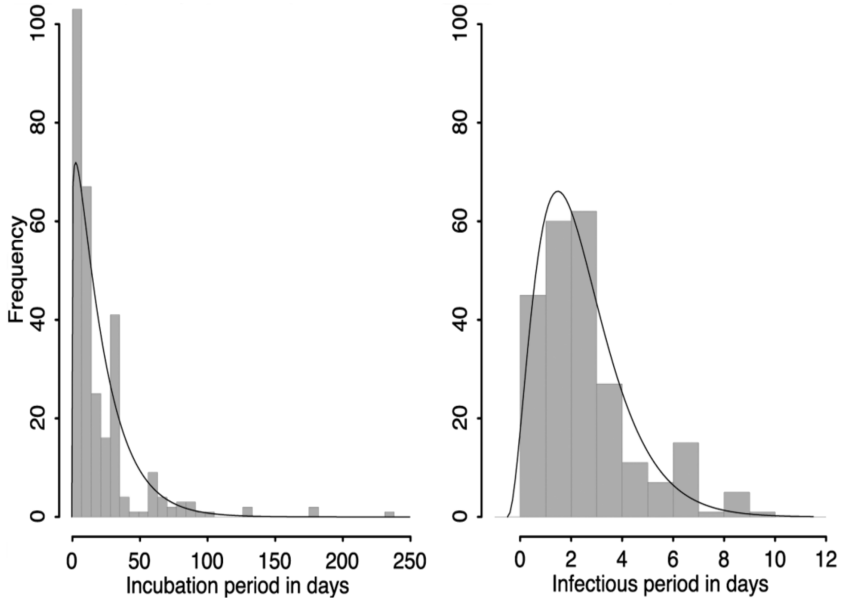

FIGURE 3.2: Dog rabies incubation and infectious period. Observed frequency distributions of dog rabies incubation period (left) and infectious period (right), by *Hampson et al.* [81] from two districts in northwest Tanzania: Serengeti, with high-density dog populations, and Ngorongoro, with a lower-density dog populations. The best fitting gamma distributions to the data are shown by black lines.

The basic reproductive number is the same for the two models, and it can be obtained using the next generation matrix approach:

$$R_0 = \frac{\rho\beta\sigma_I}{(\sigma_I + \kappa)(\gamma + \kappa)} \tag{3.33}$$

The last model considers only non lethal infection and temporal immunity so it can be derived directly from equation (3.21):

$$\begin{aligned}
\frac{dS(t)}{dt} &= bN - \beta\frac{S(t)I(t)}{N} - \mu S(t) + \omega R(t) \\
\frac{dE(t)}{dt} &= \beta\frac{S(t)I(t)}{N} - (\sigma + \mu)E(t) \\
\frac{dI(t)}{dt} &= \sigma E(t) - (\gamma + \mu)I(t) \\
\frac{dR(t)}{dt} &= \gamma I(t) - (\omega + \mu)R(t)
\end{aligned} \tag{3.34}$$

The basic reproductive number is identical to the one obtained in equation (3.29).

Rabies infection in dogs

RABV infection in dogs has a well defined pathogenesis (see Section 2.4) and the disease is considered always lethal so the R class is for the removed individuals that do not

participate to the dynamics:

$$\begin{aligned}
\frac{dS(t)}{dt} &= bN - \beta\frac{S(t)I(t)}{N} - \kappa S(t) \\
\frac{dE(t)}{dt} &= \beta\frac{S(t)I(t)}{N} - (\sigma+\kappa)E(t) \\
\frac{dI(t)}{dt} &= \sigma E(t) - (\gamma+\kappa)I(t) \\
\frac{dR(t)}{dt} &= \gamma I(t)
\end{aligned} \tag{3.35}$$

where, also in this case, $\kappa = \mu + (b-\mu)\frac{N}{K}$ represents the density dependent death rate, N is the total population and K is the carrying capacity. Using the NGM approach (see Section 3.2.3), the basic reproductive number is:

$$R_0 = \frac{\beta\sigma}{(\sigma+\kappa)(\gamma+\kappa)} \tag{3.36}$$

However, the peculiarity of rabies infection in dogs is related to the process of dissemination of the virus within the host's body (see Section 2.4). This may lead to heterogeneous and potentially long lasting exposed period as empirically observed in a recent study on dog rabies transmission in rural Tanzania made by *Hampson et al.* [81] (see Figure 3.2.3) and in a more recent study developed using data from the 1948-1954 rabies epidemic in Tokyo (Japan) [158].
All the compartmental models previously discussed does not allow such heterogeneity because the sojourn time in each compartment is exponentially distributed (as showed in equation (3.3)). While this assumption is mathematically very convenient and it is commonly used in epidemiology, it is unrealistic not only for rabies in dogs but also for diseases like measles, chicken pox and polio which exhibit an incubation with a strong central tendency [153, 159, 160].
In mathematical epidemiology it is well established that using non-exponentials incubation (EPDs) and infectious (IPDs) periods distributions changes some dynamical properties of the system [161–166]. In the SIR model, for example, a less dispersed infectious period can reduce the stability of the endemic equilibrium [162, 165], decrease the persistence time (time to fade-out) of the disease in the population [164, 165], outbreaks take off faster and have a higher peak number of cases [166].
In SEIR models the effects are more related to the relative length of the incubation and infectious periods [164]. If the incubation period is short relative to the infectious period, since SEIR can be well approximated by a SIR model, a less dispersed infectious period distribution will decrease also in this case the long term persistence time and stability [164, 165]. On the other hand, if the incubation period is much longer than the infectious period the opposite behaviour is observed: persistence times and model stability increase when less dispersed distributions are used [165].
As a result of all of these effects, the dispersions of the EPD and IPD are important also for the basic reproductive number R_0 [166]. Models using over-dispersed EPDs or IPDs result in an underestimation or overestimation of R_0 respectively [161, 165, 166].
The inclusion of non-exponential distributions can be achieved in several ways, like through integro-differential equation (IDE) formulation [163, 167] or a partial differential equation (PDE) formulation (as employed in age-structured models [114]). In this work we consider a simple formulation which involves the method of stages [161, 162, 165, 168], already used for measles [166, 169], because the resulting model is more amenable for analysis and numerical simulations.

I describe this mathematical approach considering the SEIR model of equation (3.35). Both the incubation and infectious period are described by their corresponding probability density functions, $f_E(t)$ and $f_I(t)$. The probability density function, $f(\tau)$, gives the probability of an individual that entered in the compartment τ time-units ago to change compartment in the time interval $(\tau, \tau \pm d\tau)$ as $f(\tau)d\tau$. Integrating the density function we obtain the survivorship function:

$$F(y) = \int_y^\infty f(\tau)d\tau \tag{3.37}$$

this gives the probability that an individual remains in the compartment for at least y time-units. The stages method consists to replace a single infective class, i.e. the compartments E or I, with a series of consecutive stages as $E = E_1, E_2, ..., E_m$ and $I = I_1, I_2, ..., I_n$. If the time spent in each stage is assumed to be exponentially distributed with an identical average in each stage, the total time spent in each compartment results to be a sum of m or n exponential distributions that lead to gamma distributed incubation and infectious periods respectively.

$$\begin{aligned}
\frac{dS(t)}{dt} &= bN(t) - \beta\frac{S(t)I(t)}{N} - \kappa S(t) \\
\frac{dE_1(t)}{dt} &= \beta\frac{S(t)I(t)}{N} - (m\sigma' + \kappa)E_1(t) \\
\frac{dE_2(t)}{dt} &= m\sigma' E_1(t) - (m\sigma' + \kappa)E_2(t) \\
&\vdots \\
\frac{dE_m(t)}{dt} &= m\sigma' E_{m-1}(t) - (m\sigma' + \kappa)E_m(t) \\
\frac{dI_1(t)}{dt} &= m\sigma' E_m(t) - (n\gamma' + \kappa)I_1(t) \\
\frac{dI_2(t)}{dt} &= n\gamma' I_1(t) - (n\gamma' + \kappa)I_2(t) \\
&\vdots \\
\frac{dI_n(t)}{dt} &= n\gamma' I_{n-1}(t) - (n\gamma' + \kappa)I_n(t) \\
\frac{dR(t)}{dt} &= n\gamma' I_n(t)
\end{aligned} \tag{3.38}$$

To ensure that the average time spent in the exposed class is still $1/\sigma$ and in the infectious class $1/\gamma$, the rate of movement between the subclasses is defined as $\sigma = m\sigma'$ and $\gamma = n\gamma'$, respectively. This is equivalent to assuming the following probability density functions for the latent ($f_E(t)$) and infectious ($f_I(t)$) periods:

$$f_E(t) = \frac{(m\sigma')^m e^{-m\sigma' t} t^{m-1}}{(m-1)!}$$

$$f_I(t) = \frac{(n\gamma')^n e^{-n\gamma' t} t^{n-1}}{(n-1)!} \, .$$

Straightforward calculation of the next generation matrix for this model results in the following characteristic equation for the eigenvalues of the disease-free equilibrium:

$$\lambda(\lambda + \gamma' n)^n \left[\lambda(\lambda + \sigma' m)^m - R_0\gamma'(\sigma' m)^m \left(1 - \left(\frac{\lambda}{\gamma' n} + 1\right)^{-n}\right)\right] = 0 \, .$$

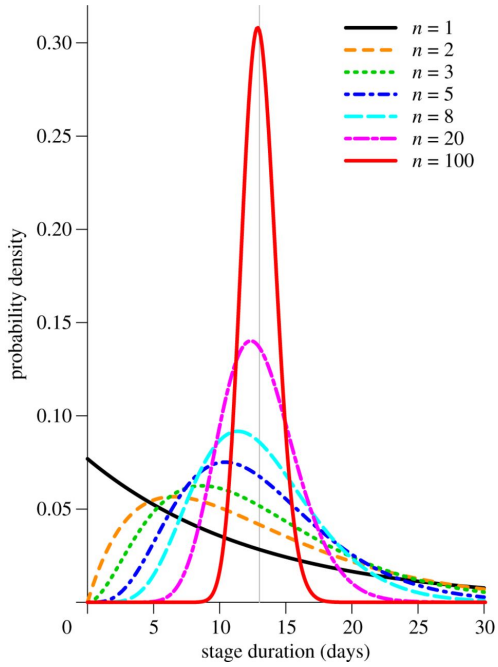

FIGURE 3.3: Gamma distributions. Probability density functions for several Gamma distributions with the same mean (13 days, marked with a vertical grey line) but different shape parameter n. The most extreme cases are the exponential distribution ($n = 1$) and the Dirac delta distribution ($n \to \infty$). (from Krylova et al. [169]).

Since we are interested in the dominant positive eigenvalue, only the expression in the square brackets is relevant. The basic reproductive number is then [170]:

$$R_0 = \frac{\beta}{m\sigma' + \kappa} \left(\frac{m\sigma'}{m\sigma' + \kappa} \right)^m \sum_{j=0}^{n-1} \left(\frac{n\gamma'}{n\gamma' + \kappa} \right)^j \tag{3.39}$$

When $n = m = 1$ and then both latent and infectious periods are exponentially distributed while if $n, m \to \infty$ the latent and infectious periods have a fixed length.

3.3 Spatial transmission models

The compartmental models introduced so far describe the epidemic spread in a single population of homogeneously mixed individuals. This picture represents a strong simplification of the reality because for directly transmitted diseases like rabies, HIV, influenza, etc. the transmission occurs with higher probability if the interaction is more intense/frequent, which implies spatial proximity. Moreover, the movement of individual among different locations may facilitate the spread of the pathogen on a wider geographical area. Human and animal communities are made by a complex structure of heterogeneous interactions that have to be introduced in a realistic epidemic model since those features have a critical role in the epidemic spread [171].
Rabies is an interesting example of infectious disease in which the diffusion is driven by the movement of the hosts and the by the spatial heterogeneity of the landscape where the host population lives [115] (see Section 2.6)
The aim of this section is to introduce space in epidemic models in particular the reaction-diffusion processes to include the spatial transmission and the metapopulation model to

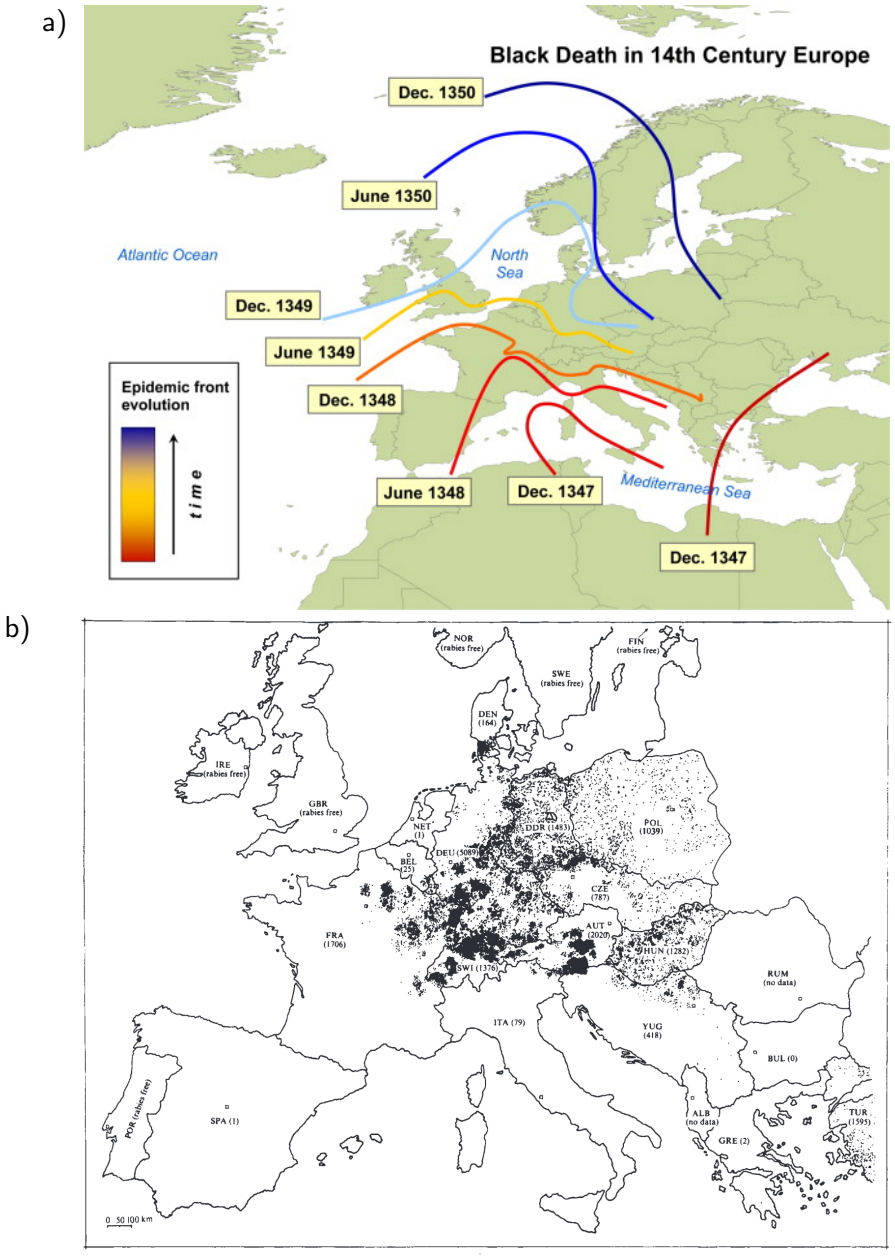

FIGURE 3.4: Top: The spread of the Black Death in 14th Century Europe was mainly a diffusive process, with an epidemic front wave crossing the continent from South to North (from *Colizza et al.* 2007 [172]). Bottom: Geographic distribution of reported cases of rabies both in domestic and wild animals, during 1979. Each dot represent a case (from *Anderson et al.* 1981 [157]).

consider the spatial heterogeneity. The resulting framework enables us to answer to important issues like: which is the rate of the spatial spreading of a pathogen, which is the influence of large and small population in the persistence and circulation and which are the mechanisms for the endemicity in the local and the broad spatial scales.

3.3.1 Reaction-diffusion process

A reaction-diffusion (RD) process is a well known modeling framework extensively applied to study chemical and physical phenomena [173, 174]. At the microscopical level it

consists of particles that diffuse in space and that are subject to some reaction process that depends on the nature of the problem considered. Space is in general a regular lattice where each particle stays in a node and diffuses through the connections between the neighboring nodes. If particles are fermions, the RD process assume the exclusion principle that limit the number of particles in each node, while if particles are bosons the RD process allows each node of the lattice to be occupied by any number of particles [175]. Bosonic RD processes have been proven useful not only in the classic field of physics, but to model a wide range of systems that includes epidemic spreading [176–179] and social contagion processes [180–183].
To better understand the role of space in the epidemic spread and to introduce the reaction diffusion method in epidemiology, let us consider two historical examples. The first one is the diffusion of the Black Death that devastated Europe during the 14th century [184]. In this case a simple way to introduce space in the epidemic model is given by spatial diffusion. Let us recall the simple SIR model without demography, where the compartments are defined by densities: $s(x,t)$, $i(x,t)$ and $r(x,t)$. The differential equations in this case are given by:

$$\begin{aligned} \frac{\partial s(x,t)}{\partial t} &= -\beta s(x,t)i(x,t) + D\nabla^2 s(x,t) \\ \frac{\partial i(x,t)}{\partial t} &= \beta s(x,t)i(x,t) - \gamma i(x,t) + D\nabla^2 i(x,t) \end{aligned} \tag{3.40}$$

where D is the diffusion rate and $D\nabla^2$ describes the diffusion process that represents the individual mobility. From equation (3.40), if $D \neq 0$ and $\beta = \gamma = 0$ the epidemics grows as $\sqrt{t}$, while if $D \neq 0$ and $\beta \neq 0$ it grows with a finite speed v. The analytical solution of the traveling wave speed can be computed [185]:

$$v = 2\sqrt{\beta D s(t=0)}\left[1 - \frac{1}{R_0}\right] \tag{3.41}$$

where $s(t=0)$ is the initial density of susceptible and $R_0 = \beta/\gamma$. Applying this simple diffusion model the resulting epidemic wave front speed is around $v \sim 140 miles/year$ which is close to the historically given estimate $v \sim 200 - 400 miles/year$.
The second example is a reaction-diffusion model introduced by *Murray er al.* in 1986 [152] to analyze the spread of fox rabies through Europe following the World War II (as already discussed in Section 3.1):

$$\begin{aligned} \frac{\partial s(x,t)}{\partial t} &= r(1-1/K)s - \beta s(x,t)i(x,t) \\ \frac{\partial e(x,t)}{\partial t} &= \beta s(x,t)i(x,t) - (\sigma + \mu + r/K)e(x,t) \\ \frac{\partial i(x,t)}{\partial t} &= \sigma e(x,t) - (\gamma + \mu + r/K)i(x,t) + D\frac{\partial^2 i(x,t)}{\partial x^2} \end{aligned} \tag{3.42}$$

where $r = b - \mu$ represent the intrinsic per capita growth rate, and D (as in equation (3.40)) is the diffusion rate. The estimated movement rate of rabid foxes was $D \sim 50 km^2/year$. The speed of the traveling wave can be computed making some reasonable approximation:

- Δt small, so the demographic processes can be neglected $b = \mu = 0$;
- since the epidemic process is driven by the movement of the infectious we can assume that for small Δt the exposed $\frac{\partial e(x,t)}{\partial t} \sim 0$

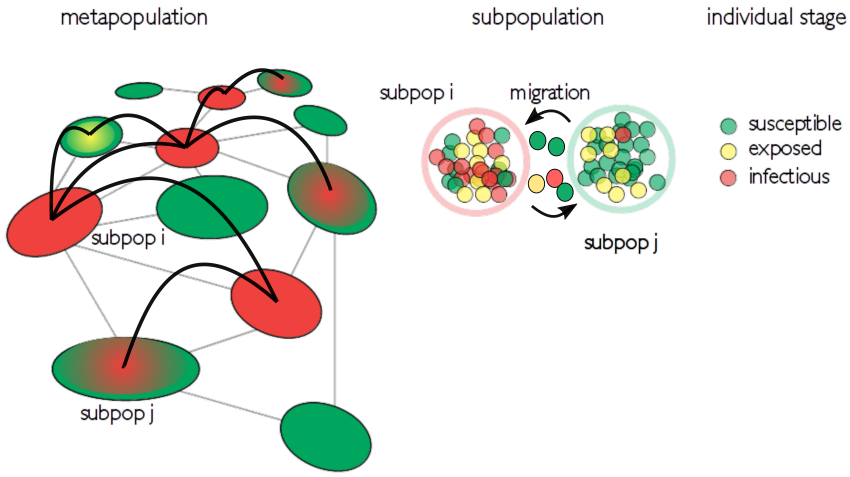

FIGURE 3.5: Schematic illustration of the modelling framework based on a metapopulation scheme. At the macroscopic level the system is composed of a network of subpopulations. At the microscopic level, each subpopulation contains a population of individuals. The infection dynamics are described by a simple compartmentalization (compartments are indicated by different colored dots in the picture). Within each subpopulation, individuals are mixed homogeneously and can migrate from one subpopulation to another following the mobility connections of the network. In this way the disease can spread at the subpopulations level.

Through these approximations the equation (3.42) can be written as:

$$\frac{\partial i(x,t)}{\partial t} = (\beta s(x,t) - \gamma) i(x,t) + D \frac{\partial^2 i(x,t)}{\partial x^2} \tag{3.43}$$

The resulting equation is similar to the well-known Fisher-Kolmogoroff equation:

$$\frac{\partial u}{\partial t} = f(u) + D \frac{\partial^2 u}{\partial x^2} \tag{3.44}$$

which gives for the wave speed $v = 2[f'(u)D]^{1/2}$, so in our case it becomes:

$$v = 2[(\beta s(t=0) + \gamma) D]^{1/2} \tag{3.45}$$

where $s(t=0)$ is the initial density of susceptible foxes. $s(t=0)$ can suggest the number of foxes that has to be targeted in vaccination or culling campaign to stop the wave, while D can give the area that should be managed [152].

3.3.2 Metapopulation model

Another useful framework for spatial transmission modeling is the one where reactions are integrated in a structured system that include explicitly spatial heterogeneities and mobility. Such framework was firstly developed in ecology and it is named *metapopulation model* [127–130]. It relies on the basic assumption that the system under study is characterized by a highly fragmented environment in which the population is structured and localized in relatively isolated subpopulation or *patches* connected by some degree of mobility [172]. Each subpopulation represents a single well-defined social or ecological entity such as a community, a pack, a herd, a refugee, a habitat, a village, a city, etc. that depends on the system under study.

The metapopulation model has multiple levels (Figure 3.5). At the microscopic level, each subpopulation i is composed by N_i individuals that follow the compartmental model dynamics: they are homogeneously mixed and they are divided into classes denoting their health status (Section 3.2). The total population is given by $N = \sum_i N_i$. At the macroscopic level the metapopulation model has a network structure (Figure 3.5) where each subpopulation is a node and each node i is connected to other k_i nodes according to his degree resulting in a network with degree distribution $P(k)$ and distribution of moments $\langle k^\alpha \rangle = \sum_k k^\alpha P(k)$. The interaction among different subpopulations is the result of the individual movements from one subpopulation to the others.

There are two different descriptions used to model the interaction given by mobility: the first is when the effective coupling is expressed as a force of infection generated by the infectious individuals in subpopulation i on the individuals of the subpopulation j [162, 186–189]; the second, which is the more realistic one, is when the interaction is given through a mechanistic approach which includes the detailed rate of movements obtained from empirical data or from mobility models [177, 178].

In the characterization of the diffusion process, the typical assumption commonly made is that in each time step the movement of individuals is given according to the matrix determined by the elements p_{ij}. This matrix expresses the probability that an individual travels from subpopulation i to subpopulation j. If w_{ij} is the number of travelers among the two subpopulations i and j, then:

$$p_{ij} \sim \frac{w_{ij}}{N_i}. \tag{3.46}$$

Such assumption has a Markovian character because it does not imply any memory of the individual movements. The individuals are not labeled according to their origin and at each time step the same traveling probability is applied to each member of the subpopulation. In the case of large metapopulation systems with a high level of heterogeneity the analytical description of the metapopulation model in terms of specific features of each single subpopulation is extremely complicate.

Let us now consider the metapopulation approach to model the disease spread in animals. In general, for animal populations the circulation of a pathogen is due to the migration or permanent movement of individuals. There are multiple ways to model that behavior, the simplest is to let animals move randomly among subpopulations [190–192], although assumptions based on data [118] or known dispersal behavior of specific species leading to different dynamics [193–195] are more appropriate. The general formulation of the metapopulation approach for a SEIR infectious dynamics is then:

$$\begin{aligned}
\frac{dS_i(t)}{dt} &= b_i N_i(t) - \beta_i \frac{S_i(t) I_i(t)}{N_i(t)} - \mu_i S_i(t) + \sum_j p_{ij} S_j(t) - \sum_j p_{ji} S_i(t) \\
\frac{dE_i(t)}{dt} &= \beta_i \frac{S_i(t) I_i(t)}{N_i(t)} - (\sigma_i + \mu_i) E_i(t) + \sum_j p_{ij} E_j(t) - \sum_j p_{ji} E_i(t) \\
\frac{dI_i(t)}{dt} &= \sigma_i E_i(t) - (\gamma_i + \mu_i) I_i(t) + \sum_j p_{ij} I_j(t) - \sum_j p_{ji} I_i(t) \\
\frac{dR_i(t)}{dt} &= \gamma_i I_i(t) - \mu_i R_i(t) + \sum_j p_{ij} R_j(t) - \sum_j p_{ji} R_i(t)
\end{aligned} \tag{3.47}$$

where the subscript i defines parameters and variables that are particular to subpopulation i, p_{ij} is the rate at which hosts move to subpopulation i from j and therefore captures both emigration and immigration.

Transition	Type	Rate
$S_j \to E_j$	Contagion	λ_j
$E_j \to I_j$	Spontaneous	σ_j
$I_j \to R_j$	"	γ_j
S_j, E_j, I_j, R_j to death	"	μ

TABLE 3.2: Transitions between compartments and their rates.

3.3.3 Stochastic and discrete integration of the disease dynamics

In this section I describe, using a stochastic and discrete approach, how I implement the infectious dynamics (Subsection 3.2.3) within each subpopulation of the metapopulation framework. Even if the infectious dynamics considered here is a general case, modifications of this classic susceptible–exposed–infected–recovered paradigm follow the same description. The force of infection λ_j is determined by interactions with infectious either from the same subpopulation j or from another connected subpopulation. The transitions described and the corresponding rates are summarized in Table 3.2. In each subpopulation the variation of the number of individuals in the compartment m (where m can be S, E, I or R) per time step is given by:

$$X_j^m(t + \Delta t) - X_j^m(t) = \Delta X_j^m. \tag{3.48}$$

In the right part of the equation, the term ΔX_j^m represents the variation given by the compartmental model dynamics.
To introduce the stochastic and discrete integration of the disease dynamics, I define an operator that act on the compartment m, which include all the possible transitions out of that compartment in the time interval Δt. The elements $\mathcal{D}_j(m, n)$ of this operator are random variables extracted from a multinomial distribution that determines the number of transitions in Δt from compartment $m \to n$.
To obtain the total variation ΔX_j^m in the time interval of the compartment m:

$$\Delta X_j^m = \sum_n -\mathcal{D}_j(m, n) + \mathcal{D}_j(n, m) \tag{3.49}$$

where the sum is on all the random variables $\mathcal{D}_j(m, n)$.
Here I discuss a concrete example of this formulation, the evolution of the susceptible compartment S_j. All possible transitions from this compartment are: to the exposed, and to the natural death given by demography.
The random variables for these transitions are extracted from the multinomial distribution:

$$Pr^{Multin}(S_j, P_{S_j \to E_j}, P_{S_j \to \text{death}}) \tag{3.50}$$

with the transition probabilities:

- $P_{S_j \to E_j} = \lambda_j \Delta t$
- $P_{S_j \to \text{death}} = -\mu \Delta t$

These two transitions cause a reduction of the size of the compartment S_j. On the other hand the increase is given by the birth of new susceptible, which is a random number extracted by a binomial distribution:

$$Pr^{Bin}(S_j, P_{\text{birth} \to S_j}) \tag{3.51}$$

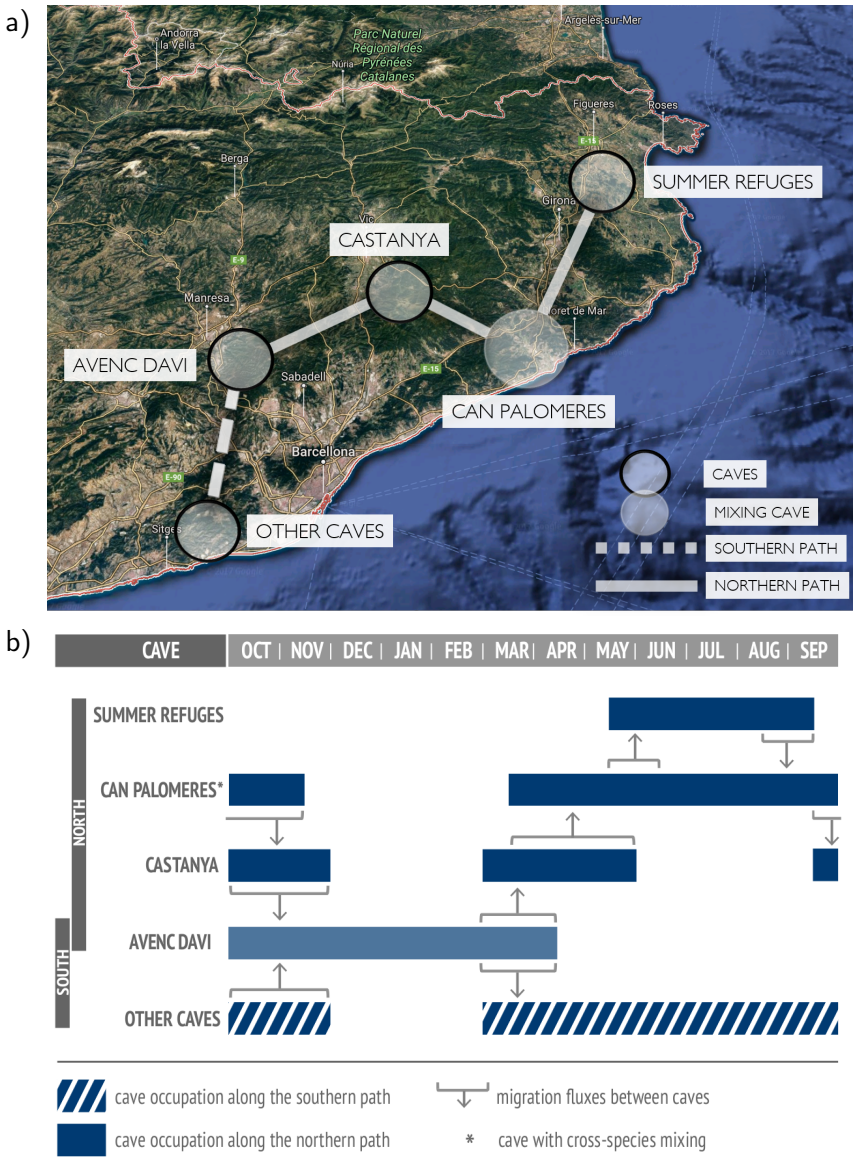

FIGURE 3.6: a) Geographical diagram of the roosting caves (circles) along the migratory path (links) of *M. schreibersii* in the region of Catalunya. Can Palomeres (white border) is the cave where cross-species mixing may occur. b) Temporal representation of the annual seasonal migration of *M. schreibersii*. Cave occupation is represented with filled rectangles (northern route) and striped ones (southern route).

with probability $P_{\text{birth}\to S_j} = b\Delta t$. After extracting these numbers from the corresponding distributions it is possible to compute the stochastic variation of the population size of the compartment S_j:

$$\Delta S_j(t) = S_j(t+1) - S_j(t) = -[\mathcal{D}_j(S_j, E_j) + \mathcal{D}_j(S_j, \text{death})] + \mathcal{D}_j(\text{birth}, S_j) \quad (3.52)$$

Origin cave	Destination cave	Period	Δt (days)
Avenc Davì	Castanya	1^{st} March - 16^{th} April	46
Avenc Davì	Other caves	1^{st} March - 16^{th} April	46
Castanya	Can Palomeres	15^{th} March - 1^{st} June	78
Can Palomeres	Summer refugee	15^{th} May - 15^{th} June	31
Summer refugee	Can Palomeres	10^{th} August - 15^{th} September	36
Can Palomeres	Castanya	15^{th} September - 15^{th} November	61
Castanya	Avenc Davì	1^{st} October - 30^{th} November	60
Other caves	Avenc Davì	1^{st} October - 30^{th} November	60

TABLE 3.3: Migration estimates for *Miniopterus schreibersii*.

Sampling date	Population
Dec 2008	16 150
Dec 2009	18 050
Dec 2010	17 100
Dec 2011	17 100
Dec 2012	17 100
Dec 2013	15 200
Dec 2014	17 100
Dec 2015	18 050
Dec 2016	17 100

TABLE 3.4: Average population estimates for *Miniopterus schreibersii* in Avenc Davì.

Sampling date	Population
Dec 2009	537
Dec 2010	577
Dec 2011	460
Dec 2012	441
Dec 2013	528
Dec 2014	520

TABLE 3.5: Average population estimates for *Myotis myotis* in Can Palomeres.

3.3.4 Metapopulation structure starting from field data: EBLV-1 infection in non-synanthropic bats populations

In this part I report original results of the work where we studied the endemicity of European Bat Lyssavirus subtype 1 (EBLV-1) in two non-synanthropic bats, *Myotis myotis* and *Miniopterus schreibersii*, in Catalonia (North-East of Spain). *M. myotis* live as a single colony of few hundred individuals in a cave called Can Palomeres (Figure 3.6 panel a), while *M. schreibersii* is a regional migratory bat species that follows a complex annual migration in a five caves system (Figure 3.6 panels a and b). The two species share the same habitat in Can Palomeres during summer months.
Here I describe how a metapopulation structure for the migratory *M. schreibersii* bat species can be built starting from population and migration data.

Data description

Empirical data provides population estimates for both bat species and migration estimates for *M. schreibersii*. Seasonal movements estimates for *M. schreibersii* (Table 3.3) were based on banding and recovery of individuals. Bats were captured inside the roosts with long-handled butterfly nets during the day or with mist nets at sunset, when they emerged to forage, if access to the roost interior was not possible [196, 197]. Individual bats were banded with a uniquely coded alloy ring on the forearm. The colony size of the *M. schreibersii* (Table 3.4) was determined in Avenc Davì in December (hibernation period) in order to avoid underestimations that can be given by the spring migratory displacements. For each sample, the colony size was computed from the estimated area in m^2 occupied by the bats and the average colony density obtained through processing photos of the colony. The colony size of *M. myotis* was estimated similarly from observations in Can Palomeres (Table 3.5).

Metapopulation structure

At the microscopic level, the disease dynamics is implemented considering the discrete and stochastic approach explained in Section 3.3.3, choosing the compartmental model which is appropriate for the host-pathogen interaction considered.
The migratory path defines the directed connections of *M. schreibersii* migration among patches, as schematically represented in the map of Figure 3.6. We indicate with $\phi^{p\to p'}(t)$ the migration rate from cave p to cave p' on day t during the year, with annual seasonality. We assume that migration rate is homogeneous in time and simply defined by the total duration of migration $\Delta t^{p\to p'}$ given by empirical estimates (Figure 1b, Table S1), i.e. $\phi^{p\to p'}(t) = 1/\Delta t^{p\to p'}$. The migration is implemented through a stochastic approach informed by the data in Table 3.3 (Figure 3.6 panel b).
The number of *M. schreibersii* in the compartment X^p traveling from patch p to patch p' in the discrete time interval is an integer random variable extracted from a multinomial distribution. As a concrete example let us consider the spring migration out from Avenc Davì of bats in the X^{AD} compartment. The two possible destinations are the compartment X^C in Castanya and the compartment X^{OC} in Other caves. The random variables are extracted from:

$$Pr^{Multin}(X^{AD}, P_{X^{AD}\to X^C}, P_{X^{AD}\to X^{OC}}) \tag{3.53}$$

with migration probabilities:

- $P_{X^{AD}\to X^C} = \eta^{AD\to C}\phi^{AD\to C}\Delta t$
- $P_{X^{AD}\to X^{OC}} = (1-\eta^{AD\to C})\phi^{AD\to OC}\Delta t$

where X^{AD} is the number of *M. schreibersii* in Avenc Davì in the compartment X at time t; $\phi^{AD\to C}$ and $\phi^{AD\to OC}$ are the migration rates from Avenc Davì to Castanya and from Avenc Davì to Other caves, respectively; $\eta^{AD\to C}$ and $(1-\eta^{AD\to C})$ are the proportions of bats that migrate to the two destinations, respectively. After extracting these numbers from the corresponding distributions, we can calculate the change in the X^{AD} population.

3.3.5 Metapopulation structure without field data: RABV infection domestic dogs

In this part I present an original work where we analyze the persistence of RABV virus in domestic dogs population of Central African Republic (CAR). As showed in the previous

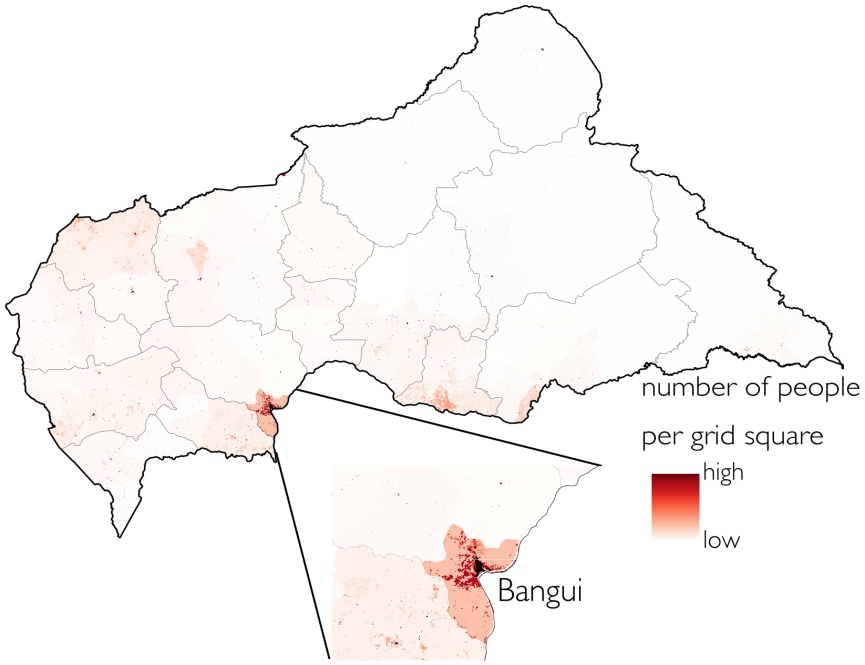

FIGURE 3.7: WorldPop CAR. 2015 estimates of numbers of people per grid square of Central African Republic, with national totals adjusted to match UN population division estimates. Resolution of 0.000833333 decimal degrees (approx 100m at the equator).

example, to build a metapopulation network we need the distribution of host population in well-defined subpopulations and the movement pattern that couple these subpopulations. Unfortunately, there is not availability of such kind of data for CAR so we used a different approach.

Population

Domestic dogs are naturally tied to human population therefore we infer dog densities starting from human demographics and human geography [1, 102]. To capture the highly fragmented and complex landscape given by the distribution of dogs communities in CAR we employed as a proxy a high resolution dataset on human population called *WordPop* [198]. WorldPop contains estimates for the geographic distribution of the population in terms of population density and settlement patterns for 126 countries in Africa, America, and Asia [198]. Fifty African countries, including Central African Republic, are represented in the database. For our analyses, we used the alpha version of the WorldPop data set for CAR; this version contains 2015 estimates of the number of people/100 m^2. The dataset is a raster image, and it is composed by a set of discrete uniform cells (pixels) that contain an estimation of the human population and that are based on a gridded surface, where each pixel on the grid represents a defined square area in a specific geographic location.The WorldPop database was constructed by using satellite data on surface imagery, specifically imagery on land cover patterns, to map the settlement patterns. The surface imagery data were used to reallocate the population census data to settlements; settlements may vary from cities to small rural homesteads. Satellite data were taken from NASA's Landsat spacecraft, which uses Enhanced Thematic Mapper imagery to monitor Earth's land cover. The details of the methodologies used by *Linard et al.* [199] to construct the database are described on the WorldPop website [198].

Resolution (m^2)	Minimum population per m^2	#patches	Human population in Bangui (734 350 in 2012)
100	20	196	677 107
	40	162	677 107
	60	95	677 107
400	20	430	685 820
	40	189	683 621
	60	132	681 190
800	20	335	779 749
	40	137	765 098
	60	91	763 610
1000	20	283	797 933
	40	114	765 562
	60	83	760 798

TABLE 3.6: Number of patches and Bangui's human population size obtained varying the resolution of the raster matrix and the minimum number of the minimum population per m^2. In red the parameters' combination selected to rearrange the raster matrix.

The CAR dataset comprises 165 076 538 cells of which 72 939 427 are populated. To design the metapopulation model we aggregate data from the raster dataset to satisfy two conditions:

- neighbouring inhabited cells are merged together in a single patch that aim to represent human settlements;
- Bangui, the capital city of the country has to be described as a single subpopulation in the metapopulation network for epidemiological reasons [107].

To fulfill those requirements firstly we adjusted the raster dataset varying the resolution in a interval between 100 m^2 to 1 km^2 hierarchically aggregating the pixel cells. Subsequently, we filtered out the scarcely populated cells considering a threshold with respect to the minimum population size in each 100 m^2. In order to build communities all remaining cells that have at least one side in common are merged together. The resulting scenario is an ensemble of geolocalized subpopulations of human communities with a certain size, spatial extension and density.
To select the optimum combination of resolution and minimum threshold we considered for which values of these parameters: the number of subpopulations remain stable (Figure 3.8) and the population size in Bangui is similar to the official estimation (734 350 inhabitants in 2012) (Table 3.6). In the evaluation process we preferred a higher resolution and a lower threshold conditions, thus we choose as optimal pixel size 800 m^2 and a threshold for the minimum population size equal to 40 inhabitants per 100 m^2 (Table 3.6 (shaded red line)). Finally, considering the mean human to dog ratio for African

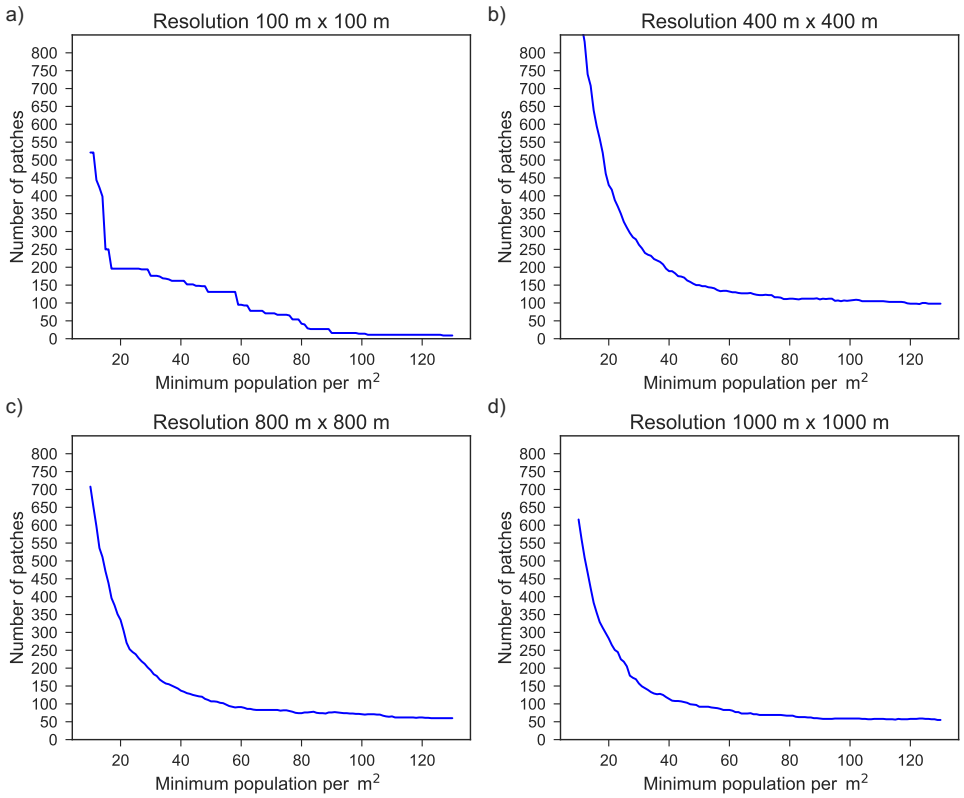

FIGURE 3.8: Subpopulations. The variation of the number of subpopulations in the metapopulation framework in function of the resolution considered and of the threshold on the minimum number of human population per m^2.

countries [1], we estimated the domestic dogs population considering two possible kinds of environments: *urban patches*, with more than 1 000 individuals per kilometers squared and with a human to dog ratio equal to 21.20; *rural patches*, with less than 1 000 individuals per kilometers squared and a human to dog ratio equal to 7.40. The total domestic dogs population estimated for the whole Central African Republic is 76 992 dogs divided in 137 subpopulations, of which 69 250 live in urban patches and the remaining 7 742 live in rural patches. Bangui, the capital city of the country, hosts 36 089 dogs which is close to half of the total population. The major concentration of subpopulations is located on the West and Central side of the country since in the east part are located three national parks named *Bamingui-Bangoran*, *Saint-Floris* and *Zemongo*. The area around Bangui is characterized by a high density of both urban and rural settlements. In Figure 3.9 it is shown: in panel a, the geographic distribution of the dogs subpopulations within the Central African Republic; in panel b, the distribution of the size the the dogs subpopulations.

Movements

The other crucial input for the metapopulation model is the coupling among subpopulations, which corresponds in this case to canine movements within the country. Unfortunately for domestic dog movements no data is available for Central African Republic. In a recent work made by *Talbi et al.* [113], they used a probabilistic approach [200] to determine the spatial and temporal dynamics of dog RABV transmission from a large-scale gene sequence study. Combining spatial epidemiology and a Bayesian phylogeographic

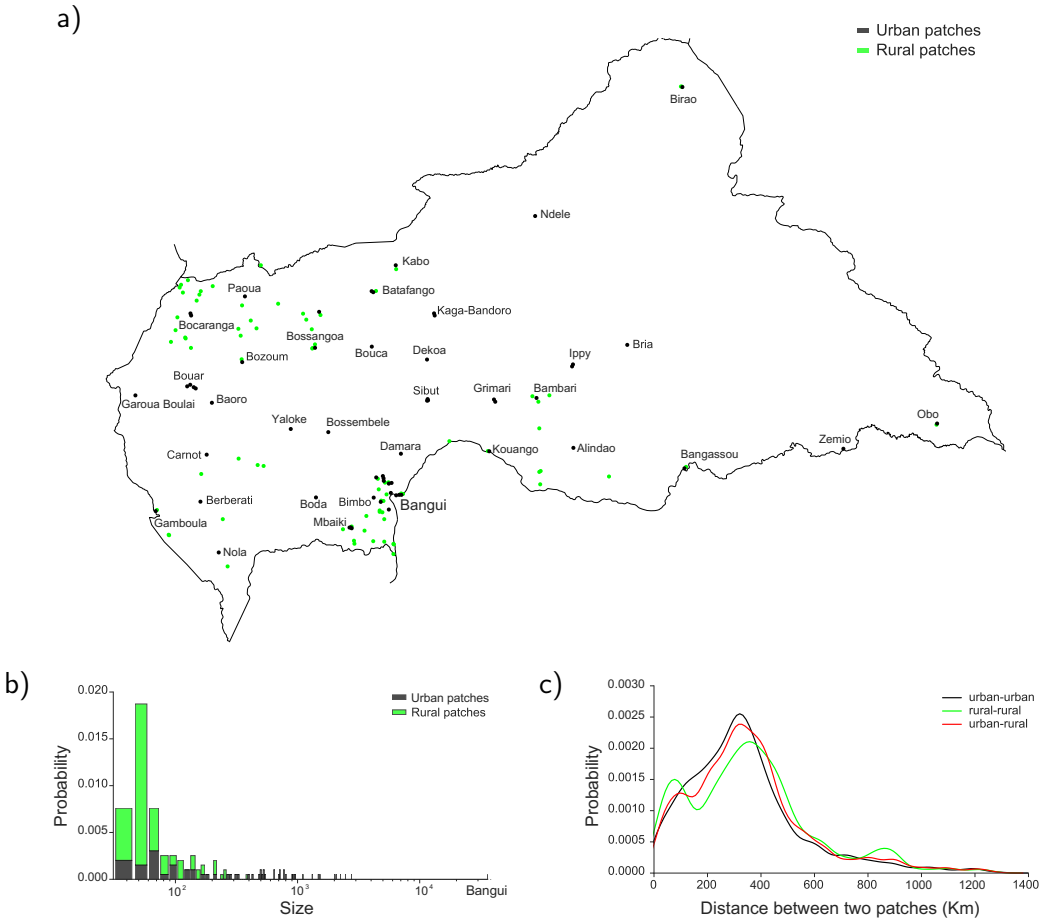

FIGURE 3.9: a) Geographical distribution of the obtained subpopulations divided in: rural (green), if the number of humans per squared kilometer is less than 1 000; urban (black), if the number of humans per squared kilometer is more than 1 000. b) Distribution of the estimated number of domestic dogs in rural (green) and urban (black) patches. c) Distribution of the distances among patches: in black if the patches are both urban; in green if the patches are both rural; in red between urban and rural patches.

approach, they tested multiples diffusion predictor to determine which of them can predict dog RABV dissemination in Algeria and Morocco. Marginal likelihood estimates of the model fit of all the different predictors considered suggests that RABV spatial dynamics are best described by road distances and geographical (Euclidean) distances provided only a marginally lower fit.

For sake of simplicity, as already done in [194], we use the Euclidean distance model to evaluate the number of migrating dogs between patch i and patch j, defined as:

$$w_{ij} = \frac{C}{d_{ij}}. \tag{3.54}$$

Where C is a normalization factor that fix the maximum number of dogs that can daily escape from each subpopulation to 1% of the patch population, and d_{ij} is the great circle distance between i and j, defined as the shortest distance between the two centroids on a surface of a sphere.

The distribution of Euclidean distances among urban-urban, rural-rural and urban-rural

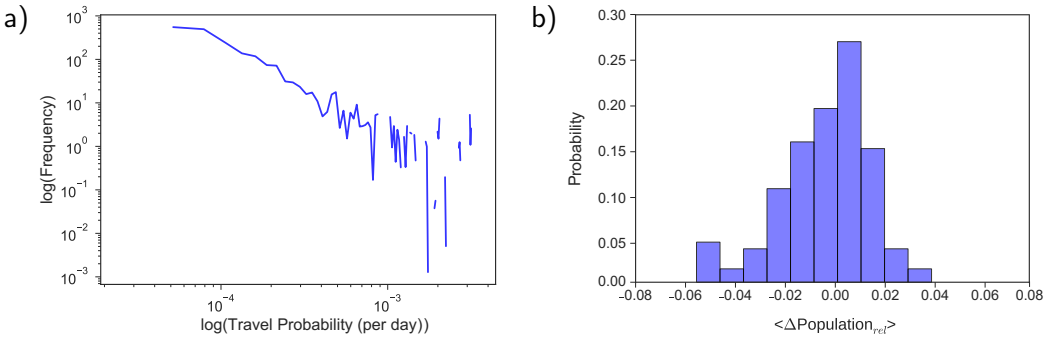

FIGURE 3.10: Mobility model. a) The distribution of the daily travel probability obtained by the model represented by equation (3.54). Subpopulation stability. b) The distribution of the average relative variation of the subpopulations size considering the dynamics give by the migration model after 10^3 time steps.

subpopulations is shown in Figure 3.9. The average distances, in the three cases, are respectively 334, 362 and 352 km and the shape of the three distributions is similar. The rural-rural distance distribution, however, is characterized also by an additional short distance peak around 75 km which represents the high concentration of rural patches around the Bangui area and in the north west side of the country. The distribution of the daily travel probability for each subpopulation is heterogeneous and the population size of each patches is maintained in equilibrium through the migration dynamics (Figure 3.10).

Metapopulation structure

At the microscopic level, the disease dynamics is implemented considering the discrete and stochastic approach showed in the Section 3.3.3, choosing the compartmental model which is appropriate for the host-pathogen interaction considered.
The dogs movements were modeled considering the equation (3.54), with an integration time scale of $\Delta t = 1$ day and with symmetric travels, $w_{ij} = w_{ji}$. The number dogs in the compartment X_i that travels between the two patches is an integer random variable extracted from a multinomial distribution. As a concrete example let us consider the migration out from Bangui in the X^{Bangui} compartment. The possible destinations are all the other 136 patches of the network with a probability that decline with the Euclidean distance. The random variables are extracted from:

$$Pr^{Multin}(X^{\text{Bangui}}, P_{X^{\text{Bangui}} \to X^{\text{Patch}_1}}, ..., P_{X_{\text{Bangui}} \to X^{\text{Patch}_{136}}}) \tag{3.55}$$

with migration probabilities:

$$P_{X^{\text{Bangui}} \to X^{\text{Patch}_j}} = \frac{w_{\text{Bangui},j}}{N_{\text{Bangui}}} \Delta t \tag{3.56}$$

where: X^{Bangui} is the number of dogs in Bangui in the X compartment at time t; N_{Bangui} is the total number of dogs in Bangui at time t. After extracting these numbers from the corresponding distributions, we can calculate the change in the population.

3.4 Conclusions

In this Chapter I presented the mathematical and computational modeling background of my research. In Section 3.1 I introduced a brief history of mathematical epidemiology applied on rabies with special attention the public health motivations. In Section 3.2 I introduced some basics of mathematical theory of infectious diseases, with special attention to compartmental models which will be extensively used in the rest of the thesis. In particular I focused on the SEIR model because it is commonly used to model rabies infectious dynamics. In Section 3.2.3 I considered the different compartmental model used in this work to analyze bats infection dynamics. Subsequently in Section 3.2.3, I illustrate a SEIR model for dog rabies infection. Than in the same framework I introduced realistic distribution of the incubation and the infectious periods that permit the inclusion of heterogeneous incubation and infection periods that are peculiar in dog rabies. In Section 3.3 I illustrated the importance of space in epidemiology in particular for modeling a direct contact host to host disease like rabies. In Section 3.3.1, I introduced the role of the diffusion in space and in Section 3.3.2 I integrate the Reaction-Diffusion approach into a metapopulation structure that is particularly indicated to model the spread of rabies in a heterogeneous population structure. From here I continue the presentation of my research following two main directions. One one hand I apply the described modeling framework to understand the persistence of European Bat Lyssavirus-1 in two bats species in Catalunya (Spain) using field data on population and on migration (Chapter 4). On the other hand, in Chapter 5 I present a novel approach to analyze the persistence of RABV virus in domestic dogs communities in Central African Republic. In particular I study the role and interplay between the heterogeneous incubation period, the human-mediated dog movements and the spatial fragmentation of the domestic dog population in that country.

4 EUROPEAN BAT LYSSAVIRUS-1 PERSISTENCE IN CATALUNIA

4.1 Abstract

Lyssaviruses are pathogens of bat origin of considerable zoonotic concern. Knowledge about persistence remains incomplete, mainly due to the complex interplay of bats ecology and immune response to infection. Leveraging an extensive ecological field survey characterizing *Myotis myotis* and *Miniopterus schreibersii* bat species in the Catalonia region, we develop a data-driven mathematical model to identify the mechanisms of persistence of *European Bat Lyssavirus* subtypes 1 (EBLV-1) in the region. We consider different disease progressions accounting for lethal infection, immunity waning, along with potential cross-species transmission when the two populations share the same refuge. Comparison with serological data suggests that EBLV-1 circulation is ensured by the spatial migration of *M. schreibersii* mixing with *M. myotis*, offering novel numerical evidence to support non-lethal infection in bats with a transient immunity of few months. Shelters hosting multi-species colonies are critical for virus exchange, suggesting they should be targeted for public health surveillance.

4.2 Introduction

Bats are reservoir hosts of numerous emerging viruses that can cross the species barrier to infect other wild and domestic animals, and also humans [201, 202]. These include lyssaviruses, the agents of rabies, that probably originated in bats and progressively diverged from a common ancestor to infect many recipient host species. To date, bats were found to serve as reservoirs of 15 of the 17 lyssavirus species currently known [14, 203]. *European Bat Lyssavirus* subtypes 1 (EBLV-1) has been reported in Europe for the first time in 1954 [9], and is the lyssavirus species more largely found in the continent (see Section 2.5.1) [204]. It is widely distributed throughout Europe (including Germany, the Netherlands, Denmark, France, Spain) [9, 10, 57, 66, 204, 205], and infects mainly insectivorous bat species [206]. EBLV-1 virus has the potential to cross the species barrier and infect other domestic and wild mammals [9–11], although such events seem relatively rare. Infections of humans by EBLV-1 have also been reported [205], including fatal cases [203, 207]. The mechanisms for lyssaviruses persistence in bats are still undefined, mainly because of paucity of knowledge of the phenomenology and data scarcity. Disease progression following lyssavirus infections in bats is largely debated and controversial (see Section 2.4 and Section 2.5). With the isolation of live virus being rare and the bat

response mechanisms to infection remaining largely unknown, discordance between different studies suggests that disease progression may depend on bat species and rabies virus variant. Finally, even when disease progression is partially known, data is often missing to parameterize it so that important determinants for transmission dynamics cannot be fully defined (see Section 2.5.1).
Host ecology may also drive the mechanisms underlying virus persistence in bats population (see Section 2.5.1) but only few modeling studies have explored this possibility with lyssaviruses. For *Eptesicus fuscus* in North America, persistence of bats rabies virus was found to be likely associated with bats dispersal and interaction between colonies [76]. Roost ecology, colony size and bat species richness were found to be associated with an increased EBLV-1 seroprevalence in Spain [43, 61]. A high number of species might not only increase the rates of contact between bat populations, but could also facilitate virus dispersal. Pathogen entry and re-entry through the higher mobility of individuals could indeed act as a strong spatial disseminating factor, as discussed for many bat species harboring zoonotic viruses [78, 117, 208–210]. This is especially relevant when bats exhibit migratory seasonal behavior [118, 211]. Finally, the dependence of host contacts rates on population size [212] is still a matter of debate, with previous modeling works adopting either frequency-dependent [77, 118] or density-dependent [76] transmission rates.
Considering both disease progression and ecological factors in the same theoretical framework is therefore crucial to comprehensively understand the mechanisms for lyssaviruses spread and persistence among colonies and improve their control to limit the risk of cross-species exposure. Our study aims at characterizing the epidemiological, immunological, and ecological context responsible for EBLV-1 persistence observed in the *M. schreibersii* and *M. myotis* non synanthropic insectivorous bat species in the system of caves in Catalonia (North-East of Spain) already presented in Section 3.3.4. Evidence of sustained EBLV-1 infection is found in both species at different times of the year [43, 213]. Through a mathematical modeling framework accounting for disease progression dynamics and bats ecology, and parameterized with empirical data on bats population and migration, we explore several hypotheses regarding unknown epidemiological, immunological and ecological aspects to identify the mechanisms responsible for EBLV-1 persistence in the two species. Specifically, we test three different disease progression models, including or not lethal infection and temporary immunity, to shed light on the unknown rabies biology in these bat species. In absence of estimates, we explore range of values to quantify virus transmissibility, its seasonal variation, and immunity periods and evaluate their impact on the transmission dynamics. In addition, we assess the role of cross-species mixing in Can Palomeres cave and of spatial dispersal through migration to explore which ecological factors have a prominent role in rabies persistence. Finally, we compare model predictions with collected EBLV-1 serological data for both species to identify the epidemiological and ecological contexts most consistent with reality. A sensitivity analysis on unknown parameters is also performed to assess the robustness of our modeling results to missing data.

4.3 Materials and Methods

4.3.1 Data

Seasonal movements were obtained for *M. schreibersii* through banding and recovery [196] as showed in Section 3.3.4 allowing us to trace the migration flows from cave to cave during the annual cycle in the North-East of Spain (Figure 3.6 panel a). A total of five caves are visited during the migration. Following hibernation in Avenc Davì, *M.*

Sampling date	Cave	Species	Sampled	Positive	Prevalence [95%CI]
23/03/10	Avenc Davì	Ms	29	3	0.10 [0.04-0.26]
24/03/11	Avenc Davì	Ms	31	4	0.13 [0.05-0.29]
28/03/12	Avenc Davì	Ms	30	3	0.10 [0.03-0.26]
28/03/13	Avenc Davì	Ms	31	0	0.00 [0.00-0.11]
20/03/14	Avenc Davì	Ms	29	0	0.00 [0.00-0.12]
22/07/10	Can Palomeres	Ms	24	13	0.54 [0.35-0.72]
09/06/11	Can Palomeres	Ms	26	0	0.00 [0.00-0.13]
16/05/12	Can Palomeres	Ms	30	14	0.47 [0.30-0.64]
03/07/13	Can Palomeres	Ms	22	2	0.09 [0.03-0.28]
05/06/14	Can Palomeres	Ms	27	4	0.15 [0.06-0.32]
22/07/10	Can Palomeres	Mm	6	3	0.50 [0.19-0.81]
09/06/11	Can Palomeres	Mm	4	1	0.25 [0.01-0.70]
16/05/12	Can Palomeres	Mm	5	3	0.60 [0.23-0.88]
03/07/13	Can Palomeres	Mm	9	3	0.33 [0.12-0.65]
05/06/14	Can Palomeres	Mm	1	0	0.00 [0.00-0.95]

TABLE 4.1: Number of bats sampled and tested positive to EBLV-1 serology, prevalence and 95%CI, in Avenc Davi and Can Palomeres, for both bats species. Where Ms stands for *M. schreibersii* and Mm stands for *M. myotis*

schreibersii population splits between Northern and Southern migration routes from March to mid-April (Figure 3.6 panel b). On the Northern route, *M. schreibersii* reach Castanya for mating when the hibernation is over, then they progressively start migrating to Can Palomeres for mating and birthing (mid-March to end-May). An important fraction of *M. schreibersii* follow their migration further North to other refuges composed of breeding or summer colonies ("Summer refuges" in Figure 3.6 panel a), where they stay approximately from mid-May to mid-September. During the same period, the remaining bats stay instead in Can Palomeres and share the refuge with *M. myotis*. Once summer is over, the entire *M. schreibersii* colony returns to Avenc Davì following the Northern route in the opposite direction: from Summer refuges to Can Palomeres, to Castanya, to Avenc Daví for hibernation to conclude the annual migration. Bats following the Southern route from Avenc Daví reach a set of caves near the coast ("Other caves" in Figure 3.6 panel a) from March to the end of November and return to Avenc Daví for hibernation, reuniting with the bats following the northern route. The detailed list of migration flows is reported in Section 3.3.4 Table 3.3.
Total population sizes of the two species are estimated to be 16 994 individuals (95% confidence interval CI [16 451-17 538]) for *M. schreibersii* (data from Avenc Daví, Table 3.4), and 525 individuals (95% CI [492-559]) for *M. myotis* (data from Can Palomeres, Table 3.5). EBLV-1 serological data were collected once a year, in Avenc Davì (for *M. schreibersii*) and Can Palomeres (for both species), between 2010 and 2014 (Table 4.1). From the 279 *M. schreibersii* and 25 *M. myotis* sampled, 15.41% (95% CI [11.49-20.31], n=43) and 40% (95% CI [21.81-61.11], n=10) were EBLV-1 seropositive, respectively.

4.3.2 Model formulation

We develop a mathematical modeling framework based on a multi-species metapopulation model with five patches corresponding to the five caves encountered by *M. schreibersii* along the migration route, and couplings between patches corresponding to the migration flows described in the former paragraph. Since *M. myotis* bats constitute a single colony with rare and short-range movements [73], we model them as a single subpopulation.

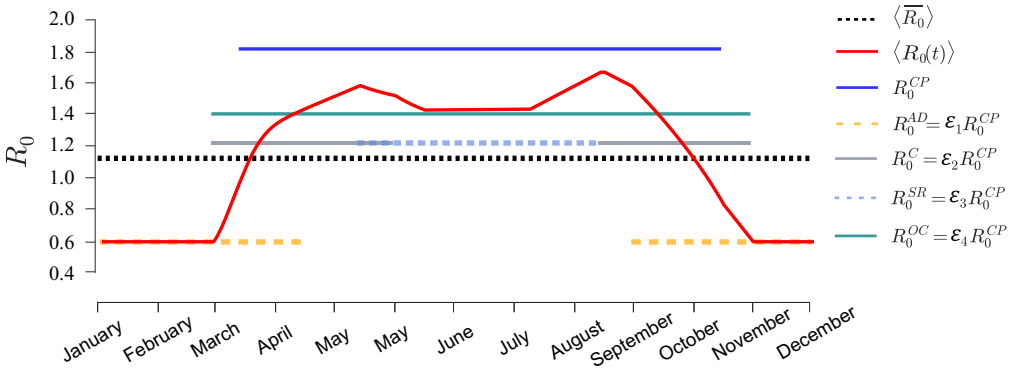

FIGURE 4.1: Reproductive numbers R_0^p of each patch p of the *M. schreibersii* migration over time. Parameter values are set to default (Table 4.4), and the reproductive number in Can Palomeres is set to $R_0^{CP} = 1.8$. The seasonal reproductive number of the metapopulation model, $\langle R_0(t) \rangle$ (red curve) and its yearly average $\langle \overline{R_0} \rangle$ (black dashed curve) are also shown.

The model, as showed in Section 3.3.4, is spatially explicit and based on a two-level dynamics: a local dynamics, representing the disease transmission in bat populations (*M. schreibersii* and *M. myotis*, single-species and cross-species infection dynamics) within each cave (patch of the metapopulation model) and modeled through a compartmental model with homogeneous mixing; and a migration dynamics, representing the spatial spread of EBLV-1 infection among caves occuring through the migration of infected hosts (*M. schreibersii*). Cave-specific transmission is considered to model the bats activities (Figure 4.1), as detailed in the following.

Single-species infection dynamics

To account for the different hypotheses existing on the biology of lyssavirus infection, we analyze three formulations of the EBLV-1 disease progression dynamics within the host, based on a susceptible-exposed-infected compartmental approach discussed in detail in Section 3.2.3. Model 1 was introduced by *George et al.* in 2011 [76] for bat rabies virus in *Eptesicus fuscus* species, an insectivorous bat species (Figure 4.2 panel a). It assumes that bats can experience nonlethal and lethal rabies virus infection, and tracks individuals in the following compartments: susceptible (S), exposed (E_I leading to an infectious state, E_R leading to an immune state), infectious (I, followed by death because of lethal infection), immune to the virus (R). Lethal infection occurs with probability ρ. To test the hypothesis on the existence of a temporary immunity following rabies disease progression in *M. schreibersii* and *M. myotis* [70, 71], we introduce model 2 as a variation of model 1 by adding loss of immunity with rate ω, while all other processes remain the same (Figure 4.2 panel b). In both model 1 and model 2, total population size is regulated by a carrying capacity K, as in [76]. The mathematical formulation of model 1 and model 2 are described in detail in Section 3.2.3 by the equations (3.31) and (3.32) respectively. Finally, to test the hypothesis of nonlethal infection [60, 73], we introduce model 3 as a SEIRS compartmental model, where bats do not die following infection but progress to an immune state (R) of average duration ω^{-1}, after which they become susceptible again (Figure 4.2 panel c). The mathematical formulation of model 3 is described in Section 3.2.3 equation (3.34).
In all three models bats die at a constant natural death rate μ. Births occur seasonally and

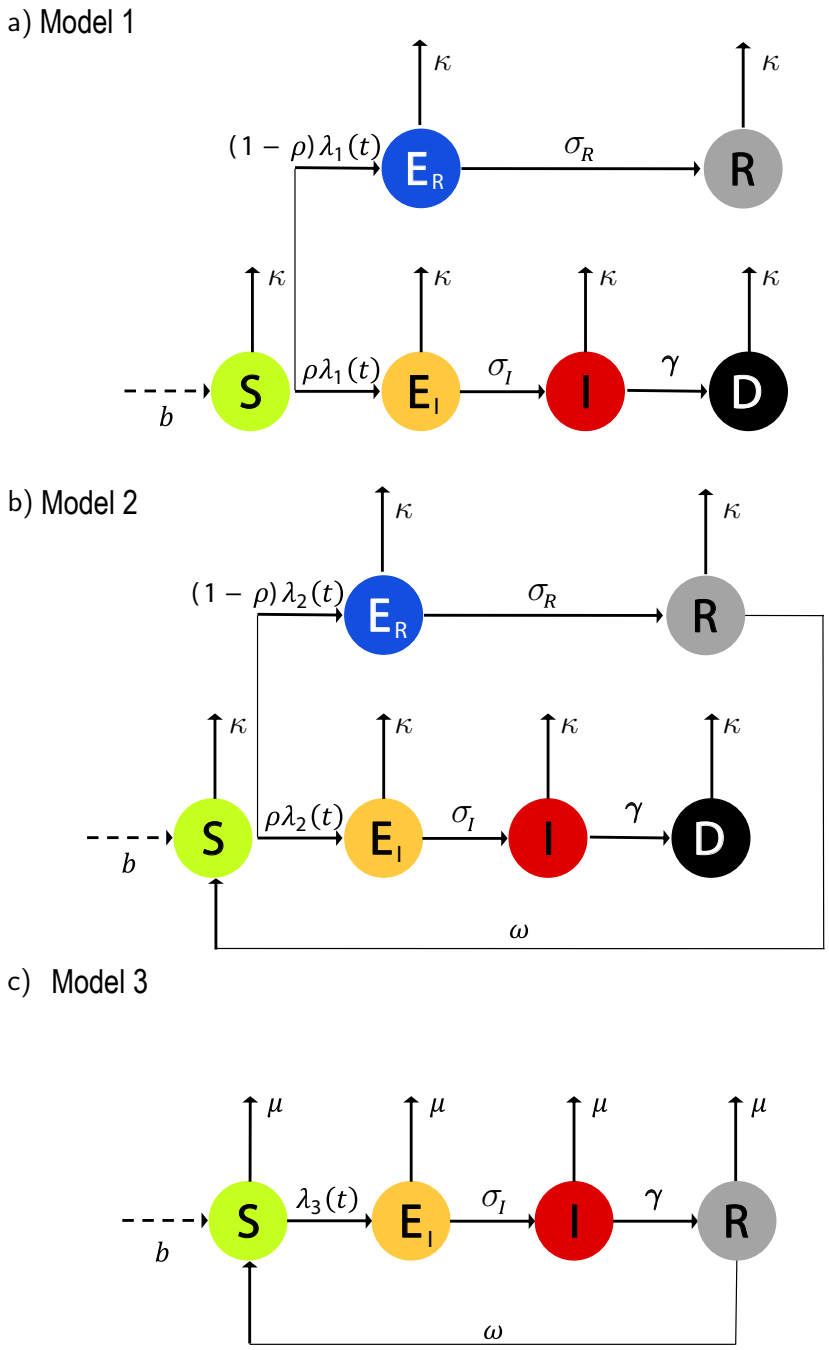

FIGURE 4.2: Compartmental models. a) Compartmental structure for model 1, including susceptible (S), lethally exposed (E_I), non-lethally exposed (E_R), infectious (I), recovered (R) and dead hosts (D). The model considers lethal infection to occur with probability ρ. b) As in a) for model 2, where waning of immunity with rate ω is also considered. c) Compartmental structure for model 3, where no infection-induced mortality is considered, and immunity wanes with rate ω.

are modeled through a uniform birth pulse during the birthing summer season (mid-May to mid-September) in Can Palomeres cave. The same models are applied to both bat species and consider frequency-dependent transmission (density-dependent transmission

is tested for sensitivity analysis).
Seasonality affects transmission intensity, as it varies upon the degree of bats activity in the specific seasonal conditions. We model the seasonal variation of transmission intensity as a function of time. For *M. schreibersii*, we consider a patch-dependent variation, as caves visited along the migration route are associated with specific bats activities. The reproductive number measures the average number of secondary cases that an infectious individual can generate during the infectious period [114]. The highest reproductive number was assumed in Can Palomeres, R_0^{CP} , where mating and birthing takes place, i.e. where the highest interaction between bats occurs, and for which a plausible range of values was explored in absence of prior estimates (see Model parameterization). Lacking estimates of bats interaction and associated transmissibility, we expressed the reproductive numbers in the other patches as linear functions of R_0^{CP} with scaling factors smaller than 1: Avenc Davì $R_0^{AD} = \varepsilon_1 R_0^{CP}$; Castanya $R_0^{C} = \varepsilon_2 R_0^{CP}$; Summer refuges $R_0^{SR} = \varepsilon_3 R_0^{CP}$; Other caves $R_0^{OC} = \varepsilon_4 R_0^{CP}$. We simplify the model by assuming $\varepsilon_2 = \varepsilon_3$, as Castanya and Summer refuges refer both to mating and breeding activities. We consider ε_4 to be the average of the scaling factors defined for Castanya, Can Palomeres and Summer refuges, i.e. we assume that the transmission intensity experienced by bats in the Southern migration route is equal to the one experienced in the Northern route, in the same period of the year. Finally, we assume that $\varepsilon_1 \leq \varepsilon_2$, as bats experience hibernation in Avenc Davì, corresponding to minimum degree of interaction.
To compare numerical results across different models and hypotheses, we consider two metapopulation summary measures for *M. schreibersii* species: (1) the time-dependent population-weighted seasonal reproductive number, defined at each day t as:

$$\langle R_0(t) \rangle = \frac{\sum_p R_0^p N^p(t)}{\sum_p N^p(t)} \tag{4.1}$$

where R_0^p represents the reproductive number of patch p, and $N^p(t)$ indicates the population of patch p at time t; (2) the average reproductive number of the metapopulation model, i.e. the yearly average value of $\langle R_0(t) \rangle$, $\langle \overline{R_0} \rangle = \frac{1}{365} \sum_t \langle R_0(t) \rangle$. The seasonal variation of transmission intensity in each cave for *M. schreibersii* is reported in Figure 4.1. For *M. myotis*, a seasonal variation of the transmissibility is also considered to account for hibernation in Winter months (low transmissibility, $R_0^{\text{low}} = \varepsilon_1 R_0^{CP}$, as for *M. schreibersii* in Avenc Davì), and for breeding and mating season during the rest of the year (high transmissibility, $R_0^{\text{high}} = R_0^{CP}$, as for *M. schreibersii* in Can Palomeres).

Cross-species infection dynamics

Cross-species transmission between *M. schreibersii* and *M. myotis* may occur in Can Palomeres only, for a limited period of time. We model it through a reduced transmissibility, $R_0^{\text{mix}} = \alpha R_0^{CP}$, with α between 0 and 1 in the hypothesis that cross-species interaction would be at most equal to same-species interaction. $\alpha = 0$ refers to non-mixing conditions. As illustrative example, here we show the differential equations for the

Sensitivity analysis	Modeling tests performed	Definition
SA1	Seasonal degrees of transmission ε_1 ,ε_2	ε_1 ,ε_2 in [0-1], $\varepsilon_1 \leq \varepsilon_2$
SA2	Cross-species mixing intensity α	in α in [0-1]
SA3	Average infectious period	2.5, 10 days
SA4	Ecological parameters from empirical estimates: population sizes, migration (starting, duration)	*M. schreibersii* size: [16,000-18,000] *M. myotis* size: [400-600] Starting date & migration events: default value $\pm\epsilon$ ϵ from Gaussian distribution (m = 0, std = 1 week)
SA5	Density-dependent transmission rates	Density-dependent transmission assumed for EBLV-1 dynamics in both species
SA6	Seasonal single population	No metapopulation structure, single population with seasonal transmission
SA7	No-seasonal metapopulation	Transmission is constant in time and space $\langle \overline{R_0} \rangle = \frac{1}{165} \sum_t \langle R_0 \rangle$
SA8	Numerical tests	Seeding numbers, caves, length of simulation time and number of stochastic runs

TABLE 4.2: Modeling tests performed for sensitivity analysis.

cross-species mixing between the species 1 and the species 2 for model 1:

$$\begin{aligned}
\frac{dS^{CP}(t)}{dt} &= bN^{CP} - \beta^{CP} S^{CP}\Big(\frac{I^{CP}(t)}{N^{CP}} + \alpha\frac{I^{CP}_{\text{spe}_2}(t)}{N^{CP}_{\text{spe}_2}}\Big) - \kappa S^{CP}(t) \\
\frac{dE^{CP}_R(t)}{dt} &= (1-\rho)\beta^{CP} S^{CP}\Big(\frac{I^{CP}(t)}{N^{CP}} + \alpha\frac{I^{CP}_{\text{spe}_2}(t)}{N^{CP}_{\text{spe}_2}}\Big) - (\sigma_R + \kappa)E^{CP}_R(t) \\
\frac{dE^{CP}_I(t)}{dt} &= \rho\beta^{CP} S^{CP}\Big(\frac{I^{CP}(t)}{N^{CP}} + \alpha\frac{I^{CP}_{\text{spe}_2}(t)}{N^{CP}_{\text{spe}_2}}\Big) - (\sigma_I + \kappa)E^{CP}(t) \\
\frac{dI^{CP}(t)}{dt} &= \sigma_I E^{CP}_I(t) - (\gamma + \kappa)I^{CP}(t) \\
\frac{dR^{CP}(t)}{dt} &= \sigma_R E^{CP}_R(t) - \kappa R^{CP}(t)
\end{aligned} \tag{4.2}$$

CP represent the Can Palomeres cave, where actually the two species may interact, $\kappa = \mu - (b-\mu)\frac{N^{CP}}{K}$ is the density dependent death rate, N^{CP} and $N^{CP}_{\text{spe}_2}$ are the population size of the two species in Can Palomeres. The cross-species interaction is given by the factor $\alpha\beta^{CP} S^{CP}\frac{I^{CP}_{\text{spe}_2}(t)}{N^{CP}_{\text{spe}_2}}$ where: $N^{CP}_{\text{spe}_2}$ is the total population of species 2, $I^{CP}_{\text{spe}_2}(t)$ indicate the number of infected of species 2 and α is the mixing intensity between the two species.

Migration dynamics

The migratory path defines the directed connections of *M. schreibersii* migration among the patches, as schematically represented in Figure 3.6. We indicate with $\phi^{p\to p'}(t)$ the migration rate from cave p to cave p' on day t during the year, with annual seasonality. We assume that migration rate is homogeneous in time and simply defined by the total duration of migration $\Delta t^{p\to p'}$ given by empirical estimates (see Figure 3.6 and Table 3.3).

4.3.3 Model parameterization

We model the *M. schreibersii* species to be composed of 17 000 individuals, and *M. myotis* species of 500 individuals, based on available estimates (see Table 3.4 and Table 3.5

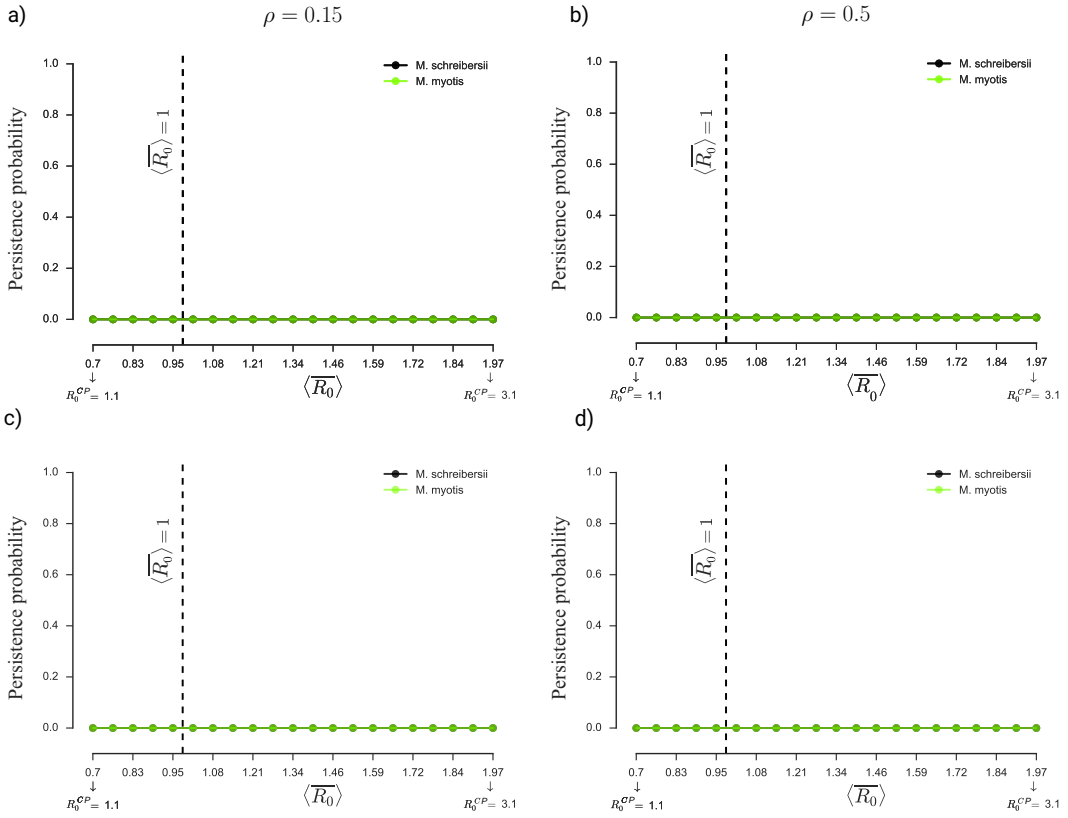

FIGURE 4.3: Persistence probability of EBLV-1 in *M. schreibersii* and in *M. myotis* for model 1. a), b) Persistence probability as a function of the average reproductive number of the metapopulation system for *M .schreibersii* (black) and *M. myotis* (green) for a proportion of exposed that becomes infectious $\rho = 0.15$ a) and $\rho = 0.5$ b) in mixing scenario. c), d): as in a), b) in the non-mixing conditions. In a), b), c) and d), the dashed horizontal line indicates $\langle \overline{R_0} \rangle = 1$.

respectively). For *M. schreibersii*, population size per patch and their temporal variation are obtained by computing migration events, as defined above. Disease progression dynamics in *M. myotis* bats is parameterized with available estimates from previous studies [73, 118]. Since no estimate for *M. schreibersii*'s disease progression is available, we use values of *M. myotis* for the average incubation period and infectious period, as in [118]. This was further supported by similar estimates of previous works on other species [76, 77, 118]. Models are tested by fully exploring ranges of plausible values [73, 77, 118] of the reproductive number R_0^{CP} (all models) and of the immunity period ω (models 2 and 3), as these are unknown and expected to be critical for the resulting epidemic dynamics. In addition, the non-mixing scenario ($\alpha = 0$) is compared to the mixing scenario ($\alpha > 0$) in all three models. All parameters for which estimates are not available (e.g. seasonal variations of the transmission intensity ε_1 and ε_2, degree of cross-species mixing α) are set to default values and ranges are explored in the sensitivity analysis. All parameters with their description and considered values are reported in Table 4.4.

4.3.4 Numerical simulations, persistence analysis and validation

The epidemic is seeded with 100 infected *M. schreibersii* bats and 10 infected *M. myotis* bats in the hibernation period. Simulations are discrete and stochastic to account for the discrete nature of hosts and for stochastic extinction events that may be favoured

by small host population sizes. Simulations evolve in discrete time steps, representing days in the annual seasonality. Each simulation provides at each time step the number of *M. schreibersii* and *M. myotis* in each compartment in each cave, and the number of *M. schreibersii* that moves from one cave to another. For each scenario analysed, we ran 10^3 stochastic simulations starting from the same initial conditions and lasting 20 years to reach the endemic equilibrium. The metapopulation framework is implemented in C++, and technical details for simulations are explained in detail in the Section 3.3.4. A sensitivity analysis on numerical aspects of the simulations was also performed (see Section 4.3.5). For each model and scenario under study, we compute the persistence probability of EBLV-1 in each bat species (P_{Ms} and for *M. schreibersii* and P_{Mm} *M. myotis*, respectively) as the fraction of stochastic simulations for which the pathogen still circulates in the host population once endemic equilibrium is reached.
Finally, we compare the simulated proportion of EBLV-1 seropositive (R compartment) at equilibrium with the serological EBLV-1 prevalence to identify portions of the parameter space that are compatible with observations. The proportion Θ of simulations falling into the 95% CI of the serological estimates is used as an indicator of model agreement with observed data.

4.3.5 Sensitivity analysis

We performed a sensitivity analysis with eight different tests to assess the impact of modeling assumptions regarding unknown ecological and biological features, and to identify key mechanisms for persistence (Table 4.2). First, we explored the values of the scaling factors ε_1 and ε_2 in the range [0, 1] to assess the role of the seasonal dependency of transmission across caves (Table 4.2 , SA1). Second, we varied the degree of cross-species mixing intensity α ($0 < \alpha \leq 1$) to evaluate the impact of the intensity of mixing between species in Can Palomeres on EBLV-1 persistence (SA2). Third, we explored different values of the average period of infection for EBLV-1 in the *M. schreibersii* population (SA3). Fourth, we tested variations in ecological parameters that were informed by empirical estimates: bats population sizes, starting date of migration flows, and duration of migration flows (SA4). Fifth, we considered density-dependent transmission rates for

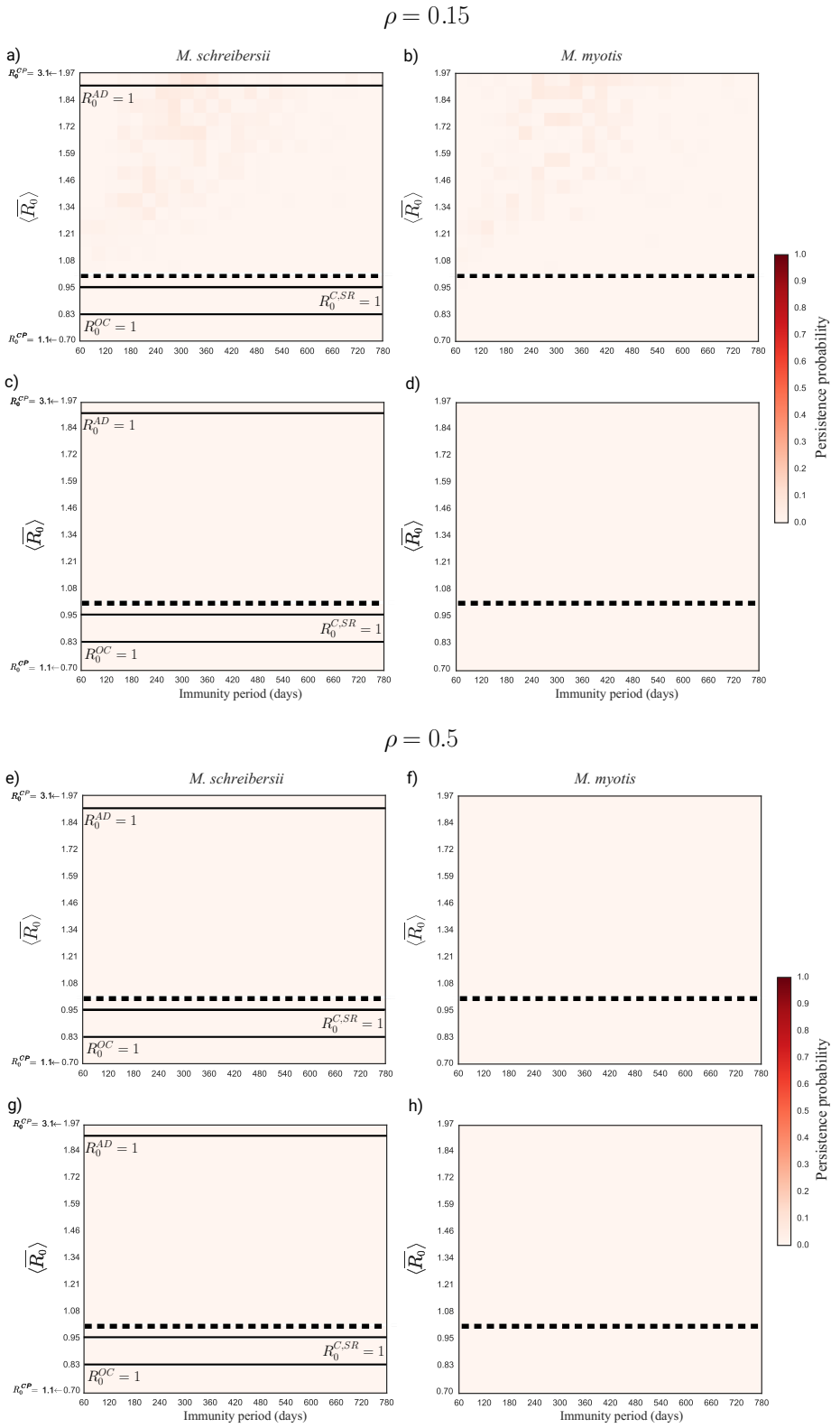

FIGURE 4.4: Persistence probability of EBLV-1 in *M. schreibersii* and in *M. myotis* in model 2. a), b), e), f): Persistence probability as a function of the average reproductive number of the metapopulation system $\langle \overline{R_0} \rangle$ and of the immunity period ω^{-1} for *M. schreibersii* (a, e) and for *M. myotis* (b, f) in the mixing scenario with probability of lethal infection $\rho = 0.15$ (left, panels a and b) and $\rho = 0.5$ (right, panels e and f). c), d), g), h): as in a), b), e), f) in the non-mixing conditions. The dashed horizontal line refers to $\langle \overline{R_0} \rangle = 1$. Solid horizontal lines refer to threshold conditions ($R_0^p = 1$) for the all caves.

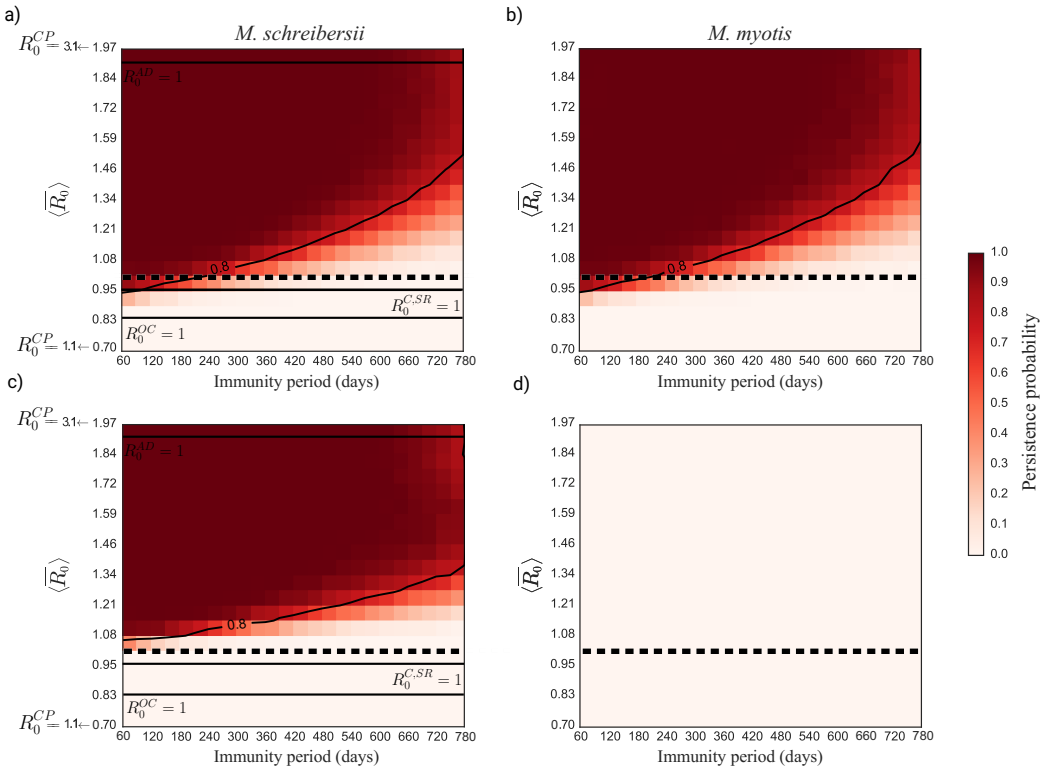

FIGURE 4.5: Persistence probability of EBLV-1 in *M. schreibersii* and in *M. myotis* in model 3. a), b): Persistence probability as a function of the average reproductive number of the metapopulation system $\langle \overline{R_0} \rangle$ and of the immunity period ω^{-1} for *M. schreibersii* a) and for *M. myotis* b) in the mixing scenario. c), d): as in a), b) in the non-mixing conditions. Contour lines indicate a persistence probability of 80%. The dashed horizontal line refers to $\langle \overline{R_0} \rangle = 1$. Solid horizontal lines refer to threshold conditions ($R_0^p = 1$) for the caves.

EBLV-1 dynamics in both species (SA5). Then, to assess independently the role of spatial migration and of seasonal activity on the persistence of EBLV-1, we compared our findings to the ones obtained from two variations of the modeling framework, each lacking one of the above two ingredients. First, we considered a *seasonal single population* epidemic model simulating the entire *M. schreibersii* population in Can Palomeres with no migration (Table 4.2, SA6), keeping the seasonal variation of the basic reproductive number in time in order to mimic the effect of the seasonal interaction. Second, we built a *no-seasonal metapopulation* epidemic model with the same spatial structure of the metapopulation framework, but with no variation in the transmissibility associated to the caves. The reproductive number was assumed to be constant in time and space, and equal to $\langle \overline{R_0} \rangle$ (SA7). Finally, we tested results robustness against numerical choices, like changing initial conditions, length of simulation time and number of stochastic runs performed (Table 4.2, SA8).

4.4 Results

To test the existence and the role of temporary immunity following rabies disease and the potential existence of non lethal infection, three susceptible-exposed-infected compartmental models were tested for EBLV-1 persistence.
EBLV-1 persistence is only observed in the model accounting for non lethal infection and

Reproductive number	Lowest bound with $\Theta \geq 90\%$	Point (1), highest Θ (Fig 4.6)	Point (2), longest immunity and $\Theta \geq 90\%$ (Fig 4.6)
$\langle \overline{R_0} \rangle$	1.02	1.16	1.29
R_0^{CP}	1.6	1.8	2
R_0^{AD}	0.53	0.6	0.67
R_0^{C}	1.07	1.2	1.3
R_0^{SR}	1.07	1.2	1.3
R_0^{CP}	1.24	1.4	1.5

TABLE 4.3: Values of the reproductive number for different epidemiological and immunological conditions leading to persistence probability larger than 80% in both species, for model 3 in the mixing scenario.

transient immunity (model 3) (Figure 4.5). In the cross-species mixing scenario (Figure 4.5, panels a and b, persistence occurs in both *M. schreibersii* and *M. myotis*, while the non-mixing scenario allows EBLV-1 persistence in *M. schreibersii* only (Figure 4.5, panels c and d). Pathogen persistence for *M. schreibersii* in both mixing and non-mixing scenarios (Figure 4.5 panels a and c, respectively) exhibits a similar pattern, with persistence made possible under slightly lower values of the reproductive number in the mixing scenario. More specifically, for a 2-months immunity period, the transition from extinction to $P_{\mathsf{Ms}} \geq 80\%$ persistence probability occurs with $\langle \overline{R_0} \rangle$ in the range 0.77-0.95 in the mixing scenario, compared to the range 0.89-1.46 in the non-mixing condition. For a 2-years immunity period, the same transition occurs for $\langle \overline{R_0} \rangle$ values ranging between 0.90 and 1.08 in mixing condition, and between 1.03 and 1.34 in non-mixing conditions. These results show that EBLV-1 persistence in *M. schreibersii* is reached also for values of the average metapopulation reproductive number below unity ($\langle \overline{R_0} \rangle \leq 1$) if mixing is assumed, contrary to the non-mixing scenario. For *M. myotis,* EBLV-1 persistence is observed only in the mixing scenario (Figure 4.5 panel b), with a pattern very similar to the one observed in *M. schreibersii*.

Models 1 and 2, i.e. accounting for infection-induced mortality with or without temporary immunity, showed very low ($< 9\%$) or null probability of persistence in any of the species for the parameter values explored (Figure 4.3 and Figure 4.4). Also, density-dependent transmission would not allow persistence of the pathogen in any of the models tested (Figures A.3.1, A.3.2, A.3.3).

Comparison with serological data was conducted on the sole modeling framework allowing for persistence in both species, as observed in reality, i.e. model 3 in the mixing scenario. Focusing on the conditions leading to a persistence probability above 80% in both *M. schreibersii* and *M. myotis*, we find the majority of numerical simulations to fall within the 95% CI of serological data ($\Theta \geq 50\%$) for immune periods lasting about a year and a half or shorter and moderate transmissibility ($\langle \overline{R_0} \rangle$ between 1.2 and 1.3), and for $\langle \overline{R_0} \rangle$ values larger than 0.95 and short immunity periods (Figure 4.6). A higher agreement with empirical data ($\Theta \geq 90\%$) is observed for moderate transmissibility and short immunity periods (from $\langle \overline{R_0} \rangle$ between 1.21 and 1.42 with $\omega^{-1} = 60$ days, to $\langle \overline{R_0} \rangle = 1.02$ with ω^{-1} between 120 and 210 days).

Simulated proportion of infected and serological data collected for both species are shown for two points in the space of $P_{\mathsf{Ms}} \geq 80\%$ and $P_{\mathsf{Mm}} \geq 80\%$: point (1) with $\langle \overline{R_0} \rangle = 1.16$ and $\omega^{-1} = 90$ days corresponding to the conditions having the largest compatibility with observations ($\Theta = 97\%$) (Figure 4.6); point (2) with $\langle \overline{R_0} \rangle = 1.29$ and $\omega^{-1} = 570$ days corresponding to the longest temporary immunity conditions having $\Theta \geq 50\%$ (Figure 4.6). In addition, Table 4.3 shows values of the reproductive numbers computed for each

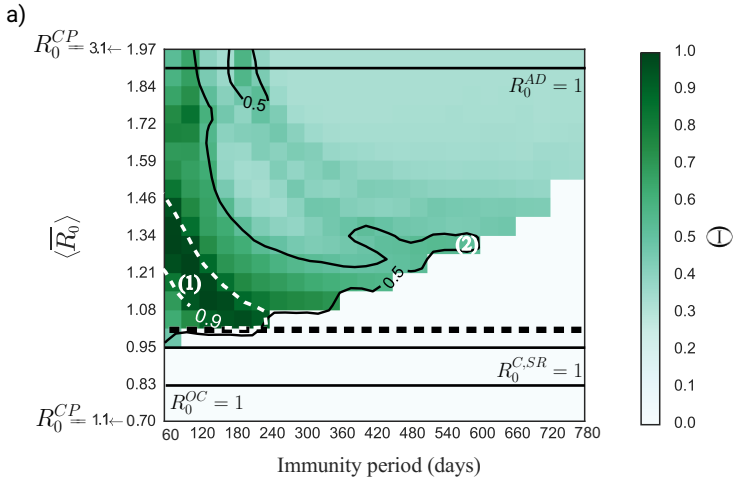

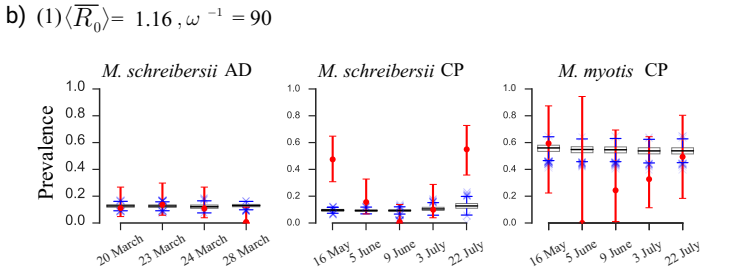

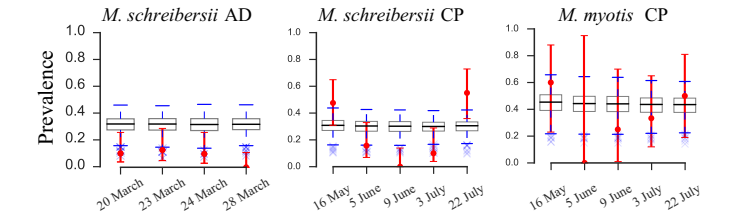

FIGURE 4.6: Model 3 comparison. a) Proportion Θ of simulations falling within the 95% CI of the serological estimates as a function of the average reproductive number of the metapopulation system $\langle \overline{R_0} \rangle$ and of the immunity period ω^{-1}. Only values allowing a persistence probability above 80% in both *M. schreibersii* and *M. myotis* are shown. The dashed horizontal line refers to $\langle \overline{R_0} \rangle = 1$. Solid horizontal lines refer to threshold conditions ($R_0^p = 1$) for the caves. Contour lines indicates $\Theta = 50\%$ (solid) and $\Theta = 90\%$ (dashed). b) Comparison between simulated prevalence of immune bats (boxplots) and serological data (median and 95% CI, red symbols) collected in Avenc Davì (for *M. schreibersii*) and in Can Palomeres (for both species). Simulations refer to point (1) highlighted in panel a), i.e. the point of the space of parameters having the largest agreement with empirical data ($\Theta = 97\%$), corresponding to $\langle \overline{R_0} \rangle = 1.16$ and $\omega^{-1} = 90$ days. c) As in b) for point (2) highlighted in panel a), i.e. the point of the space of parameters having the longest immunity period with ($\Theta \geq 50\%$), corresponding to $\langle \overline{R_0} \rangle = 1.29$ and $\omega^{-1} = 570$ days. All results are obtained with model 3 in mixing conditions.

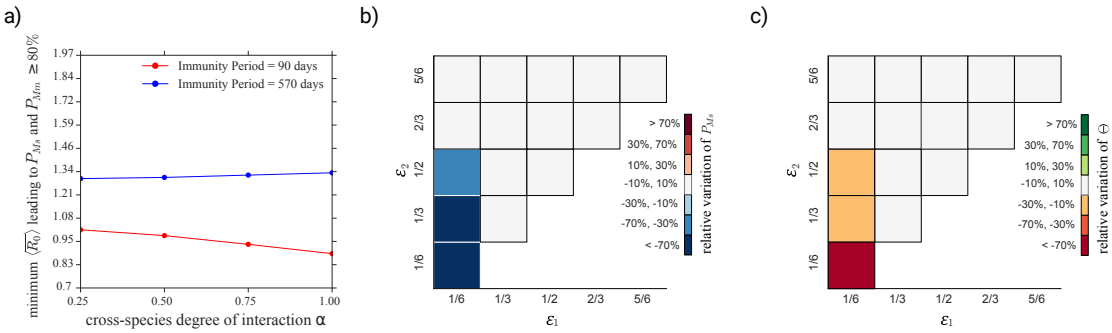

FIGURE 4.7: Impact of cross-species transmission and seasonal transmission. a) Minimum $\langle \overline{R_0} \rangle$ needed to reach 80% persistence probability of EBLV-1 in both species as a function of cross-species degree of interaction in the mixing conditions (sensitivity analysis test SA2). Two values of immunity periods are explored, corresponding to points (1) and (2) of Figure 4.6. b) Relative variation of the persistence probability P_{Ms} in *M. schreibersii* for scaling factors for seasonal transmission ε_1 and ε_2 in the range [0,1] compared to default values (SA1). Numerical results are obtained for model 3 in the mixing scenario and epidemiological and immunological conditions leading to the highest compatibility with empirical data (point (1) in Figure 4.6). c) As in b) but showing the relative variation of the agreement Θ between simulations and empirical data.

cave and corresponding to point (1) and point (2), and to the lowest bound of transmissibility for $\theta \geq 90\%$. The reproductive number in Avenc Davì (R_0^{AD}) was always found to be below unity in these three conditions, whereas its value in Can Palomeres (R_0^{CP}, largest transmissibility conditions across the annual seasonality) was found to vary between 1.6 and 2.

Results of Figures 4.5 and 4.6 are obtained using default values for the unknown parameters, therefore we tested how variations of these values may affect the resulting epidemic outcomes. The intensity of cross-species interaction has limited impact on EBLV-1 persistence in *M. schreibersii* (Figure 4.7). For the longest possible immunity period (570 days, as for point (2)), the minimum $\langle \overline{R_0} \rangle$ values needed for $P_{\text{Ms}} \geq 80\%$ is stable at around 1.28-1.34. For shorter immunity periods (90 days, as for point (1)), a slight decrease in the minimum $\langle \overline{R_0} \rangle$ value is observed (from 1.02 to 0.89), once α ranges from 0 to 1. Persistence and validation results were also considerably robust against variations of the seasonal scaling factors for transmissibility, in the region of high agreement with real data (Figure 4.7 for point (2)). For 12 combinations of values in the space of parameters of ε_1 and ε_2 out of the 15 explored (80%), results show less than a 10% variation from those obtained in the default parameterization, for both simulated persistence and validation with serological data. Larger deviations are only obtained when scaling factors assume very small values.

Additional tests performed in the sensitivity analysis allowed us to assess the role of seasonality versus spatial migration. Persistence was found to be stable when neglecting the seasonal variation in transmissibility, even through changes of the immunity period (Figure 4.8), reinforcing results of Figure 4.7. In the absence of *M. schreibersii* migration, persistence in *M. schreibersii* would instead strongly decrease for immunity periods longer than one year compared to the default metapopulation scheme (Figure 4.8).

Finally, persistence was not altered by varying the length of the infectious period in *M. schreibersii* between 2.5 and 10 days (Figure A.1 of the Appendix A). No variations were

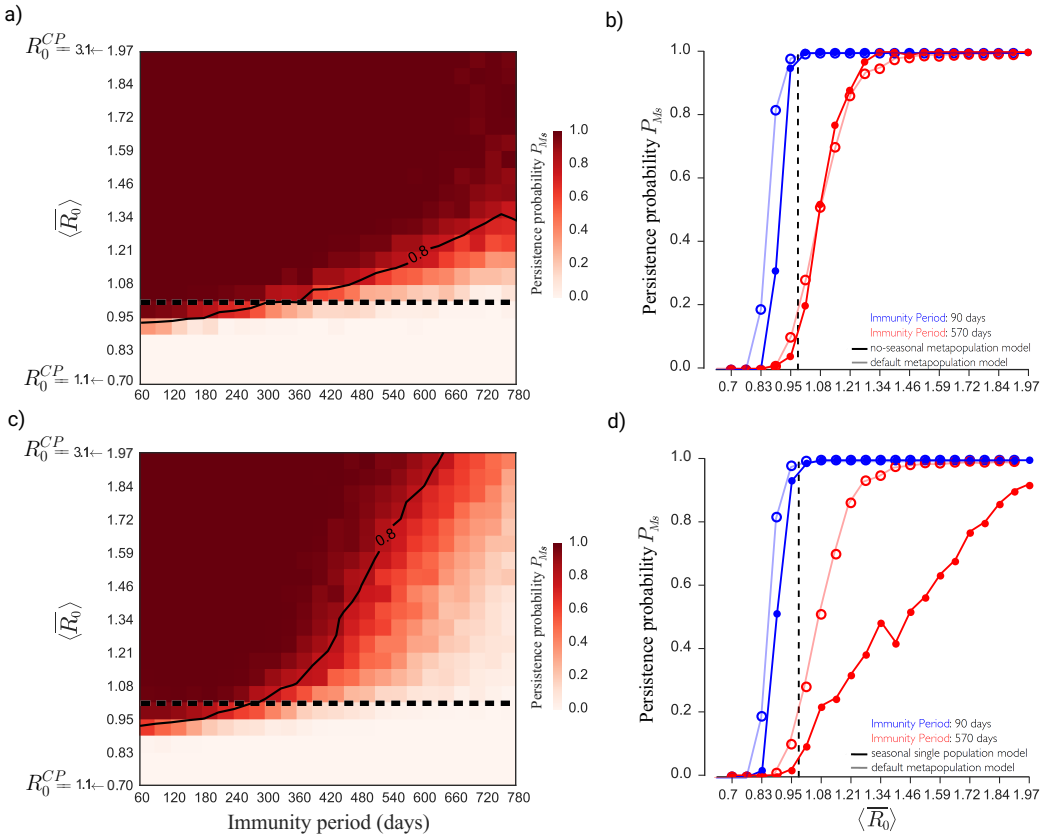

FIGURE 4.8: Impact of spatial migration and seasonality. a) Persistence probability as a function of the average reproductive number of the metapopulation system $\langle \overline{R_0} \rangle$ and of the immunity period ω_{-1} for *M. schreibersii* in the *no-seasonal metapopulation* sensitivity analysis test (SA7). Numerical results are obtained for model 3 in mixing conditions. b) Persistence probability P_{Ms} as a function of $\langle \overline{R_0} \rangle$ for two values of the immunity period ($\omega_{-1} = 90$ and $\omega_{-1} = 570$ days, of points (1) and (2) of Figure 4.6, respectively), comparison of the *no-seasonal metapopulation* with the default metapopulation model. c) As in a) for the seasonal single population sensitivity analysis test (SA6). d) As in b) for the comparison of the seasonal single population with the default metapopulation model.

observed with changes in bats population sizes (Figures A.2.1 and A.2.1), starting date of migration events (Figures A.2.2), and duration of migration events (Figures A.2.3) around the estimated values. Numerical aspects did not affect results.

4.5 Discussion

We developed a mathematical modeling framework accounting for roosts ecology, seasonal effects, migratory paths, disease progression, and bat species richness, based on estimates from a field survey in Catalonia. The study aimed to identify the mechanisms responsible for the empirically observed EBLV-1 persistence in *M. schreibersii* and *M. myotis* species, shedding light on several unknown epidemiological, immunological and ecological factors.

In the ecosystem under study, numerical evidence suggests that persistence of EBLV-1 is possible in both bat species only if all animals survive infection and acquire a transient immunity, and if the two species mix allowing cross-species transmission (model 3, mixing

conditions). In the absence of interaction between species, EBLV-1 infection would not be sustained in *M. myotis* population. Finally, no persistence is predicted to occur in any of the two bat species if we consider infection-induced mortality (models 1 and 2). While our study confirms the importance of bats' ecology (species richness, interaction) on lyssaviruses persistence in line with previous work [60, 61, 76, 78, 202, 209] , our model provides data-driven numerical evidence supporting bats may not only survive from EBLV-1 infection but furthermore may also acquire transient immunity. This is consistent with the findings on rabies virus infection in free-ranging bats [78, 79, 214], in bats in a captive colony [71], and also in naïve bats born in captivity [72].

The model identifies a parameter region with the largest compatibility of numerical trajectories with empirical data, characterized by small values of the average reproductive number of the metapopulation system and small immunity periods, of the order of few months. In these conditions, several caves are associated to seasonal transmission close to the critical threshold, and persistence is mainly supported by transmission in Can Palomeres. Numerical findings also provide a lower bound for the birthing reproductive number ($R_0^{CP} \geq 1.6$) and for the hibernation reproductive number ($R_0^{AD} \geq 0.5$), for which no direct estimations from epidemiological data are currently available for this type of lyssavirus.

The model predicts cross-species mixing to be the most important ecological factor allowing persistence in both species. Multi-species colonies and habitats sharing are a phenomenon largely observed in the field that is known to favor virus exchange. Also, migratory species are generally found to host more viruses than sedentary species [211]. Our findings indicate that the small size of *M. myotis* population would probably not allow maintaining alone the circulation of the virus. Structuring the hosts into smaller subpopulations to account for longer and more frequent displacements observed in other ecological settings [73] would further strengthen this result.

The mixing intensity between species is largely unknown, but persistence in our case was robust to a large range of mixing intensity values. Seasonal migration of *M. schreibersii* bats is another ecological factor of primary importance affecting the probability of persistence in our context, as also recognized elsewhere [76, 116, 118, 209]. Its role is increasingly important for longer immunity periods, when immunity duration becomes comparable to or longer than the annual timescale of migration process. In these conditions, the smaller renewal of susceptibles following immunity tends to hinder virus survival whereas movements along the migratory route allow its maintenance as already observed in theoretical studies [215].

The regional migratory species is therefore responsible for large-scale spatial diffusion of the virus and its persistence on a larger range of epidemiological and immunological conditions, and it can contribute to pathogen persistence in species encountered along the migration path. In addition, given that *M. schreibersii* make seasonal movements of long distance (exceeding 350km in the region) [43, 196], our findings also suggest that they might represent one of the dispersion vectors of EBLV-1 in southern Europe, where that bat species is abundant, ensuring spatial diffusion and local persistence in other species. This is consistent for example with the regional reservoir role found for *M. schreibersii* in a 4-bat species ecological setting in the Balearic islands [118].

We found one factor to have a negligible impact on virus persistence, i.e. seasonality of transmission. Seasonality may act for ecological reasons due to the diverse activities of bats over time affecting interactions and transmission [216] and also on modulating transmissibility because of immunological drivers, e.g. facilitating virus multiplication and activating immune response [217].

While more precise estimates of the rescaling factors of transmissibility (for hibernation,

mating, birthing, and breeding) would be useful, our model suggests that seasonal variation in transmissibility is not critical in order to achieve accurate predictions of viral persistence, as long as the migratory path is well described. Large deviations would be obtained only for extremely low values of transmissibility during Fall/Winter period, unlikely to occur because of the rather mild environmental conditions in Catalonia even during hibernation period. The robustness of our results on variations of seasonal transmissibility represents an important point for future studies, as no quantitative data exist now to better describe the ecological features of the system (mixing rate and variation by activity) beyond cave occupation. Our findings suggest that efforts should be invested first in accurately tracking hosts' movements.

Besides ecological factors, numerical findings rule out any possibility of virus persistence assuming infection-induced mortality, regardless of the loss of immunity (models 2 and 3), differently from the conclusions of [76, 77] reached in other ecological settings. Lyssavirus infections are generally lethal for mammals, and intra-bat infection dynamics may exhibit a large variation of possible epidemic and immunologic outcomes depending on bat species and lyssavirus [60, 216]. For example, while rabies virus infection may cause death in *Eptesicus fuscus* [77], lethal infections of other lyssavirus may be very rare for bats [60, 216]. Our findings indicate that *M. schreibersii* and *M. myotis* might survive infection.

In addition, we find that persistence compatible with reality is most likely to occur assuming transient immunity of seven months or less. While detailed experimental data on EBLV-1 infection in *M. schreibersii* is missing to confirm our numerical evidence, previous findings suggest that there may be conditions for a mid-term serological response in healthy bats [60]. For example, antibodies were detected during 3 months following the experimental infection of *Eptesicus fuscus* [70]. Natural observational studies reported the occurrence of a positive seroconversion (i.e. from seronegative to seropositive antirabies status) followed by a negative one 6-12 months later in vampire bats in French Guiana [78], and the loss of detectable immunity to EBLV-1 in the majority of seropositive recaptured *M. myotis* bats in the following recapture sessions at various time intervals [216]. Given the little current knowledge on the mechanisms on bats immune response, survival from infection and loss of immunity are not excluded [117, 218]. Finally, for unknown *M. schreibersii* epidemiological parameters we used those obtained from *M. myotis* fieldwork [73, 118], also consistent with the estimates for *E. fuscus* [76]. Variations of the infectious period for *M. schreibersii* bats did not affect the predicted persistence behaviour, consistently with previous findings [118].

While the debate on the dependence of disease transmission on animal population size [219–222] still remains, our mathematical framework suggests frequency-dependent transmission to be in place in the ecological setting under study, ruling out other hypotheses. This conclusion may find support in the fact that many species of bats are known to form communities (families) that are stable over short (daily and nocturnal activities) and long terms (between migrations) thus including members of different generations, and whose sizes are independent on the colony size [223, 224]. Due to the regularity of social interactions, the restricted number of daily contacts, the way virus can be transmitted (through bites and scratch), a frequency dependent approach appears to be a good modeling choice. Our findings are in contrast with those of Refs. [76] and suggest that ecological aspects such as roosting behavior may affect the relation between population size and contact rates for a given species and disease transmission.

The prevalence estimates used to compare our model trajectories are yielded from relatively small sample sizes. However, bats were captured every year, in the same cave, and point prevalence estimates are rather consistent across the 5 years of the study, especially in Avenc Davì. In Can Palomeres, all confidence intervals are overlapping, except for the sampling on July 22nd, which is slightly higher than the other ones. For *M. myotis*,

the confidence intervals are very large, because very few animals were caught each time. Positive animals were found however every year, except in 2014 when only one animal was sampled. These data, although limited, show reasonable evidence of endemic circulation of EBLV-1 virus that find qualitative agreement only with the predicted persistence scenario of model 1. Quantitative comparison in this scenario is then performed to reduce the space of unknown parameters to realistic intervals.
EBLV-1 is mainly associated to the serotine bat (*Eptesicus serotinus*) in Europe, accounting for 99% of detected cases [60, 67], however it was not considered in our study for several reasons. The distribution of EBLV-1 cases per bat species can indeed hardly be used to identify a reservoir species, because of biases in active and passive surveillance (e.g. towards more populous species or those most affected clinically or closer to humans). Moreover, an exception to this strong association is found in the region of Spain, where the virus has been reported in a number of other species, including *M. myotis* and *M. schreibersii* [43, 73]. Most importantly, *E. serotinus* has a synanthropic behavior, whereas *M. schreibersii* and *M. myotis* are non-synanthropic, as they roost in natural caves and abandoned mines, showing a strong troglophile character [43]. For these reasons, we considered *E. serotinus* not to be in contact with the bat species in the ecosystem under study. On the other hand, Can Palomeres cave also hosts other non-synanthropic bat species of smaller population sizes that were not tracked in the field study therefore not considered here. The major role of these caves in the spatial circulation of EBLV-1 suggests that an increased public health attention should be made on caves hosting multiple species, along with targeted ecological fieldwork to be performed to improve our understanding of the system.
Bat species have a wildly variable range of habitats, life cycles, population sizes and spatial distributions. Some species display a more localized nature like *M. myotis*, while others exhibit rather long migratory behaviors similar to *M. schreibersii* (e.g. *E. helvum* [225]). Knowledge of the topology and size of these structured populations may be used to inform the theoretical and computational framework proposed here for application to other settings, of even higher complexity, and greatly enhance our understanding of the potential for lyssavirus maintenance and transmission. Finally, bats are reservoir hosts of numerous emerging zoonotic viruses. Our framework can readily be extended also to other zoonotic viruses of public health concerns circulating in spatially fragmented bat populations.

4.6 Conclusions

Our mathematical modeling framework shows that EBLV-1 persistence in Catalonia is ensured by the regional migration of *M. schreibersii* mixing with a colony of *M. myotis*. In addition, our work provides novel numerical evidence supporting frequency-dependent transmission of EBLV-1 in the considered species and non-lethal infection followed by a transient immunity of few months, thus improving our knowledge on disease progression. Our approach suggests that those caves hosting multi-species colonies may represent hotspots for virus exchanges and should therefore be targeted for public health surveillance and control.

	Parameter description	***M. myotis***		***M. schreibersii***	
		Default value	Ref.	Default value	Range
N	Total population size	500 [400-600]		17 000	[16 000-18 000]
σ_I^{-1}	Average incubation period leading to infectiousness	30 days	[60, 76, 118]	30 days	
σ_R^{-1}	Average incubation period leading to immunity (models 1,2)	15 days	[76]	15 days	
γ^{-1}	Average infectious period	5 days	[73, 118]	5 days	2.5, 10 days
ω^{-1}	Average immunity period (models 2,3)	2 years	[61]	–	[60 – 730] days
ρ	Proportion of exposed that becomes infectious (models 1, 2)	0.15, 0.5	[76]	0.15, 0.5	
μ	Natural death rate	1/15 years^{-1}	[61]	1/15 years^{-1}	
b	Pulsing birth rate (birthing season only)	$b(t) = \mu$	[61]	$b(t) = \mu$	
κ	Density dependent death rate (models 1, 2)	$\kappa = \mu - (b - \mu)N/K$	[76]	$\kappa = \mu(b - \mu)N/K$	
K	Carrying capacity (models 1, 2)	$7 \cdot 10^5$	[76]	$2.55 \cdot 10^7$	
R_0^{mix}	Basic reproductive number relative to cross-species mixing	$R_0^{\text{mix}} = \alpha R_0^{CP}$			
α	Cross-species interaction	[0 – 1]			
R_0^{CP}	Basic reproductive number of *M. schreibersii* in Can Palomeres	N/A		–	[1.1 – 3.1]
R_0^{AD}	Basic reproductive number of *M. schreibersii* in Avenc Davì	N/A		$R_0^{AD} = \varepsilon_1 R_0^{CP}$	
R_0^{C}	Basic reproductive number of *M. schreibersii* in Castanya	N/A		$R_0^{C} = \varepsilon_2 R_0^{CP}$	
R_0^{SR}	Basic reproductive number of *M. schreibersii* in the Summer refuges	N/A		$R_0^{SR} = \varepsilon_3 R_0^{CP}$	
R_0^{OC}	Basic reproductive number of *M. schreibersii* in the Other caves	N/A		$R_0^{OC} = \varepsilon_4 R_0^{CP}$	
ε_1	Scaling factor for	N/A		1/3	[0 – 1]
ε_2	Scaling factor for	N/A		2/3	[0 – 1]
ε_3	Scaling factor for	N/A		$\varepsilon_3 = \varepsilon_2$	see ε_2
ε_4	Scaling factor for	N/A		$\varepsilon_4 = (\varepsilon_1 + \varepsilon_2 + \varepsilon_3)/3$	see $\varepsilon_1, \varepsilon_2$
R_0^{low}	Basic reproductive number of *M. myotis* in Winter months	$R_0^{\text{low}} = \varepsilon_1 R_0^{CP}$		N/A	
R_0^{high}	Basic reproductive number of *M. myotis* in Summer months	$R_0^{\text{high}} = R_0^{CP}$		N/A	

TABLE 4.4: Parameters description and values.

5

RABIES PERSISTENCE IN DOMESTIC DOG POPULATION IN CENTRAL AFRICAN REPUBLIC

5.1 Abstract

Dog-mediated rabies remains a serious public health problem in several African and Asian countries. More than 99% of human cases are related to rabies exposures mediated by dogs. However, the drivers of rabies in dogs are still largely unknown and this impairs the probability of success of mass vaccination campaign and at large the implementation of control strategies.
Rabies has an unusually heterogeneous incubation period related to the entry route of the virus and its process of dissemination in the infected body. Moreover, since the transmission is induced by direct contact between infectious and susceptible hosts environment features like host distribution and mobility may have a strong impact in the spread and maintenance of the disease. To study the role and interplay of these factors on RABV epidemiology we introduced a novel stochastic compartmental model with realistic data-driven distributions for incubation and infectious periods. Then we explored through numerical simulations the conditions that can lead RABV persistence in a network of geographical fragmented populations, taking the Central African Republic as a model. In this spatial explicit framework we found that the virus can persist even for low transmissibilities keeping the total population substantially stable in agreement with empirical observations. Interestingly, once exponentially distributed incubation and infection periods are considered, higher values of R_0 are needed to have endemicity. Our study provides further understanding of the fundamental role of host population's spatial structure in rabies circulation and of the impact of heterogeneous periods of latency and infectiousness in the persistence of the rabies infection at country level.

5.2 Background

Rabies is a multi-host viral encephalitis caused by rabies virus (RABV), a lyssavirus genotype (see Section 2.2) maintained in domestic and wild mammals and characterized by a complex epidemiological situation [226]. Dogs are the most important reservoirs for human exposure (see Section 2.5.2). Although the disease has been successfully eliminated in domestic dogs in developed countries, in low-income countries of Asia and Africa it still affects urban and rural areas. Even if human and canine vaccines for rabies exist, the scarce availability and accessibility in risky areas represents an additional challenge for public health. Moreover, rabies post-exposure prophylaxis (PEP) often represents a considerable financial burden for developing countries where this disease is endemic [227,

228] (see Section 2.5.2).
Recent studies conducted in Central African Republic (CAR) and in its capital city Bangui [106, 107, 229] show that rabies is endemic in the country at least in the last 20 years. However, given the extreme political and economical instability of the country, no dogs mass vaccination campaign has been recently implemented [106]. Surveillance data collected in 2012 [106] shows that the vast majority of persons exposed are from Bangui or its suburban area i.e. Bimbo and Bégoua (93.2%) [106]. The rest of the cases came from two Bangui's neighbouring prefectures named Ombella M'Poko and Ouaka [106]. Phylogenetic and virological analysis of isolates sampled in Bangui, showed the presence of several subtypes sequentially circulating in the domestic dogs population, characterized by a basic reproductive number [114, 149] R_0 close to one (see Section 2.5.2).
Our aim is to understand which are the principal mechanisms underlying the maintenance or the extinction of the RABV virus in domestic dogs and to analyze this problem we have adopted, as case of study, the endemic condition of Bangui and of the Central African Republic. Three elements may be at play: the hosts movement patterns, the spatial fragmentation of the domestic dogs population and the variability of the incubation period of rabies in dogs (see Section 2.4).
Domestic dogs movements can be classified in natural and human mediated (see Section 2.6). Natural dispersal is given by free-roaming movements that are in general around few kilometers per day for a healthy dog [88, 119] and even less for a rabid one [81]. Human mediated dispersal, on the contrary, can drive movements of orders of magnitude higher respect to the natural one, and it can be potentially predictable since it is strictly related to human migration patterns and commuting [82, 112, 119, 121]. The crucial role of human mediated movements in the spread of various diseases in wildlife [124, 230, 231], in livestock [232] and in domestic animals [82, 112] has already been established (see Section 2.5.2 and Section 2.6). As recently observed in Bali (Indonesia) [145], frequent human-mediated dog movements (daily and monthly time scale) drastically reduce the probability of the disease elimination in a heterogeneous vaccination coverage scenario. Finally, a recent study [113], based on phylogeographic analyses, shows that the observed RABV spread patterns can only be explained considering long distance human mediated dispersal, suggesting a critical connection between human migrations (long time scale) and human commuting (short time scale) with the geographical diffusion of the virus.
Given that rabies is a direct host-to-host contact transmitted disease (see Section 2.3) also spatial heterogeneities like natural barriers (water bodies, mountains, etc.) [124, 233], anthropogenic features (political borders, human settlements, bridges, roads, etc.) [112, 234] and the spatial distribution of the host population may have a role in the diffusion and endemicity of the pathogen [235] (see Section 2.6).
Compared to other encephalitis, rabies has an unusually heterogeneous incubation period with a median close to one month and a range from 10 days to more than one year [81, 158] (see Section 2.4). These peculiarities lead to irregular and potentially long lasting asymptomatic periods which may allow the translocation of infected animals over a wide range of distances [115].
Various mathematical and computational models have been used to study the diffusion and the endemicity of rabies, however, despite the public health relevance of this disease, a precise identification of the mechanisms underlying persistence is still missing. Non-spatial models helped to identify some important features such as the high renewal of the naive domestic dogs population, given by the average short life-span and the high fecundity rate, or the minimum threshold dogs density for rabies persistence (4.5 dogs $\cdot$ km^2) [53, 81]. However, the main limitations of such models are related to the exclusion of key features like landscape heterogeneities and dog movements [115, 124].

Once space is explicitly considered, modeling studies were able to uncover additional critical aspects such as the optimal vaccination strategy in a particular environment [194, 236], the minor role of wildlife in long term persistence [91, 194, 195], the importance of human mediated dog movement for the diffusion of the virus in disease-free areas [113, 146, 237] and the critical role of the reintroduction in disease free areas [145, 146, 194, 195, 236, 237]. Those models are in general developed after an extensive data collection on dogs bite incidence and past vaccination campaigns [194, 195, 236], or on household surveys data [120, 145, 146]. Unfortunately, data collection can be extremely challenging and costly if the area under study is large also a possible generalization of the results obtained may depend on the environment considered [145, 146, 237]. Finally, only few of those models [194, 195, 236] consider the potentially long lasting asymptomatic periods characteristic of dog rabies.
The aim of this work is to propose a framework which extends and tries to generalize prior approaches considering the spatial structure, the host movements and also realistic data-driven distributions for incubation and infectious periods.

5.3 Results

To analyze the RABV dynamics in the domestic dog population of the Central African Republic we built a spatially explicit modeling framework where each dog settlement represents a patch (sub-population) and all patches are coupled together through dogs' movements (see Section 3.3.5). The model is based on a two-level dynamics: a local dynamics, representing the disease transmission within each subpopulation and modeled through a compartmental model approach with homogeneous mixing approximation (Figure 5.9); a network-like dynamics, representing the spatial spread of RABV infection through the translocation of infected animals in the country. The model is discrete and stochastic and all the results are obtained from 10^3 stochastic realizations of each scenario considered (see Table 5.1). If i indicates the subpopulation, the input of each realization is given by: the initial population $N_i(0)$, the carrying capacity K_i and the detection probability ρ that we use to evaluate the seeding of exposed $E_i(0)$ and infectious $I_i(0)$ in each patch (see Methods 5.6.2). Following personal communications, the most likely detection probability is $\rho = 20\%$ so we used this value as baseline, however also other values of ρ ($5\%, 10\%$ and 50%) have been explored. The output of our model, in each point of the parameters space are: the proportion of stochastic realizations where the virus still circulates after 100 000 time steps, which corresponds to approximately 274 years considering a daily time step; the prevalence, i.e. the proportion of infected, in each subpopulation; the daily number of infected dogs in Bangui. The values of R_0 explored are above 1 in order to have the spread of the pathogen (see Section 3.2.1) and below 2 as in general indicate for rabies (Table 3.1). Since birth rate is high and highly variable and it is an important factor for RABV endemicity we also explored a range of values for this parameter.

5.3.1 Model of dogs movements

Since no data is available on domestic dog movements in Central African Republic, we modeled the coupling among subpopulations considering the work made by *Talbi et al.* [113]. In our formulation, the travel probability between two patches i and j declines as the Euclidean distance d_{ij} increases (the modeling approach is described in details in Section 3.3.5 and in Section 5.6.2). We classified three different migration range according to distance: long range movements, for distances between 100 km and 1290 km

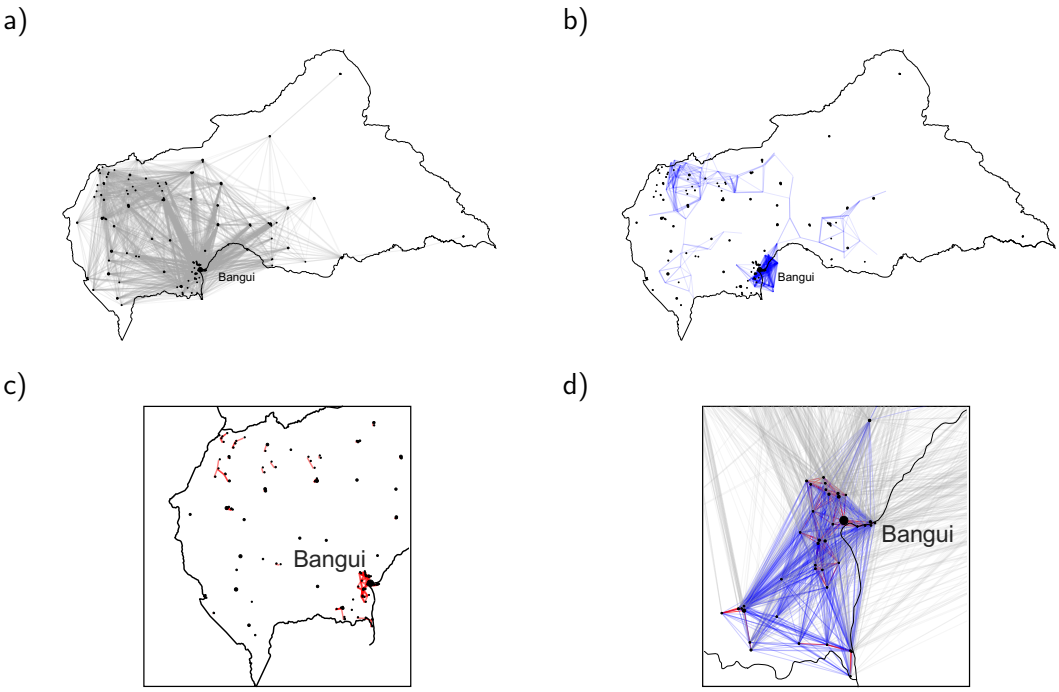

FIGURE 5.1: Geo-referenced network of the estimated domestic dog communities. Filled circles represent the position of the patches centroids with a size proportional to the squared of the estimated population. Links between patches represent the migration routes classified respect to the great-circle distances in: a) long range movements with a distance higher than 100 km and a percentage of daily migrating dogs on average equal to 0.00064; b) medium range movements with a distance between 20 and 100 km and a percentage of daily migrating dogs on average equal to 0.0046; c) short range movements with a distance lower than 20 km and a percentage of daily migrating dogs on average equal to 0.035. d) Bangui and his geographical proximity with all the possible migrating routes.

(the maximum distance between two patches in our framework) with a proportion of population involved per day $\sim 0.00064\%$; medium range movements for distances from 20 to 100 km and a proportion of population involved per day $\sim 0.0046\%$; short range movements for distances lower than 20 km (the least common ones, only 2% of the total number of links, but the most probable per day) with a population involved per day on average $\sim 0.035\%$. In Figure 5.1 panels a, b and c are showed the three geo-referenced networks that correspond to this classification. In Figure 5.1 panel d are represented all the possible daily movements around the Bangui area showing the strong presence of both short (red) and medium (blue) range movements that characterize the geographical area composed by Bangui's municipal area, the South of the prefecture of Ombella M'Poko and the East part of the prefecture of Lobaye.

5.3.2 Inferred domestic dogs demography in CAR

The spatially structured population is obtained using *WorldPop* a public database on human demography (see Section 3.3.5) and considering the average human to dog ratio for African urban and rural environments (see Methods). The estimated population in the whole CAR is composed by 76 992 dogs distributed in 137 settlements divided in

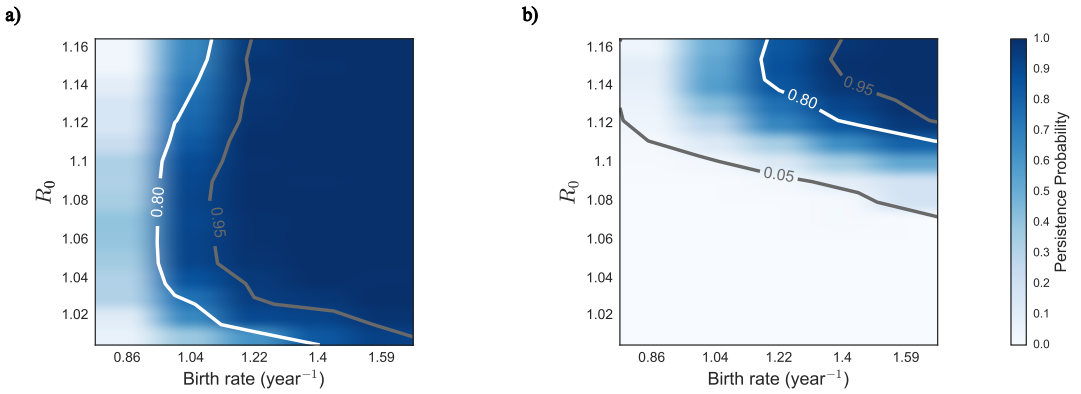

FIGURE 5.2: Rabies virus persistence probability in Central African Republic. a) Persistence probability of rabies virus in the domestic dog population of Central African Republic as a function of the basic reproductive number R_0 and of the annual dogs birth rate. Results are obtained for the realistic metapopulation modeling framework where incubation and infectious periods are distributed according to empirical data (i.e. gamma distributed). b) As in a) assuming that incubation and infectious periods are exponentially distributed. In both cases it is assumed a detection probability $\rho = 20\%$. Contour white lines indicate a persistence probability higher than 80%. The two contour grey lines indicate a persistence probability equal to 5% and 95%.

58 *urban* and 79 *rural* patches (Figure 3.9). The population size is smaller for rural patches in which about the 10% of the total population lives. 47% of the domestic dogs population lives in Bangui and the 50% of the total dog population is reached in the whole Bangui prefecture that is obtained grouping together Bangui and its suburbs composed by rural settlements and urban areas like Bimbo and Bégoua. An important fraction of settlements is distributed in the Center and in the West of the country since in the East there are numerous national parks and natural reserves. Figure 3.9 shows: in panel b, the distribution of the estimated number of domestic dogs in rural (green) and urban (black) patches; in panel c, the distribution of distances among the patches.

5.3.3 Modeling rabies persistence

We analyze the RABV circulation and persistence in the domestic dog population of Central African Republic implementing an infection dynamics with empirical distributions for incubation and infectious periods to allow the potentially long lasting asymptomatic stage characteristic of rabies (see Section 3.2.3 and Section 5.6.2 for the details). We also simulate using the same spatial structure and the same mobility model a classic infectious dynamics with exponentially distributed infected stages (see Section 3.2.3) that, differently, does not allow that possibility. Our aim is to evaluate whether and how the epidemic outcome can be affected by incubation period heterogeneity. The disease can be maintained in both cases (Figure 5.2) with different epidemic scenarios.

If incubation and infectious periods are distributed according to empirical data (Figure 5.2 panel a), the probability that the disease persists in the whole country is higher than 5% for each value of the parameters explored. A sharp transition is observed incrementing the annual birth rate from 0.86 to 1.04. If the annual birth rate is 0.86 the maximum persistence probability is reached for $R_0 = 1.06$ and is equal to 38% while for a birth rate equal to 1.04 the maximum is 90% persistence probability reached for $R_0 = 1.05$.

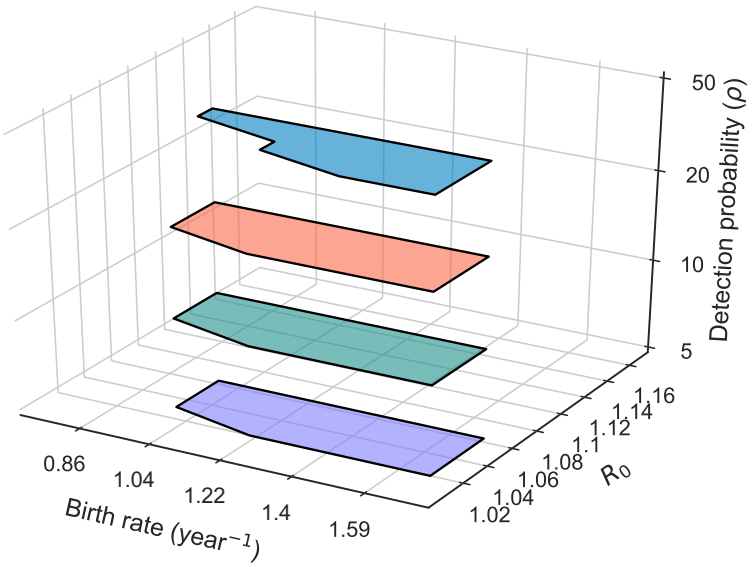

FIGURE 5.3: Shape of the region where the persistence probability is higher than 80% and where the average population of domestic dogs in Central African Republic is equal to the estimated population $\pm 20\%$ as a function of the basic reproductive number R_0 and of the annual dogs birth rate, for a detection probability $\rho = 5, 10, 20, 50\%$.

In general, increasing the annual birth rate increases the persistence probability for each value of R_0.
However, increasing R_0 and keeping the birth rate constant leads to higher persistence probabilities only for birth rates ≥ 1.22. For example, if the annual birth rate is 1.04 and we increment the transmissibility, we observe an increasing persistence probability from 40% to 70% between $R_0 = 1.01$ and $R_0 = 1.04$; then, after a stage where persistence remains constantly higher 80% (between $R_0 = 1.04$ and $R_0 = 1.1$), we observe a decrease from 80% to 60% when R_0 goes to 1.16. A possible interpretation can be that for high values of R_0 that population renewal is too low to compensate the mortality due to infection, indeed for annual birth rates higher than 1.22 the persistence probability is uniformly higher than 95%, even for $R_0 > 1.1$. Finally, the probability that RABV persist in the whole population is uniformly higher than 95% for a birth rate higher than 1.22 and for R_0 between 1.02 and 1.16.
If exponentially distributed incubation and infectious period are assumed, the epidemic scenario is extremely different (Figure 5.2 panel b). Firstly a minimum of $R_0 = 1.07$ is required to have a non-zero persistence probability. Secondly a persistence probability of 80% is reached only for R_0 higher than 1.11. The lowest birth rate to have a persistence probability of 80% is 1.22 for $R_0 \geq 1.14$. The area where the observed probability of persistence is higher than 95%, in this case, is restricted to $R_0 \geq 1.14$ if the birth rate is 1.41 and $R_0 \geq 1.13$ if the birth rate is 1.59. Similarly to the previous case also here an increasing annual birth rate leads to higher persistence probabilities.

A detailed analysis of the epidemic outcome and a comparison with empirical observations (described in Section 5.6.1) are performed only for the modeling framework where incubation and infectious periods are distributed according to empirical data, named baseline model (Figure 5.2 panel a).
Since even a single RABV epidemic may have a strong impact on the dogs population size of an entire country (see Section 2.6), we have examined the fluctuations of the average

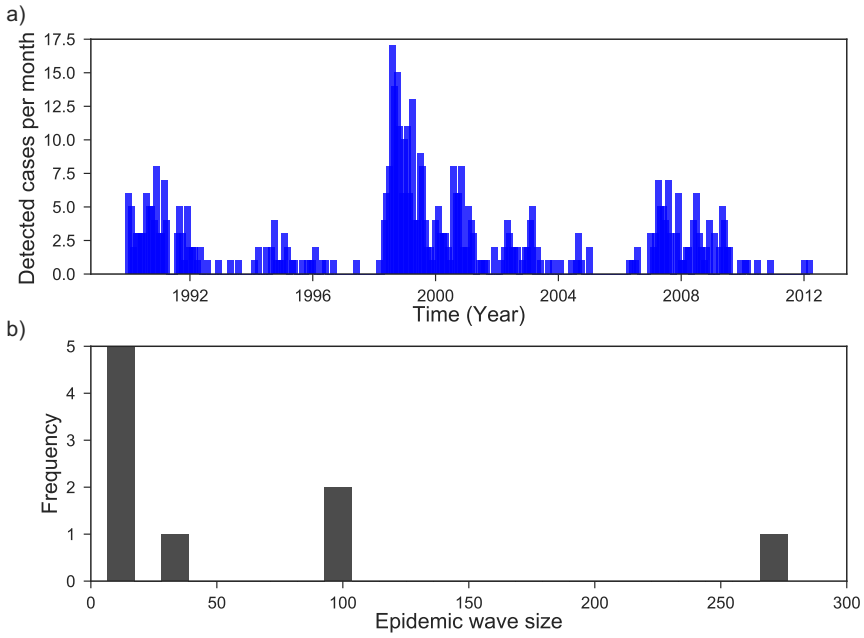

FIGURE 5.4: a) Surveillance data. Number of dog RABV cases in Bangui (CAR) in the period between 1990 to 2012 with monthly sampling [107]. b) Epidemic waves. The distribution of the size of the epidemic waves.

population of domestic dogs in the whole CAR as a function of R_0 and of the annual birth rate. The total population may vary considerably, from -45% to $+30\%$, therefore we restricted our analysis in the region where this variation is limited to $\pm 20\%$ and where the persistence probability is higher than 80%. We tested the variation of the shape of this region both varying the carrying capacity K_i per patch and keeping the detection probability constant $\rho = 20\%$ (baseline value) and varying the detection probability keeping $K_i = 3N_i(0)$ (baseline value) constant. In the first case the shape of the region changes drastically only for $K_i < 2.5N_i(0)$, while for higher values it remains substantially stable (see Figure B.3). In the second case the shape of the region remains more stable in the interval considered (see Figure 5.3). For detection probabilities equal to $5, 10, 20\%$ it exhibits always an equivalent shape: it goes from $R_0 = 1.03$ to $R_0 = 1.06$ for an annual birth rate equal to 1.04, while for higher birth rates (more than 1.22) the region is slightly larger, with R_0 between 1.02 and 1.06. Differently, for a detection probability equal to 50% the region shrinks to $R_0 = 1.06$ for a birth rate equal to 1.04, from $R_0 = 1.03$ to $R_0 = 1.06$ for a birth rate equal to 1.22 and finally for higher birth rates the regions assumes the same shape observed for the other values of ρ.

As showed in Section 5.6.1, the epidemiological data actually available are the result of 20 years of monthly surveillance on dog rabies cases in Bangui (Figure 5.4 panel a [107]). From this time-series we extracted the distribution of the size of the epidemic waves (Figure 5.4 panel b) defining a wave as a set of consecutive RABV cases that starts after at least 4 months of absence of cases and finishes when no case is detected the following month. Using the distribution of the epidemic wave obtained for Bangui we performed a maximum-likelihood analysis of the detection probability ρ, of R_0 and of the annual birth rate (see Section 5.6.2). Figure 5.5 shows the result of the logarithm of the likelihood function, called log-likelihood. Since the logarithm is a monotonically increasing function, the logarithm of a function achieves its maximum value at the same point as the function itself, and hence the log-likelihood can be used in place of the likelihood in maximum likelihood estimation.

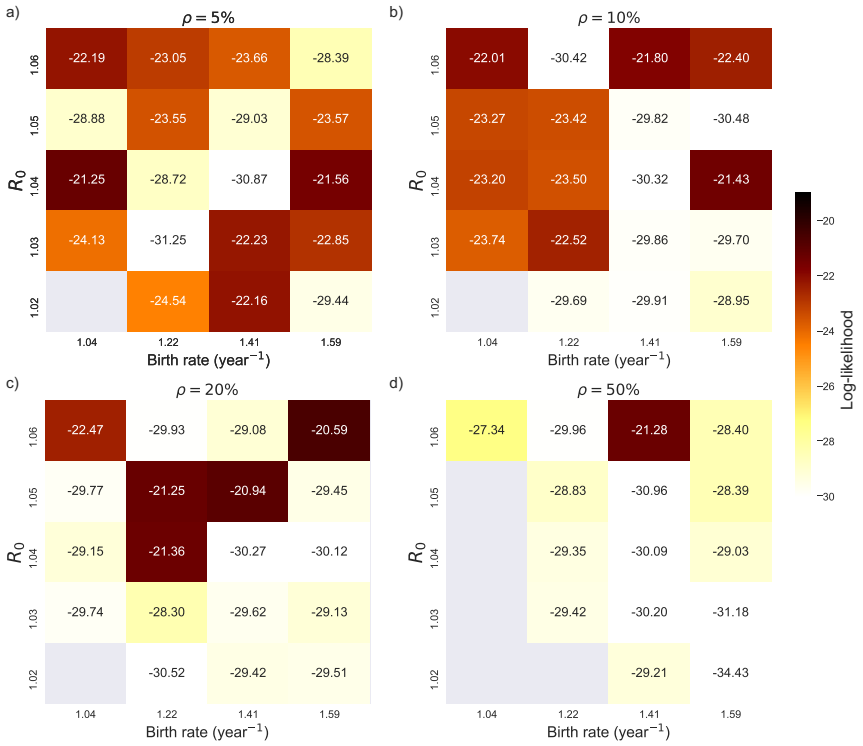

FIGURE 5.5: Heatmap of log-likelihood analysis for a detection probability $\rho = 5\%$ as a function of the basic reproductive number R_0 and of the annual birth rate of the domestic dog population in the area of the parameter space with high persistence probability and stable population. b), c) and d) as in a) for ρ equal to 10, 20 and 50% respectively.

For $\rho = 50\%$ (Figure 5.5 panel d) we obtained the worst accordance with empirical data since the log-likelihood is in general lower in respect to the other scenarios. Differently, for lower detection probabilities such as $\rho = 5\%$ and 10% (Figure 5.5 panel a and b), we observe better results even if the likelihood functions does not exhibit a smooth behaviour, i.e. with a unique and well defined maximum. For example for $\rho = 5\%$, the maximum of the likelihood function is for $R_0 = 1.04$ and the lowest birth rate considered (equal to 1.04) while, keeping the same R_0, we observe a similar likelihood also for the higher birth rate (equal to 1.59). The best estimate is obtained for $\rho = 20\%$ and for $R_0 = 1.06$ and a birth rate equal to 1.59 (Figure 5.5 panel c). Since this point is on the upper left boundary of the parameter space analyzed we verified, including also higher values of R_0 and birth rate in the analysis, that it is a proper maximum of the likelihood function (see Figure B.1). Detection probability $\rho = 20\%$ is then confirmed as baseline values for the rest of the work.

In order to further relate the outcome of our model with empirical observations, we considered the periodicity of the Bangui's surveillance time series (*Bourhy et al.* [107]), which consists in 53.4 and 89.0 months, and we compared it with the periodicity obtained, through wavelet analysis [238], in Bangui in our simulations (see Section 5.6.1). As shown in Figure 5.6 panel a, we analyze in four different points, one is the point identified through the MLE analysis (Figure 5.6 panel a) and the others are chosen to represent the behavior of the system at the boundaries of the region with high persistence and stable population. The shapes of the probability distributions of the dominant periods obtained numerically are relatively homogeneous in the four points and the two periods empirically observed, 53.4 and 89.0 months, are consistently present and around the peak of each distribution (Figure 5.6 panels b, c, d and e). In the two points with higher R_0 the

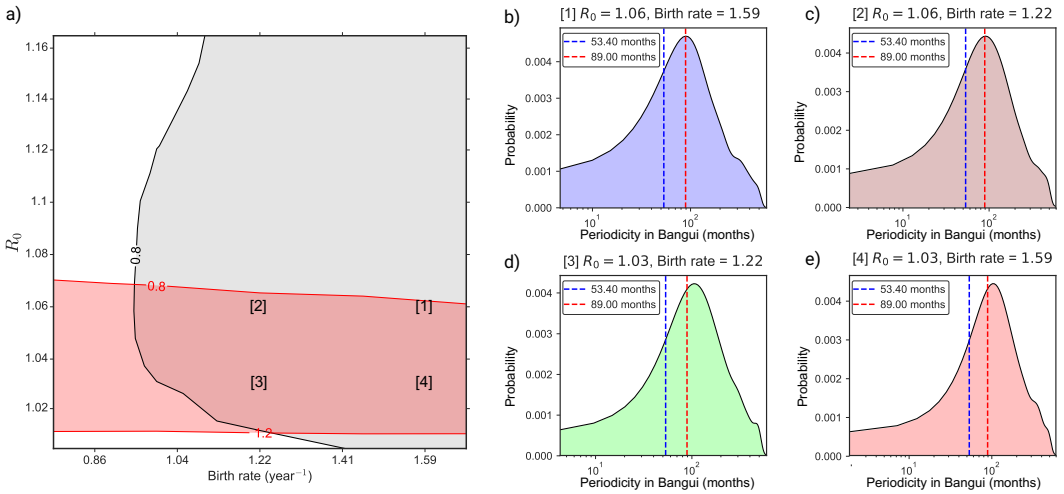

FIGURE 5.6: Detection probability $\rho = 20\%$, comparison with empirical observations. a) Parameter space expressed in terms of the basic reproductive number R_0 and of the annual dogs birth rate: in grey, the area where the persistence probability is higher than 80% (see Figure 5.2). In red the area where the modeled average dogs population in the Central African Republic is equal to the estimated population $\pm 20\%$. b) Comparison between the periods of the epidemic cycles obtained in Bangui through simulations in the points with the maximum likelihood ($R_0 = 1.06$ and birth rate equal to 1.59 dogs/year) and the two empirical oscillation periods of 53.4 and 89.0 months described respectively by the blue and the red dotted lines. c), d) and e) same comparison as in b) but in other points of the parameter space. The detection probability assumed is $\rho = 20\%$.

peak of the two numerical distributions corresponds to the maximum periodicity obtained empirically (Figure 5.6 panels b and c).

5.3.4 Role of the population structure and of the movement range

To assess the role that variations in population structure or in movements range have on the epidemic outcome we analyzed, starting from the baseline model, multiple scenarios trying to disentangle the possible effect of each element. All the models tested are listed in Table 5.1, and a synthetic analysis of the results is shown in Figure 5.7 panel a.
Firstly, to determine the combined impact of spatial structure and mobility we built a framework where both these ingredients are neglected, modeling RABV circulation only in Bangui as isolated patch without any reintroduction. The persistence probability obtained is always equal to zero (Figure 5.7 panel b), even for values of basic reproductive number (R_0) higher in respect to the range used in the other scenarios.
Then, to understand the role of the capital city on the overall epidemic we simulate the infection dynamics in the whole CAR, removing from the network only the patch that corresponds to Bangui. In this case, despite a strong and general reduction in the persistence probability the virus can be maintained (Figure 5.7 panel c). The persistence profile observed has a trend similar to the baseline (Figure 5.2 panel a), where the probability increase with R_0 and with the birth rate. An 80% persistence probability is reached for R_0 between 1.11 and 1.16 and for a birth rate equal to 1.59.
Similar results can be obtained considering, in both aforementioned examples, besides Bangui also all the settlements which are within a radius of 20 km from the capital city. In particular in the first case we built a spatial structured population composed by Bangui

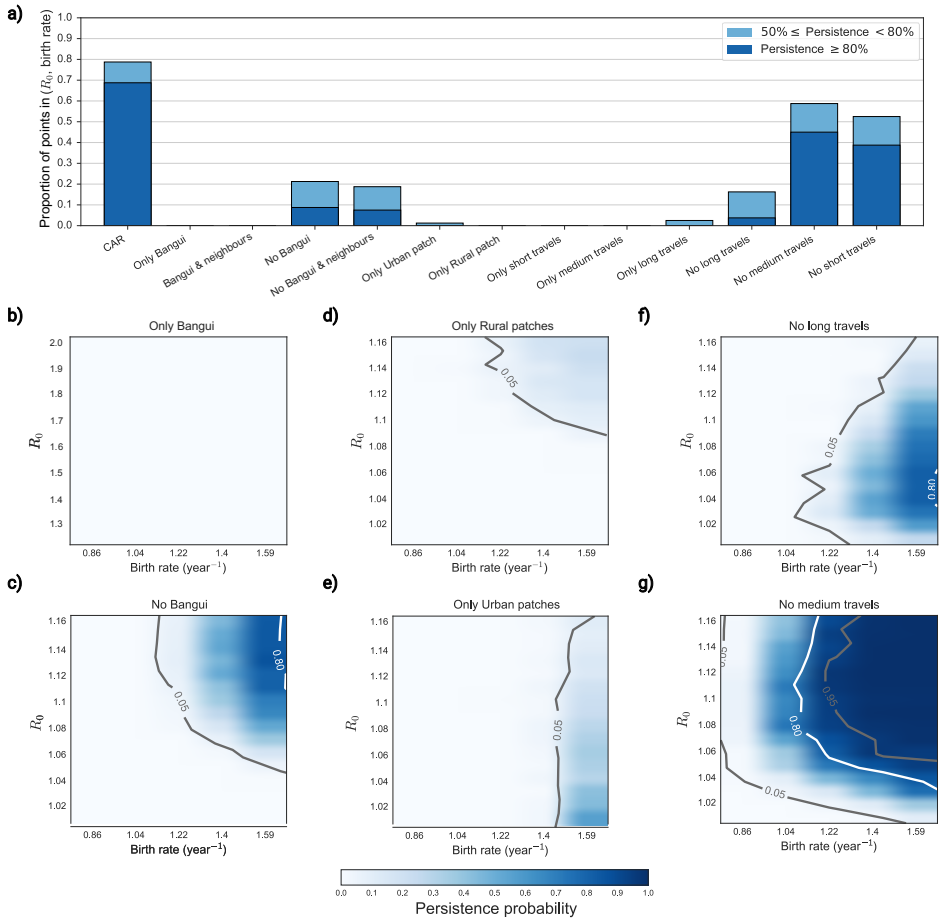

FIGURE 5.7: Rabies virus persistence probability in Central African Republic, tested scenarios. Top: a) The proportion of points within the parameter space analyzed (R_0, birth rate) where rabies persistence probability is higher than 80% (dark blue) and between $50 - 80\%$ (light blue) as a function of the different scenarios tested. Bottom b), c), d), e), f), g) Relevant examples from the scenarios listed in a) of the persistence probability of rabies virus as a function of the basic reproductive number R_0 and of the annual dogs birth rate. The compartmental model consider both the incubation and infectious periods distributed according to empirical data (i.e. gamma distributed). The detection probability assumed is $\rho = 20\%$. Contour grey and white lines indicate a persistence probability respectively larger than 5% and 80%.

and its 13 neighboring settlements (Figure B.2 panel a) and in the second case we removed those patches from the CAR population structure obtaining a network composed by 123 patches and with a population equal to the half of the baseline model in both cases (Figure B.2 panel b).

Further, we explored how the epidemic outcome may vary considering separately rural or urban settlements. In both cases is observed a drastic reduction in the persistence probability in the whole parameters space, reaching at most 20% in the former case (Figure 5.2 panel d) and 56% in the latter (Figure 5.2 panel e). If only rural patches are considered, similarly to the baseline, the persistence probability increases with R_0 and birth rate; while, in the case with a network composed only by urban settlements a nonzero persistence is observed only for a birth rate higher than 1.4 and it declines when R_0 increases reaching the maximum between 1.01 to 1.04.

Finally, to assess the role of the different movement range, we have considered several possible travel restrictions. These restrictions are applied for short (< 20 km), medium (≥ 20 and ≤ 100 km) or long (≥ 100 km) range movements and for each possible combination of two of these travel range. Neglecting long range movements changes radically the epidemic outcome lowering the persistence probability and changing the persistence profile (Figure B.2 panel f). Similarly to what is observed when only urban settlements are considered, the persistence probability does not increase linearly with R_0. The highest persistence probability (82%) is reached for a birth rate equal to 1.59 an $R_0 = 1.05$, for the same birth rate and for higher values of the basic reproductive number the probability decreases up to 6.5% for $R_0 = 1.16$. Differently, if travel restrictions are applied to medium or short range movements the epidemic outcome observed is similar to the baseline with a slightly lower persistence probability especially for low values of R_0, from 1.01 to 1.05, and for birth rate lower than 1.04 (Figure 5.2 panel g and Figure B.2 panel c). For travel restrictions that involve two simultaneous movement ranges the disease almost never persist in the population. If only short or medium travel are included in the framework the persistence probability is always zero (Figure B.2 panels d and e), while if only long range movement are considered a nonzero persistence probability is observed exclusively for $R_0 \geq 1.12$ and for birth rates higher than 1.22 (Figure B.2 panel f).

5.3.5 RABV prevalence and the epidemic concentration curve

To have a better insight into the RABV endemicity in CAR we analyzed the prevalence (i.e. the proportion of infected) that we obtain as result of our stochastic model in each subpopulation, using the values of ρ, R_0 and birth rate that better agree with surveillance data (see Section 5.3.3). Figure 5.8 panel a, provides a spatial visualization of the RABV prevalence in the country showing the percentage of domestic dog population that is infected by the virus. We found a quite different level of infected in the different regions, in particular we can divide the country in three geographical areas. In the East part, from the region on Bamingui-Bangoran to Vakaga in the North and from Basse-Kotto and Haut-Mbomou in the South, the prevalence obtained is always lower than 10% with minimum of 0.2% observed in the eastern regions. The Central part contains all the regions with higher prevalence, in particular in the South with Bangui's suburban area, Ombella-M'Poko and Lobaye. Around Bangui and in the South of the Ombella-M'Poko we observe the highest percentage of infected dogs with a prevalence that is always higher than 20% for both rural and urban patches. Finally, the West side of the country is also characterized by an average high prevalence that is however lower than 20%.
To have a quantitative estimation of the degree of urbanization and dispersion of RABV infection in rural areas we computed the epidemic concentration curve (ECC) (see Section 5.6.2). This curve shows an homogeneous level of infected in rural (green) and urban (black) area, and there is no evidence of a different behaviour in the two classes. Moreover, the RABV prevalence is on average similar: 19% in urban and 16% in rural subpopulations.

5.4 Discussion

Controlling and eliminating rabies in dogs mainly by the implementation of strict control measures including mass dog vaccination campaigns, is now considered as the most cost effective measure to prevent rabies in humans [228]. However a better understanding of the dynamics of rabies virus infection in dog population would further provide guidance in planning and implementing these control measures.
For direct host-to-host contact transmitted diseases, like rabies, transmission occurs with a higher probability if the interaction is more intense/frequent, which implies a crucial

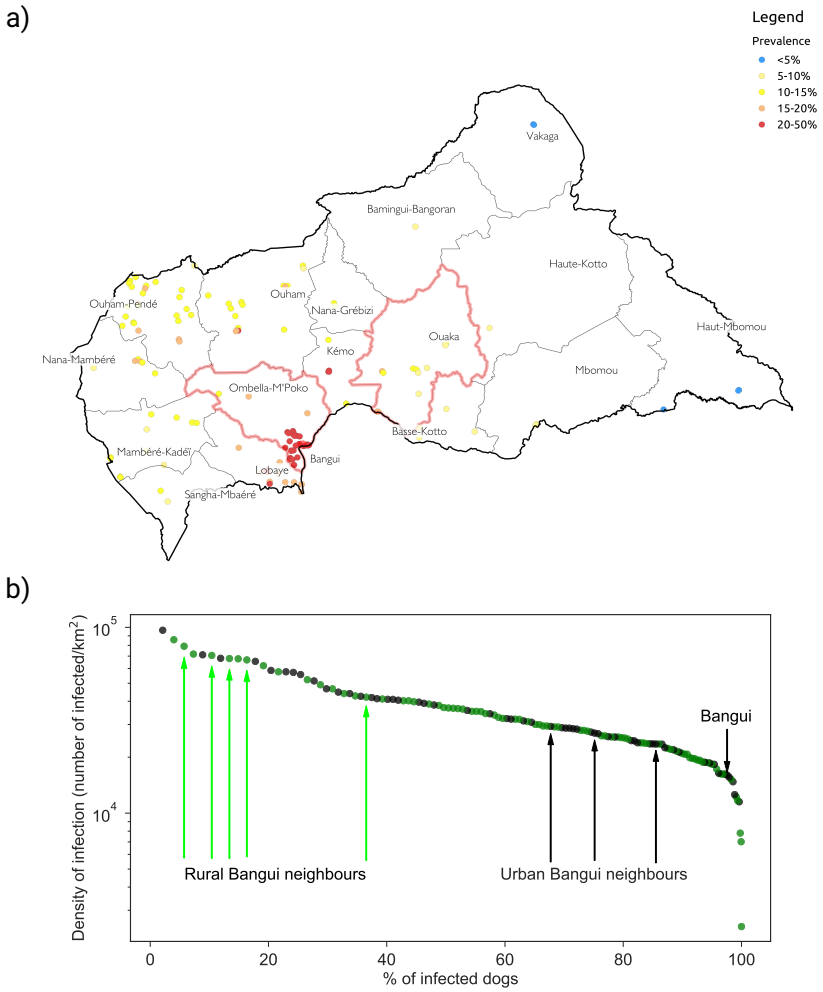

FIGURE 5.8: Rabies virus prevalence in Central African Republic. Top: a) Geo-spatial distribution of the RABV prevalence in the domestic dog population in the country, each point represents a patch centroid. The color of each point is related to the average prevalence in that subpopulation ranging from light blue, for low prevalence ($\leq 5\%$), to dark red, for prevalence between 20% to 50%. The highlighted regions (Bangui, Ombella-M'Poko and Ouaka) represent the areas where an higher number of cases have been detected in 2012 surveillance [106]. Bottom: b) Epidemic concentration curve (ECC) for RABV prevalence in domestic dog population in Central African Republic, the green points represent rural patches while black points represent the urban one.

role of spatial distribution and mobility of the host population. Considering domestic dogs as hosts, these two factors are mainly connected to human demography and spatial heterogeneities, thus RABV dynamics strongly relies on the specific geographical region examined [146, 194, 236].

All the studies made on RABV in domestic dogs are developed after extensive data collection programs [145, 146, 194, 236] and some of the conclusion achieved are specific and hardly generalizable to other environments [146, 194, 236]. In order to tackle this problem we developed a framework that can be easily extended to other context since the domestic dog population is estimated using public world database of human demography (WorldPop) [239–241] as proxy, and the mobility is based on a diffusion model which is general and already tested in the prediction of the rabies spread in domestic dogs [113].

The migration probabilities obtained in our environment corroborates with a recent observation performed on domestic dog rabies in the Philippines [146] considering, however, all the substantial differences between the two countries.
We started from the endemic context of the domestic dog population in Central African Republic [106, 107, 229] where no recent vaccination campaign has been recently implemented, and we developed a spatial explicit metapopulation model accounting for: sparse and fragmented host population, since a strong spatial structure can be crucial for the persistence of endemic pathogens [125, 162]; realistic distributions of incubation and infection periods characteristic of dog rabies [81]; local infection dynamics (in each settlement) and country level disease spread given by short, medium and long range movements of infected hosts. The aim is to determine the impact of these aspects on the RABV epidemiology and on the maintenance of the disease. Several parameters that characterize the RABV infection depend on the particular geographical area [115] thus we used numerical simulations to explore multiple values of these parameters.
The inclusion of empirical distributions in the infection stages changes considerably the epidemic scenario favoring the circulation and the maintenance of the pathogen, as the comparison between the two spatial models in Figure 5.2 shows. A potential explanation can be the different timing that exists between the infection dynamics and the hosts' migration in the two cases. Even if a short infectious period (on average 3.1 days) may reduce the spatial and temporal scale at which the host can shed the virus, a long and heterogeneous incubation period allows the migration of infected for longer time and for larger distances. In the model with exponentially distributed incubation and infectious periods many hosts remain exposed or infectious for a shorter time, so an important proportion of exposed hosts become rapidly infectious and eventually dies. Moreover, due to the restricted mobility of infectious animals [115], the spatial dispersion of the pathogen can be reduced. The impact of realistic distributed disease stage on the dynamics and persistence of an infectious disease has been already explored for several pathogens (i.e. measles, HIV, etc.) and has shown always a substantial effect on the pathogen endemicity [165, 166, 170, 242–244]. Anyway, despite these considerations, only recently it is being applied in dog rabies modelling [194, 195, 236].
Analyzing in detail the baseline framework, we characterized the values of the parameters where RABV has a high probability to persist and where the population remains stable during the dynamics (Figure 5.3). In this region of the parameter space we estimated the detection probability, the basic reproductive number and the annual birth rate of the domestic dog population through a maximum likelihood analysis of our model on the size distribution of the epidemic waves obtained through 20 years of surveillance in Bangui [107]. The best estimate is $\rho = 20\%$, $R_0 = 1.06$ and 1.59 annual birth rate (Figure 5.5). Moreover, we found that for all the detection probabilities explored it is possible to have a stable dog population in the whole CAR and a high persistence probability of the pathogen only for values of between 1.03 and 1.07 and with an annual birth rate higher than 1.04 dogs/year. This area of the parameters space is compatible with recent estimates made for rabies in domestic dogs [236]. Higher transmissibility, 100% mortality rate and an absence of vaccination could lead to a drastic reduction of the host population since a single rabies epidemic can eliminate a large proportion of the total dog population [89, 122, 145], therefore a basic reproductive number below 1.06 and a high population turnover permit the circulation of a lethal virus like rabies keeping the host population stable.
To compare the outcome of our model with the epidemic activity observed during 20 years of surveillance in Bangui (see Section 5.6.1), we considered the periods of the epidemic cycles obtained by *Bourhy et al.* in [107]. These two periods, which are respectively 53.4 and 89.0 months, are consistently present and around the peak of each numerical

distribution obtained from the different reproductive numbers and annual birth rates considered (Figure 5.6 panels b, c, d and e). In particular a better accordance is observed for $R_0 = 1.06$ regardless of the annual natality rate. Even if this comparison has limitations given the shorter time length of the surveillance data (about 267 months) in respect to the numerical time series (more than 4 000 months), similar periodic patterns have been already observed in other African countries [81, 111].

Our findings predict that spatially fragmented and heterogeneous population represents key elements in the RABV persistence in domestic dogs. The endemicity can be obtained only in spatial explicit models, instead in isolated environments (Figure 5.7 panel a, Figure B.2 panel a) the pathogen tends to fade out. This outcome is in agreement with the results obtained through the phylogenetic analysis made in Bangui [107] where the authors found that, even if the virus appears to be endemic the actual epidemiology is given by re-introduction of new lineages from outside the city.

Interestingly, considering the network of Bangui and its 13 nearby settlements, which consist of almost 50% of the total host population, the persistence probability is constantly zero for each value of the parameter space explored. Differently, the pathogen may persist, although with a reduced probability, removing Bangui or Bangui and its surrounding area from the whole network. This result points out that the most populated region in CAR is important but not critical in the disease persistence, and, on the contrary, a crucial role is played by the spatial heterogeneity of hosts distribution. An heterogeneous spatial structure of the host population coupled with the mobility plays a major role RABV circulation, because it makes possible the host's circulation that leads to a sequential reintroduction and infection of disease-free areas.

The domestic dogs movement pattern considered in our work does not include only short distance natural dispersal which for a healthy domestic dog is around 50 metres per day, from the home bases with a maximum of 3.2 km [88, 115], but also human-mediated long-range movements which seems crucial for the virus dissemination both in domestic [113, 232, 245] and in wild animals [124]. We modelled dog movements considering results obtained in [113], in particular in our model the travel probability declines as the Euclidean distance between two patches increases. The separate effect of each range in RABV endemicity is shown in Figure 5.7. Our results show that long range movements have a particular role in the virus circulation even if they are not frequent. Removing all the long range movements from the metapopulation framework can drastically reduce the persistence probability for all the values of R_0 and of the annual birth rate explored. It may happen that, even though the disease dies out in an asynchronous way in the different patches of the model, long range movements favor the occasional reintroduction and the re-synchronization of the infection (Figure B.2). Moreover, short and medium range movements restrict the hosts dynamics to a local scale therefore the infection remains confined and tends to fade out. To have a high persistence probability in a large area of the parameter space it is necessary to combine at least long range movements with short or medium range movements (Figure 5.7).

Our result indicate that large cities are not the only crucial determinant in the dynamics and maintenance of rabies and that efforts of control of rabies should target surrounding areas and villages disseminated in the country side.

Summarizing mobility, spatial explicit structure and long and heterogeneous incubation period are crucial in order to understand how the maintenance and the extinction of rabies virus occur in the domestic dog population.

Unfortunately, no information is available on the carrying capacity in the different settlements considered in our model. However, even if this quantity is hard to estimate and in literature can vary from twice the host population [236] to more [246], from the analysis that we made testing different values of K it emerges that this variable has a negligible

impact in the epidemic outcome at least if $K_i \geq 2.5N_i(0)$ (see Figure B.3). This can be related to the fact that for lower carrying capacity the threshold of the population size in each patch is too strong and it may contrast the oscillating behaviour of the population during the infection.
RABV transmission from other host reservoir species (i.e. wildlife in general) to domestic dogs is assumed not to be relevant considering that dogs are the reservoir for rabies in sub-saharan Africa [91, 104, 124], that dog to dog transmission is approximately eight times as common as transmission between dogs and other carnivores [91], that domestic dogs live mostly in human settlements where interactions with wildlife are sporadic and that epidemiological cycles of RABV maintained in non-flying wildlife mammals are geographically limited in Africa and to our knowledge not present in CAR [226]. Moreover, it seems that spillover of directly transmitted pathogens between domestic dogs and wildlife might be infrequent and rarely followed by onward transmission to other hosts [88].
Finally, since not data are available on the import and export of domestic dogs in CAR due to humans relocation we considered the whole country as an isolated system. This assumption is a simplification of the reality, as already highlighted in Section 2.5.2, since human mobility facilitated domestic dog movements and rabies diffusion also among different countries [82, 110, 121]. However, as obtained by *Talbi et al.* [113], the RABV diffusion process between countries is somehow restricted and limited by geopolitical boundaries. Therefore the reintroduction from neighboring countries, even if clearly important, can be occasional. However, as a future step it may be useful to include also this type of inter-regional movements or through a sporadic introduction of infected dogs or by adding other regions in our framework. The last choice can help to develop a more realistic model that can contribute to the identification of an appropriate control strategies also at interregional level. Actually, the African public health authorities are moving in to this direction, creating networks among different countries in order to facilitate the coordination between animal and human health sectors across national, regional and continental levels [247, 248].

5.5 Conclusions

Our model allows the exploration of parameters and conditions characterizing the RABV transmission dynamics in the domestic dogs population and improves our knowledge on the conditions for persistence and the relevant mechanisms affecting it. The interplay between the peculiar heterogeneity of rabies incubation period and a sparse and fragmented dog population is essential for the maintenance of the virus. Moreover it seems that also the rapid turnover of the domestic dogs is crucial for the disease persistence. The model developed in this work may be applicable to design efficient and cost-effective control strategies not only in the Central African Republic, the country analyzed, but also in in many different settings in countries where the disease is endemic.

5.6 Methods

5.6.1 Epidemiological data

The dataset refers to RABV cases in Bangui, the capital city of the Central African Republic, and it is obtained by *Bourhy et al.* [107]. In our analysis we considered the number of domestic dog RABV cases during the sampling period (1990-2012 with monthly sampling). This time-series was analyzed through wavelet analysis and periodogram [238] obtaining two dominant periods of oscillation: 53.4 and 89.0 months. The detection probability ρ in [107] is assumed in the range between 5%-50% to account for low surveillance

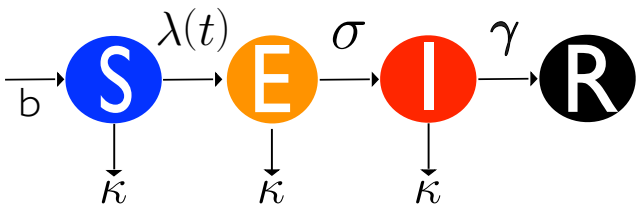

FIGURE 5.9: Compartmental structure. It is composed by susceptible (S), exposed (E), infectious (I) and removed (R). The model considers only invariably fatal infections.

efforts combined with the incubation plus infectious period reported for dogs in Africa [81].

5.6.2 Metapopulation model

Infection and vital dynamics

RABV infection dynamics in dogs is in general described by a SEIR compartmental model (see Section 3.2.3) where the hosts can be: susceptible (S), healthy individuals that may acquire the infection with a force of infection; exposed (E), the hosts who have contracted the infection but cannot shed the virus throughout the incubation period of average duration; infectious (I), the individuals who can transmit the virus during an infectious period of average duration; removed (R), the hosts after the infectious stage who are removed from the population because rabies is fatal once clinical symptoms appear (see Section 2.4). A schematic representation of the compartmental model is provided in Figure 5.9. In the classic compartmental model approach the transition rates between compartments (e.g. from exposed to infectious) are constant as a result of exponentially distributed sojourn times [114, 149]. Even if this simplifying assumption lead to an analytically convenient mathematical treatment, for RABV it may not adequately reflect the reality [170] (See Section 3.2.3). The empirical distributions of the incubation and infectious periods for RABV in African domestic canine population were obtained by *Hampson et al.* [81] through a contact tracing study on rabid dogs in Tanzania and both shapes observed are non-exponentials, but fitted with two gamma distributions (See Section 3.2.3). To incorporate the empirical gamma-distributed incubation and infectious periods in the compartmental model, we used the approach already adopted by [166, 170] and showed in detail in Section 3.2.3. Both infected compartment are divided into m and n subclasses, which are the shape of the gamma distribution of the incubation and infectious periods respectively. To keep the same average time spent in the two classes σ^{-1} and γ^{-1} the rates of movement between the subclasses are defined as $\sigma = m\sigma'$ and $\gamma = n\gamma'$, respectively.
To assess the role of the empirical shapes in the epidemic outcome, we also analyze the case with constant rates of transition σ and γ, which are the average values of the two distributions. Vital dynamics is included in both models assuming that newborns enter in the susceptible class with rate b, whereas individuals in each compartment may die with rate μ. The estimation of the natural death rate of domestic African dogs is obtained from Ref. [81] and it is given by the reciprocal of the average life expectancy. The

size of the population follows a logistic growth model, assuming that increasing mortality rates constrain population growth as the population approaches a defined limit, known as the carrying capacity K, which represents the maximum number of individuals that an environment can sustain without any infection. The carrying capacity is specific of the habitat and it is proportional to the local disease-free population [157]. The size dependent death rate is therefore defined by $\kappa = \mu + (b - \mu)N(t)/K$, where $N(t)$ is the host population at time t. Different studies analyzed the demographic parameters for domestic dog population in Africa and Asia providing estimates based on cross-sectional household questionnaire surveys of dog owners [249–251]. The birth rate obtained is in general high and it can vary drastically among different geographical areas [81, 91, 99, 102, 103, 236, 249, 252]. In order to mimic this heterogeneity and the high turnover empirically observed we have explored a range of values for this variable (Table 5.2).

Domestic dogs demography

The habitat of the domestic dog population is strictly related to the different human settlements (i.e. villages, towns and cities) and in general it is estimated administering questionnaires to a selection of households [99, 102, 103, 108, 250, 251]. Unfortunately, there is no availability of such kind of data for Central African Republic perhaps because this method is extremely challenging and costly to be applied to the whole country. As suggested in [1, 102, 108], human settlements can be considered as dog habitat, so domestic dogs population can be estimated using human population as a proxy. In particular two kinds of environment are considered: urban, with more than 1 000 individuals per kilometers squared and with a human to dog ratio equal to 21.20; rural, with less than 1 000 individuals per kilometers squared and a human to dog ratio equal to 7.40. To capture the highly fragmented and complex landscape given by the distribution of human communities in CAR we used *WorldPop* [239–241], a high resolution dataset on human population. This raster dataset is made by a gridded population matrix with a pixel resolution of approximately decimal degrees (approx. 100 meters at the equator) that can be changed hierarchically aggregating the pixel cells. In order to build communities, all the scarcely populated cells (with less than one human per pixel) are filtered and then all the cells which have at least one side in common are merged together. The resulting scenario is an ensemble of geolocalized patches of human communities with a certain size, spatial extension and density from which we finally obtain the distribution of domestic dogs sub-populations. The method used to build domestic dogs communities is described in detail in Section 3.3.5.
In each patch i, we define also the characteristic carrying capacity K_i which is proportional to the initial estimated population $K_i = 3N_i(0)$. We also considered, as sensitivity analysis, different values of carrying capacity (in the range $[2.5N_i(0) - 3N_i(0)]$) because this ecological parameter is given by a composition of multiple and non-trivial factors which are extremely challenging to estimate.

Mobility model

The other crucial input for the metapopulation model is the coupling among subpopulations, which corresponds in this case to the canine movements within the country. Unfortunately for domestic dog movements no data is available for Central African Republic. However in a recent work [113], combining spatial epidemiology and a Bayesian phylogeographic approach, some diffusion models are tested in order to determine which of them can predict the dog RABV dissemination in Algeria and Morocco. Road distance model and great-circle (Euclidean) distance model appear to fit better the spatial spread

of the pathogen. For sake of simplicity, as already done in [194], we use the great-circle distance model to evaluate the number of migrating dogs between patch i and patch j, defined as $w_{ij} = \frac{C}{d_{ij}}$. C is a scale factor that limit the maximum number of dogs that can daily escape from each patch to the 1% of the patch population, d_{ij} is the great circle distance between i and j, defined as the shortest distance between the two centroids on a surface of a sphere.

Maximum likelihood estimation

In statistics, maximum likelihood estimation (MLE) is a method of estimating the parameters of a certain statistical model given observations, by finding the parameter values that maximize the likelihood of making the observations given the parameters. In our case, the observations are the empirical size of the epidemic waves. The probability to have an empirical wave of size $\{s_i^*\}$ conditioned to ρ, R_0 and to the annual birth rate defines the likelihood function:

$$\mathcal{L}(\rho, R_0, \text{birth rate}) = \mathcal{P}(\{s_i^*\}|\rho, R_0, \text{birth rate}) \tag{5.1}$$

Maximizing this function we obtain a value for the three parameters that better agree with empirical data. The set of numerical observation of the distribution of the epidemic waves in Bangui allows the definition of the discrete probability $P_i(\{s_i\})$ as the fraction of times that an certain size $\{s_i\}$ for an epidemic wave is observed. The procedure is iterated for the different values of ρ, R_0 and birth rate to reconstruct the likelihood function $\mathcal{L}(\rho, R_0, \text{birth rate})$. Since the phylogenetic analysis conducted in Bangui [107] (Figure 2.7 panel b) suggests that the wave like behaviour observed through surveillance is given by the extinction of local chains of transmission coupled with the re-introduction of new lineages from outside, we can consider the waves sizes as statistically independent variables. Therefore we can factorize the total probability $\mathcal{P}(\{s_i\})$ in the product of the the distribution for each size of the epidemic wave:

$$\mathcal{P}(\{s_i\}) = \prod_i P_i(s_i) \tag{5.2}$$

Changes in population structure and mobility

To assess the different contributions on RABV endemicity given by all the ingredients that are part of the metapopulation model, we tested how the spatial configuration of the host population and the mobility can affect the epidemic outcome.
From the data sampling and the phylogenetic analysis made in [107] it seems that, in Bangui, the virus circulation is sustained by some accidental reintroductions from outside. To understand if those reintroduction are required to have the observed long term persistence we analyze the dynamics of the pathogen taking into account Bangui as an isolated environment.
The second scenario explored is a metapopulation model where the only patches considered are Bangui and his neighboring area (villages distant less than 20 km). In this case we want to determine if the circulation of the virus can be sustained in a localized geographical area composed by a densely populated patch (Bangui) surrounded by a lot of different smaller patches (the neighboring area).
In third and in the fourth scenarios we tested the role of Bangui and his neighboring area respect to the whole country, thus we simulate the virus circulation excluding respectively only the capital city or the capital city and the neighboring area from the network framework.

Domestic dog communities are classified in rural and urban depending on the type of human settlement they belong to, thus to understand the respective role of these communities in the dynamic and persistence of RABV we explored two other scenarios obtained removing from the network or all the urban patches or all the rural patches. In the last set of scenarios we investigate the role of the different animal movements range in the circulation of the pathogen. In particular we tested the relevance of long, medium and short range animal movements and also all the possible combination of two of them.

Epidemic concentration curve

The epidemic concentration curves is obtained following a recent work on the geospatial mapping of HIV infection in sub-Saharan Africa [253]. In particular we considered the average number of infected in our model ψ_i, where i indicates the patch, and then we ordered all the different ψ_i in ascending order as $\psi_i^{\mathsf{min}}, ..., \psi_i^{\mathsf{max}}$. The ECC is than obtained plotting the variable s_j with $j \in [0, \psi_i^{\mathsf{max}}]$ on a semilogarithmic scale where:

$$s_j = 100 \left(\frac{1}{I}\right) \sum_{\psi_i \geq j} \psi_i \tag{5.3}$$

and:

$$I = \sum_{i=1}^{N} \psi_i \tag{5.4}$$

where $N = 137$ is the total number of subpopulation in our model.

Numerical simulations

We consider discrete stochastic numerical simulations for RABV transmission in the canine populations to account for stochastic extinction events that may be favored by the small population of some settlements. A continuous formulation of the metapopulation model would not be appropriate for addressing infection extinction phenomena. Indeed, assuming individuals to be described by a continuous variable would allow for unrealistic fractions of infected individuals to indefinitely sustain the epidemic. Time is considered discrete with a daily timescale. Since the disease is endemic in the country [106], in the seeding process each patch i is seeded with a certain number of exposed $E_i(0)$ and $I_i(0)$ infectious. Those numbers are obtained defining in Bangui, the only patch for which epidemiological data are available [107], the proportion of RABV infectious dogs in endemic condition η as the median number of detected cases during the observation period divided by the estimated dog population of the city. This calculation is made rescaling the time series with the detection probability assumed. The proportion of exposed in endemic condition ν is than obtained through simple numerical calculations. Therefore, the seeding process can be done adding in each patch i with a population N_i a number of exposed and infectious equal to $E_i(0) = \nu N_i(0)$ and $I_i(0) = \eta N_i(0)$ respectively.
The persistence probability of RABV infection is defined as the fraction of stochastic simulations for which the virus still circulates in the host population at the end of the simulation time. A total of stochastic runs are simulated starting from the same initial conditions and lasting 250 years in order to reach the endemic equilibrium following the initial transient. All the simulations are implemented in C++, and technical details are reported in Section 3.3.5. Sensitivity analysis on numerical aspects of the simulations was also performed.

Scenario	Number of patches	Number of links	Population
CAR	137	9 316	76 992
Only Bangui	1	0	36 089
Bangui & neighbours	14	91	38 129
No Bangui	136	9 180	40 903
No Bangui & neighbours	123	7 503	38 863
Only Urban patches	58	1 653	69 250
Only Rural patches	79	3 081	7 742
Only short travels	137	183	7 6992
Only medium travels	137	951	76 992
Only long travels	137	8 182	76 992
No long travels	137	1 134	76 992
No medium travels	137	8 365	76 992
No short travels	137	9 133	76 992

TABLE 5.1: Scenarios tested. Properties of each scenarios tested for the RABV persistence.

Notation	Parameter description	value
σ^{-1}	average incubation period	22.11 days [81]
γ^{-1}	average infection period	3.1 days [81]
μ^{-1}	average life period	2.2 years [81]
m	shape of gamma distribution incubation period	2.0[81]
σ'	scale of gamma distribution incubation period	11.055[81]
n	shape of gamma distribution infectious period	3.0[81]
γ'	scale of gamma distribution infectious period	1.1[81]
R_0	basic reproductive number	1.01 - 1.4 (Bangui) 1.01 - 1.17 (CAR) [81]
b	annual birth rate	1 - 1.59 years [81, 236]
K_i	carrying capacity patch i	$3N_i[2 - 4.5N_i]$
ρ	detection probability	$20\%[5, 10, 50\%]$ [107]

TABLE 5.2: Parameters description and values.

6 CONCLUSIONS AND OUTLOOK

In this thesis I described how multidisciplinary knowledge can be integrated through a mathematical model and incorporated into a computational framework to identify the main mechanisms that underlie rabies persistence in different realistic settings such as: two interacting bat species in a system of caves in Catalonia (Spain), domestic dog population of Central African Republic.
My research is motivated by the challenging perspective of finding the interplay between epidemiological, virological and ecological factors in rabies spread and circulation with the aim of refining surveillance and implementing more efficients control strategies.
The development of metapopulation models in conjunction with complex networks theory led to an innovative approach that integrates those different factors in analyzing large-spatial scale transmission of emerging diseases. This powerful tool has already proven its efficacy in the analysis of the epidemics spread of diseases like influenza [254, 255], SARS [256] and MERS-Cov [257] on a global scale. It represents the proper framework to model rabies since it gives the possibility to incorporate environmental stochasticity and landscape heterogeneity among coupled subpopulations of hosts linked through animal movements.
In the first part of the thesis we employed this approach to identify the mechanisms responsible for the empirically observed EBLV-1 persistence in *M. schreibersii* and *M. myotis* species accounting for roosts ecology, seasonal effects, migratory paths, disease progression, and bat species richness based on a field survey.
Our results confirm the importance of bats' ecology on lyssaviruses persistence and provides numerical evidence supporting the fact that the two species analyzed tolerate EBLV-1 natural infection and may also acquire transient immunity. Seasonal migration of *M. schreibersii* and cross-species mixing result critical factors to have persistence in multiple species and large-scale spatial diffusion of the virus. Differently, seasonal variation in transmissibility is not critical in order to achieve accurate predictions of viral persistence. Our findings suggest that efforts should be invested in accurately tracking bats' movements and in targeting caves that host multiple species for their role in the disease maintenance.
In the second part of the thesis we tackled the problem of the RABV endemicity in domestic dog population. We considered both local-scale factors such as dogs' high reproduction rate, local transmissibility and empirical distribution for incubation and infection periods and large-scale factors such as the sparse and fragmented dog population and human-mediated dog movements. With respect to the previous approach, this is more theoretical since no data were available on domestic dog demography and on dogs' movements in the country that we used as case of study (Central African Republic).

Our work confirms the importance of the inclusion of empirical distributions in the infection stages because the characteristic heterogeneous incubation period allows the migration of the infected for longer time and for larger distances favoring the circulation of the pathogen. Spatially fragmented heterogeneous populations and long range human-mediated movements represent the other key elements in RABV persistence. Efforts in rabies control should reduce or regulate human-mediated movements to avoid the reintroduction of the pathogen in disease-free areas and target with parental vaccination not only urban areas but also the surrounding peri-urban and rural areas to contain the transmission on local scale.
Fine-scale data on within cities and villages dogs social and spatial organization would be very useful in the understanding of the different dogs ecology in the two environments. In my knowledge two different projects already started to collect data on the roaming behavior of free-roaming domestic dogs in two different geographic areas of Sub-Saharan Africa. In those projects domestic dogs are instrumented with proximity sensors or/and GPS collars to identify their position, the characteristic roaming behaviour and to measure the social structure and the daily contact network with a high spatial and temporal resolution. A better knowledge of the domestic dogs ecology will improve the accuracy of our framework helping the model calibration in order to develop a more accurate perspective on rabies transmission on local and national scale. Moreover, the model could be further developed considering the culling of rabid dogs that show the characteristic symptoms of the disease, since in reality any detected rabid dog is usually culled to stop the transmission. In conclusion, our model can be used to design efficient and cost-effective control strategies firstly in Central African Republic where rabies is endemic and a vaccination campaign is needed, but also in other countries since our modeling approach can be adapted to different contexts.

A

Sensitivity analysis on EBLV-1 Persistence in Catalonia

A.1 SA3. Sensitivity analysis on the duration of the infectious period

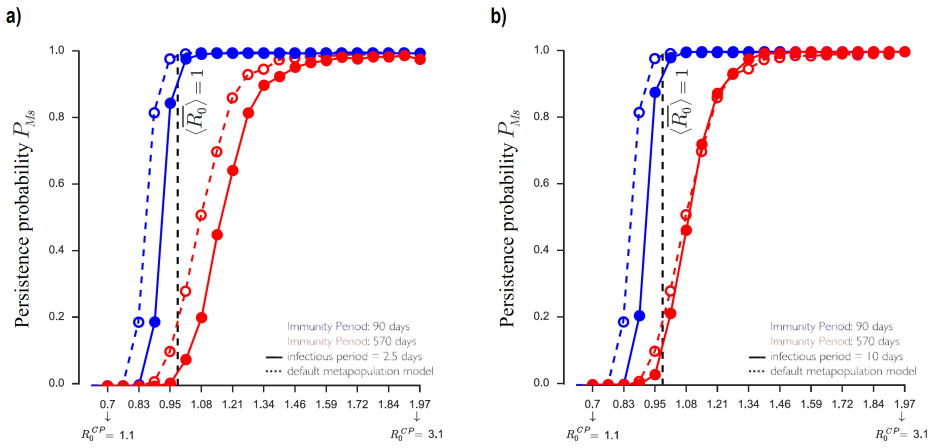

FIGURE A.1: Impact of the infectious period. a) Persistence probability P_{Ms} as a function of $\langle \overline{R_0} \rangle$ for two values of the immunity period ($\omega^{-1} = 60$ and $\omega^{-1} = 730$ days), comparison of infectious period equal to 2.5 days (continuous line) with respect to default value (dashed line). b) as in a) with infectious period of 10 days. The vertical dashed line indicates $\langle \overline{R_0} \rangle = 1$.

A.2 SA4. Sensitivity on ecological parameters from empirical estimates: population sizes, migration (starting, duration)

A.2.1 Sensitivity analysis on bats population size

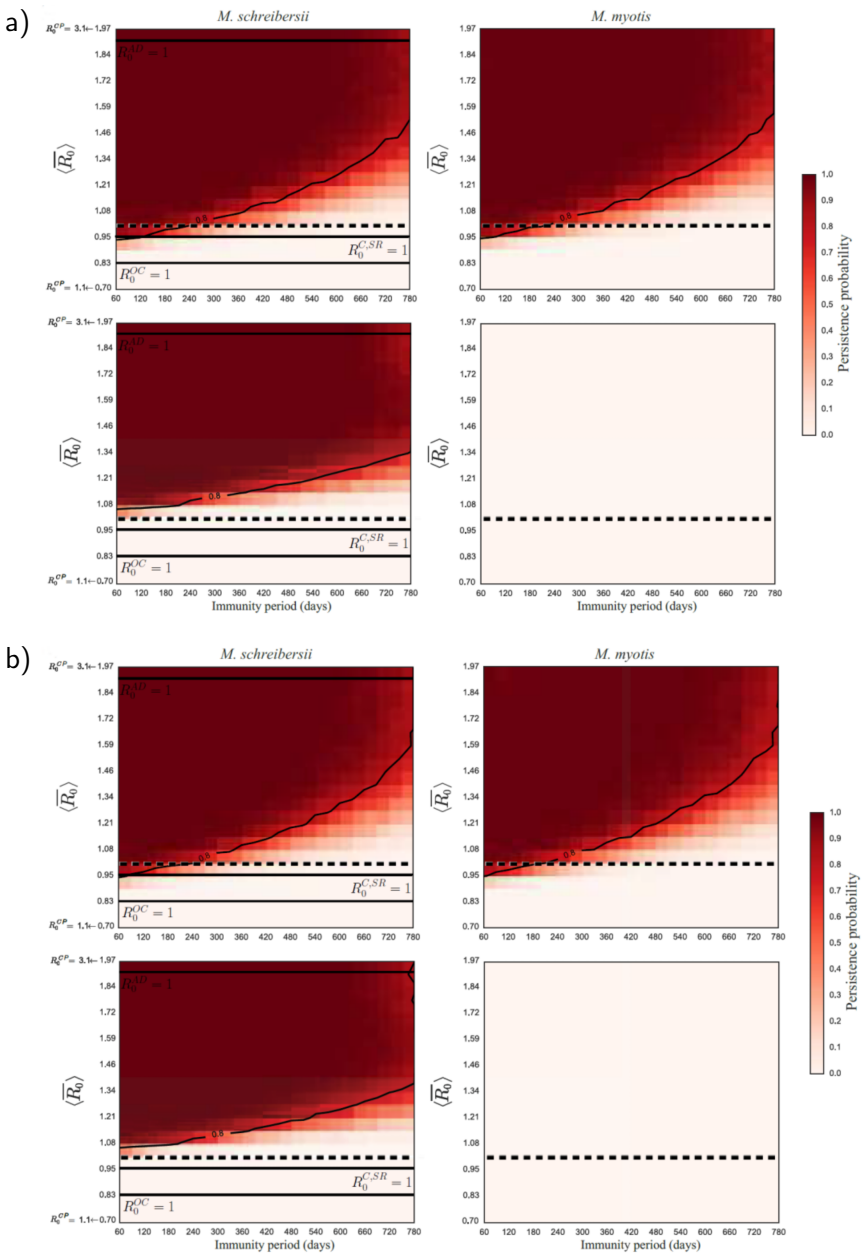

FIGURE A.2: Impact of the initial *M. schreibersii* population on the persistence probability of EBLV-1 in *M. schreibersii* and in *M. myotis* in model 3 (SA4). a) Persistence probability of EBLV-1 in *M. schreibersii* (left) and in *M. myotis* (right) as a function of the average reproductive number of the metapopulation system $\langle \overline{R_0} \rangle$ and of the immunity period (ω^{-1} , in mixing (top) and non-mixing (bottom) conditions, for an initial population of 16000 *M. schreibersii* and 500 *M. myotis*. b): as in a) but with an initial population of: 18000 *M. schreibersii* and 500 *M. myotis*. Contour lines indicate a persistence probability of 80%. The dashed horizontal line refers to $\langle \overline{R_0} \rangle = 1$. Solid horizontal lines refer to threshold conditions ($R_0^p = 1$) for the all caves.

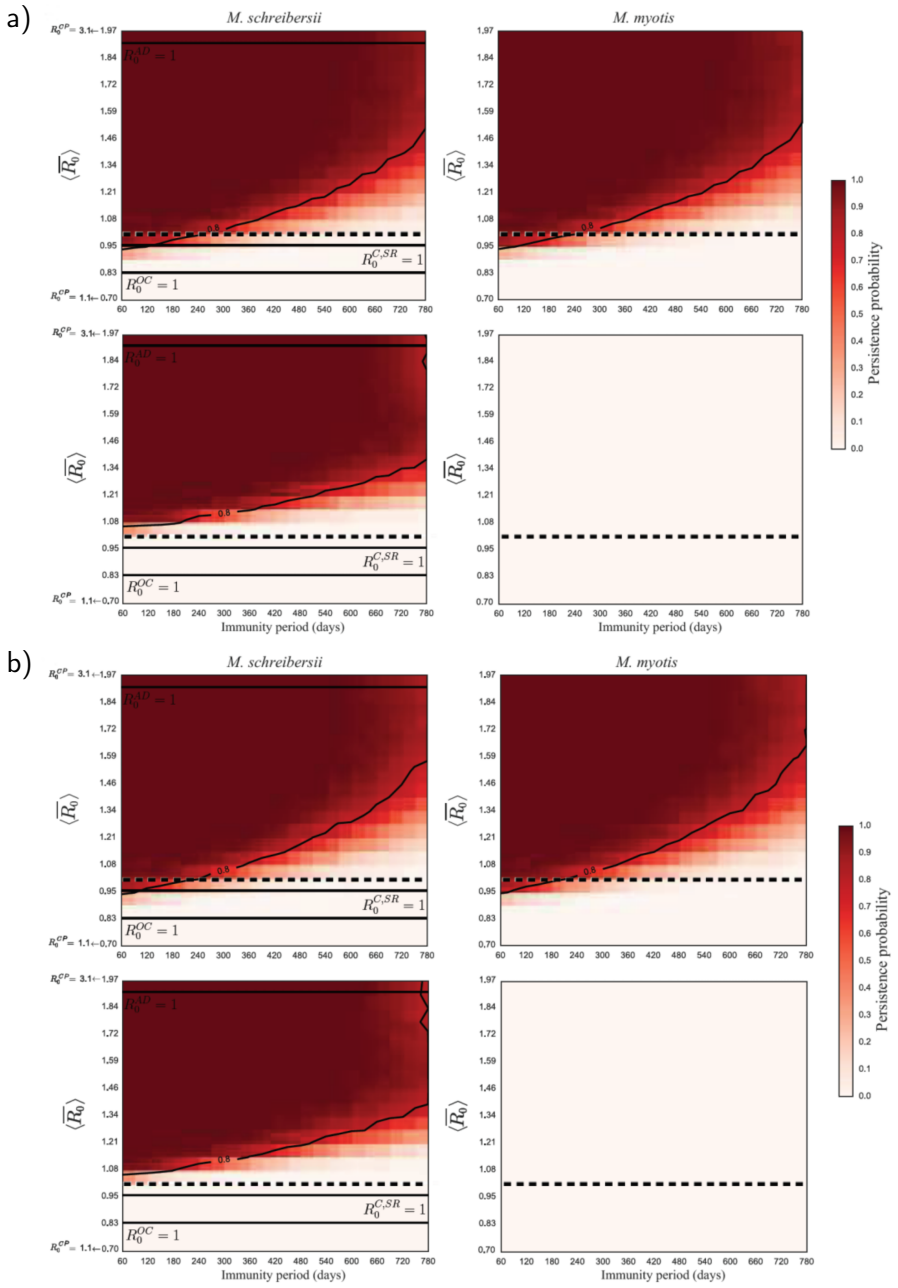

FIGURE A.3: Impact of the initial *M. myotis* population on the persistence probability of EBLV-1 in *M. schreibersii* and in *M. myotis* in model 3 (SA4). a) Persistence probability of EBLV-1 in *M. schreibersii* (left) and in *M. myotis* (right) as a function of the average reproductive number of the metapopulation system $\langle \overline{R_0} \rangle$ and of the immunity period (ω^{-1} , in mixing (top) and non-mixing (bottom) conditions, for an initial population of 17000 *M. schreibersii* and 400 *M. myotis*. b): as in a) but with an initial population of: 17000 *M. schreibersii* and 600 *M. myotis*. Contour lines indicate a persistence probability of 80%. The dashed horizontal line refers to $\langle \overline{R_0} \rangle = 1$. Solid horizontal lines refer to threshold conditions ($R_0^p = 1$) for the all caves.

A.2.2 Sensitivity analysis on starting date of migration events

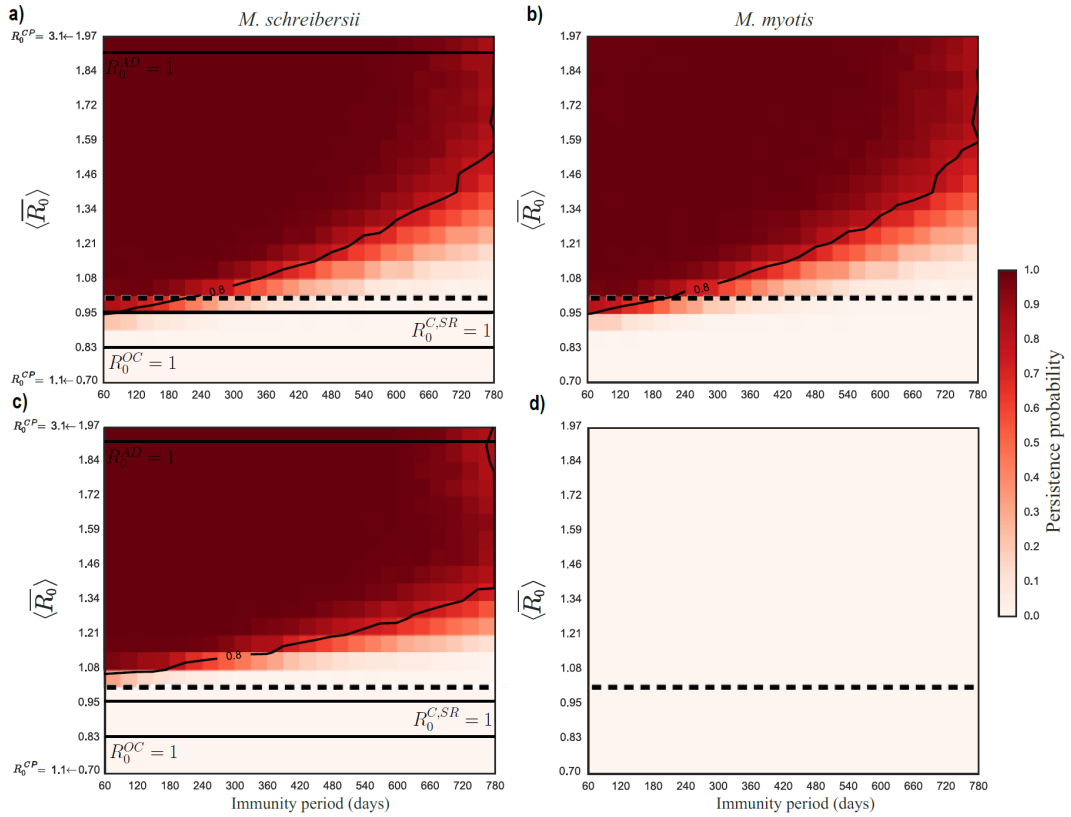

FIGURE A.4: Impact of the starting date of migration on the persistence probability of EBLV-1 in *M. schreibersii* and in *M. myotis* in model 3 (SA4). a), b): Persistence probability as a function of the average reproductive number of the metapopulation system $\langle\overline{R_0}\rangle$ and of the immunity period ω^{-1} for *M. schreibersii* a) and for *M. myotis* b) in the mixing scenario, for starting dates of migration changed by a factor ϵ, where ϵ is randomly extracted from a Gaussian distribution with a zero mean and a standard deviation of 1 week. c), d): as in a), b) in the non-mixing conditions. The dashed horizontal line refers to $\langle\overline{R_0}\rangle = 1$. Solid horizontal lines refer to threshold conditions ($R_0^p = 1$) for the all caves.

A.2.3 Sensitivity analysis on duration of migration events

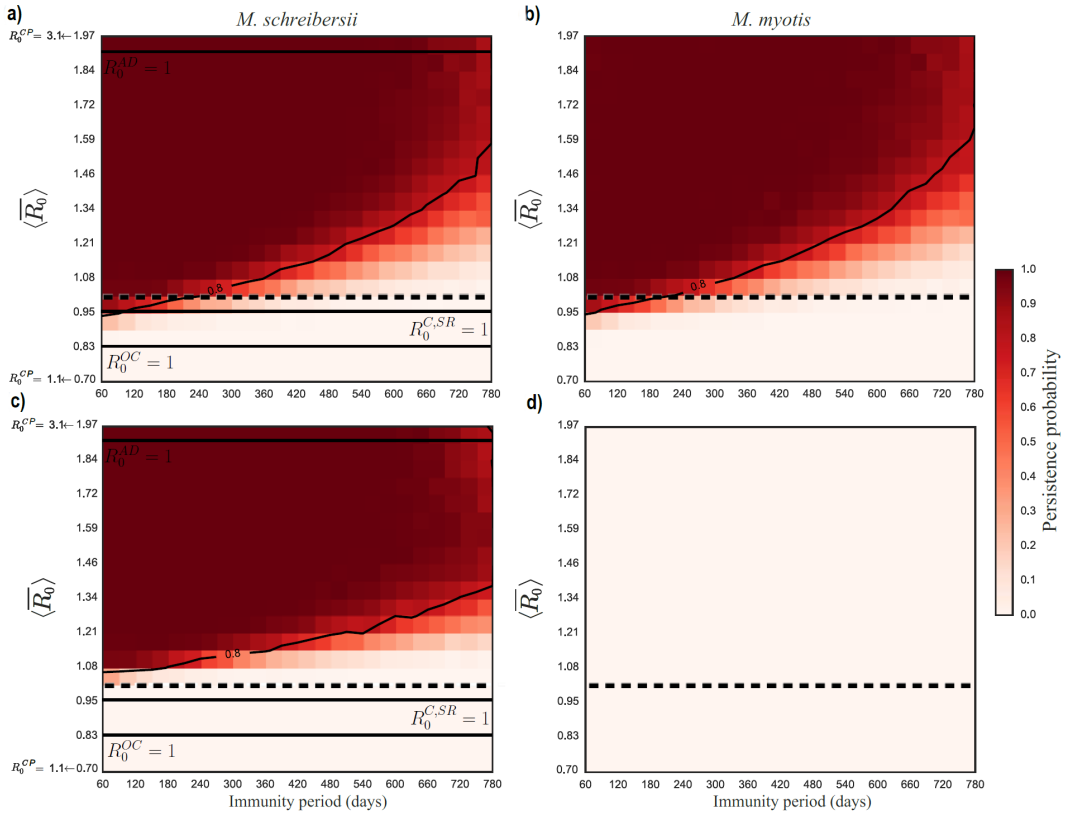

FIGURE A.5: Impact of the migration duration on the persistence probability of EBLV-1 in *M. schreibersii* and in *M. myotis* in model 3 (SA4). a), b): Persistence probability as a function of the average reproductive number of the metapopulation system $\langle \overline{R_0} \rangle$ and of the immunity period ω^{-1} for *M. schreibersii* a) and for *M. myotis* b) in the mixing scenarioin the mixing scenario for migration durations Δt changed by a factor ϵ, where ϵ is randomly extracted from a Gaussian distribution with a zero mean and a standard deviation of 1 week. c), d): as in a), b) in the non-mixing conditions. The dashed horizontal line refers to $\langle \overline{R_0} \rangle = 1$. Solid horizontal lines refer to threshold conditions ($R_0^p = 1$) for the all caves.

A.3 SA5. Sensitivity analysis on type of transmission, density-dependent transmission rates

A.3.1 Model 1

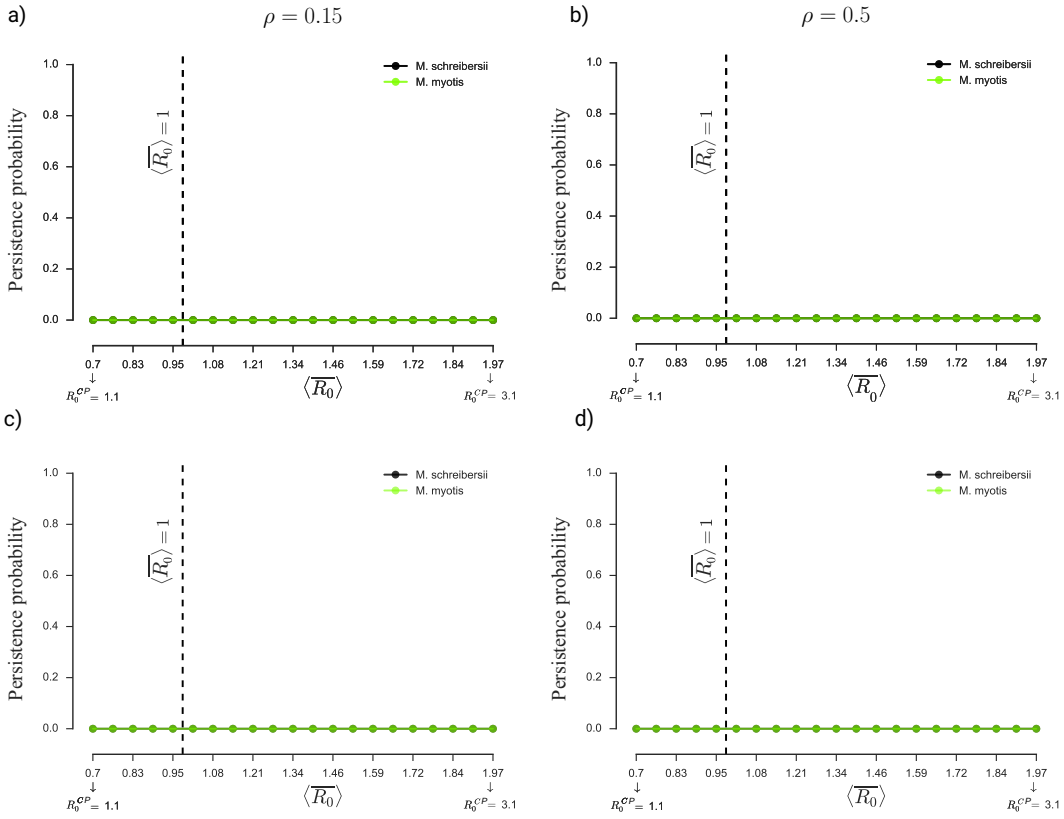

FIGURE A.6: Persistence probability of EBLV-1 in *M. schreibersii* and in *M. myotis* for model 1 for density dependent transmission. a), b) Persistence probability as a function of the average reproductive number of the metapopulation system for *M .schreibersii* (black) and *M. myotis* (green) for a proportion of exposed that becomes infectious $\rho = 0.15$ a) and $\rho = 0.5$ b) in mixing scenario. c), d): as in a), b) in the non-mixing conditions. In a), b), c) and d), the dashed horizontal line indicates $\langle \overline{R_0} \rangle = 1$. The smallest and largest values of the reproductive number of Can Palomeres cave explored are indicated on the horizontal axis.

A.3.2 Model 2

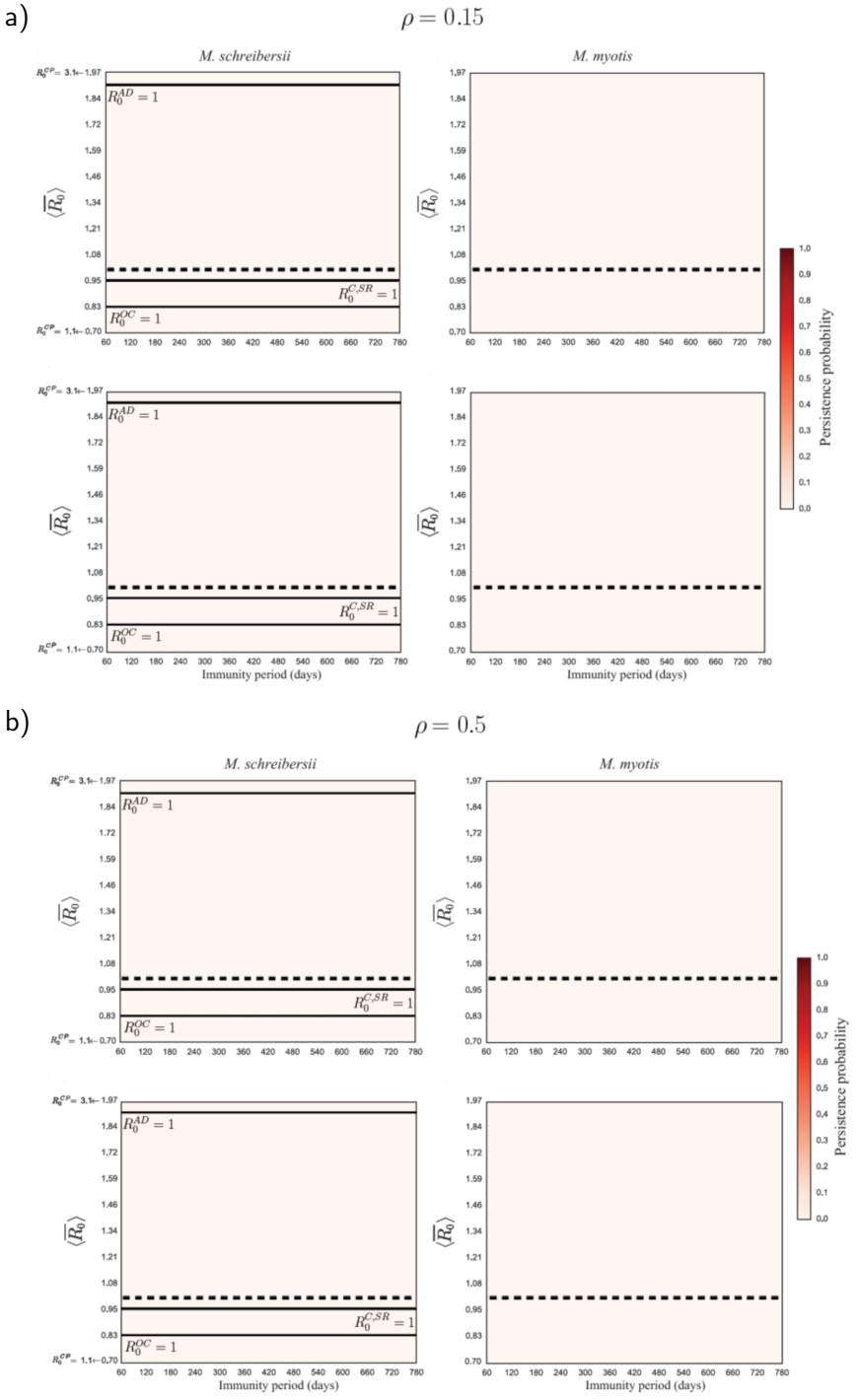

FIGURE A.7: Persistence probability of EBLV-1 in *M. schreibersii* and in *M. myotis* in model 2 for density dependent transmission. a) Persistence probability as a function of the average reproductive number of the metapopulation system $\langle \overline{R_0} \rangle$ and of the immunity period ω^{-1} for *M. schreibersii*(left) and for *M. myotis* (right) in mixing (top) and non-mixing (bottom) scenario with probability of lethal infection $\rho = 0.15$. b) same as a) but with probability of lethal infection $\rho = 0.5$. The dashed horizontal line refers to$\langle \overline{R_0} \rangle = 1$. Solid horizontal lines refer to threshold conditions ($R_0^p = 1$) for the all caves.

A.3.3 Model 3

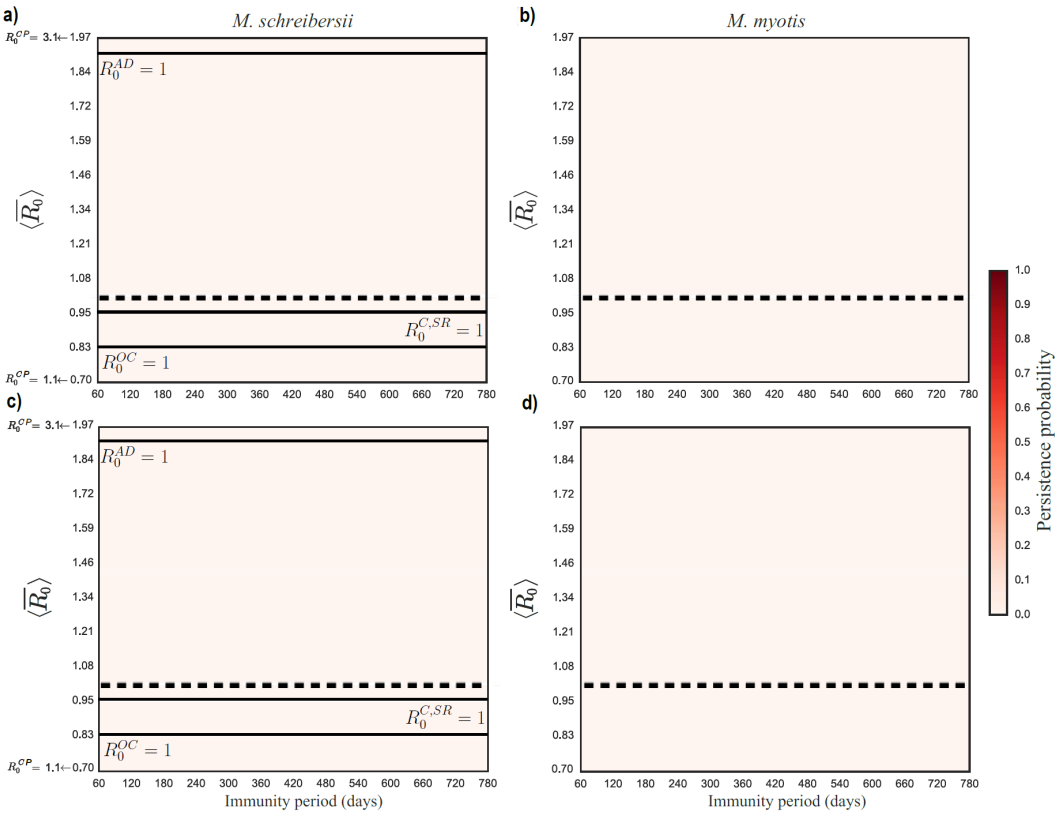

FIGURE A.8: Persistence probability of EBLV-1 in *M. schreibersii* and in *M. myotis* in model 3 for density dependent transmission. a), b), c), d): Persistence probability as a function of the average reproductive number of the metapopulation system $\langle \overline{R_0} \rangle$ and of the immunity period ω^{-1} for *M. schreibersii* a) and c) and for *M. myotis* b) and d) in the mixing scenario. The dashed horizontal line refers to$\langle \overline{R_0} \rangle = 1$. Solid horizontal lines refer to threshold conditions ($R_0^p = 1$) for the all caves.

B

Sensitivity analysis on rabies persistence in domestic dog population in Central African Republic

B.1 Log-likelihood estimation

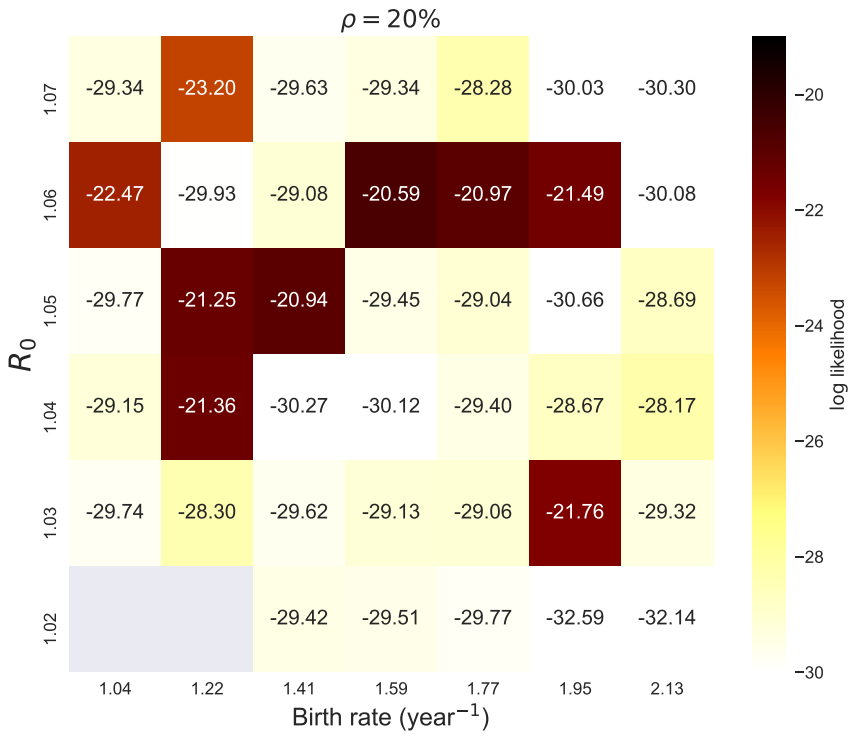

FIGURE B.1: Heatmap of the resulting log-likelihood for a detection probability $\rho = 20\%$ as a function of the basic reproductive number R_0 and of the annual birth rate of the domestic dog population.

B.2 Role of the population structure and of the movement range

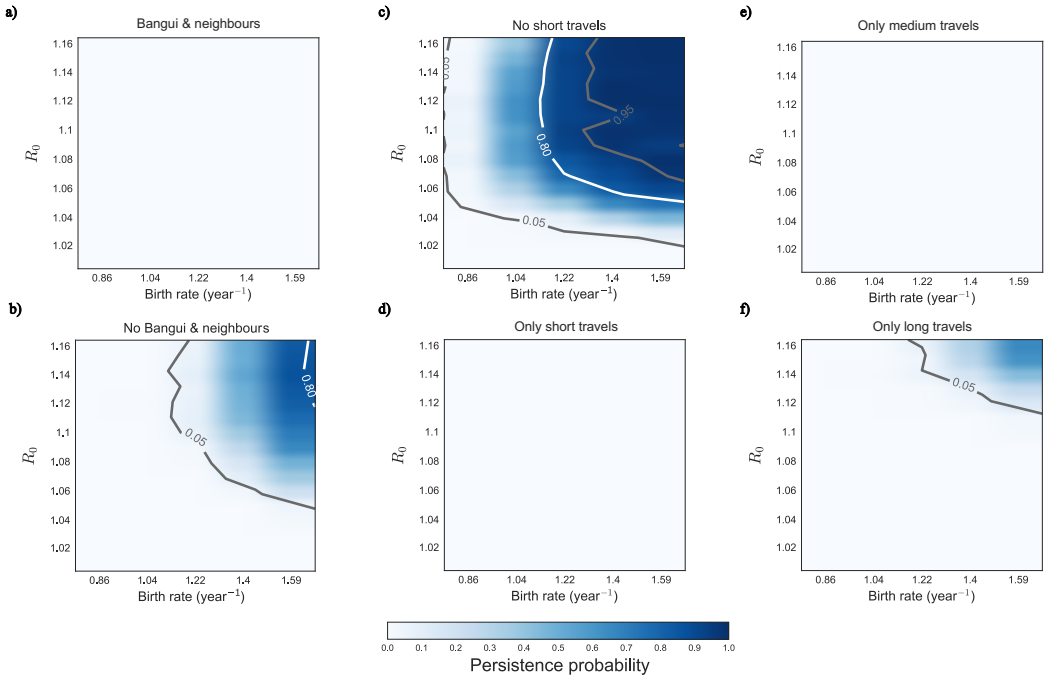

FIGURE B.2: Rabies virus persistence in a subgroup of scenarios tested. a) Persistence probability of RABV of domestic dog population in Bangui as a function of the basic reproductive number R_0 and of the annual birth rate of the dog population. This is the outcome of the non spatial explicit model where we explored also larger values of R_0. b) As in a) but with a spatial explicit model that consideres Bangui and his neighboring area (all the village distant less than 20 km). c) Persistence probability in the whole CAR considering only rural patches (human settlement with less than 1 000 individuals per kilometers squared). d) Persistence probability of RABV of domestic dog population of the CAR as a function of the basic reproductive number R_0 and of the annual birth rate of the dog population, restricting the possible daily movement to the short range movement (< 20km). e) As in d) but restricting the possible daily movement to the medium range movement (≥ 20km and ≤ 100 km). e) As in d) but restricting the possible daily movement to the long range movement (> 100 km).

B.3 Sensitivity analysis on Carrying capacity

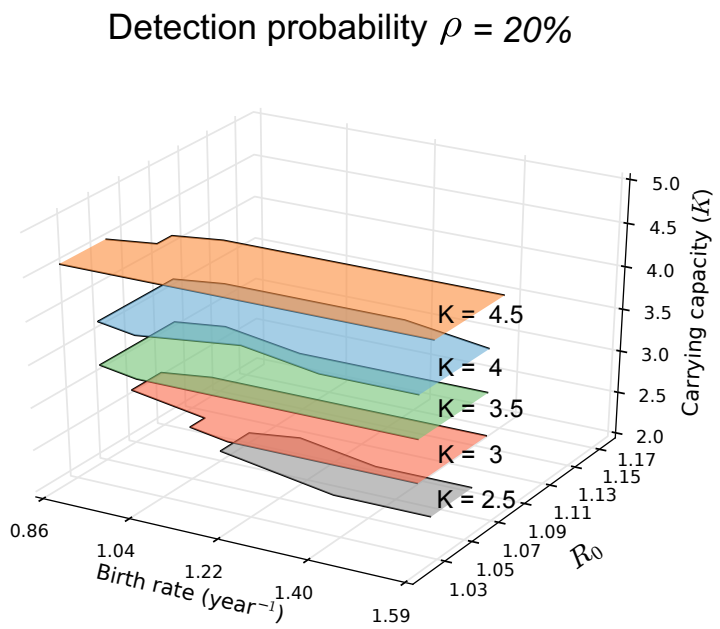

FIGURE B.3: Impact of the carrying capacity K on the epidemic scenario. Shape of the region where the persistence probability is higher than 80% and where the average population of domestic dogs in Central African Republic is equal to the estimated population $\pm 20\%$ as a function of the basic reproductive number R_0 and of the annual dogs birth rate, for a range of carrying capacities explored: $K_i = 2.5N_i(0)$ (grey), $K_i = 3N_i(0)$ (red), $K_i = 3.5N_i(0)$ (green), $K_i = 4N_i(0)$ (light blue), $K_i = 4.5N_i(0)$ (orange). The detection probability is assumed constant and equal to $\rho = 20\%$.

Bibliography

[1] Darryn L. Knobel et al. "Re-evaluating the burden of rabies in Africa and Asia." In: *Bull World Health Organ* 83.5 (May 2005), pp. 360–368. ISSN: 0042-9686. URL: http://www.ncbi.nlm.nih.gov/pmc/articles/PMC2626230/ (visited on 06/20/2016).

[2] Klaus Dietz and JAP Heesterbeek. "Daniel Bernoulli's epidemiological model revisited". In: *Mathematical biosciences* 180.1 (2002), pp. 1–21.

[3] Leung AK. "Rabies: Epidemiology, pathogenesis, and prophylaxis". In: *Adv Ther* 24 (2007), p. 1340.

[4] "World Health Organization Expert Committee on Rabies, First report. 2005". In: *WHO Technical Report Series, 931* (2005), p. 1.

[5] Wyatt J. "Rabies-Update on a global disease". In: *Pediatr Infect Dis J* 26 (2007), p. 351.

[6] Jackson AC. "Human rabies: a 2016 Update". In: *Curr Infect Dis Rep* 18 (2016), p. 38.

[7] Otolorin GR. "A review on human deaths associated with rabies in Nigeria". In: *J Vaccines Vaccin* 6 (2015), p. 262.

[8] Rupprecht CE. "Clinical practice. Prophylaxis against rabies". In: *N Engl J Med* 351 (2004), p. 2626.

[9] T. Müller et al. "Epidemiology of bat rabies in Germany". en. In: *Archives of Virology* 152.2 (Feb. 2007), pp. 273–288. ISSN: 0304-8608, 1432-8798. DOI: 10.1007/s00705-006-0853-5. URL: http://link.springer.com/10.1007/s00705-006-0853-5 (visited on 02/04/2017).

[10] Laurent Dacheux et al. "European Bat Lyssavirus Transmission among Cats, Europe". In: *Emerging Infectious Diseases* 15.2 (Feb. 2009), pp. 280–284. ISSN: 1080-6040, 1080-6059. DOI: 10.3201/eid1502.080637. URL: http://wwwnc.cdc.gov/eid/article/15/2/08-0637_article.htm (visited on 02/04/2017).

[11] Juliane Schatz et al. "Enhanced Passive Bat Rabies Surveillance in Indigenous Bat Species from Germany - A Retrospective Study". en. In: *PLoS Neglected Tropical Diseases* 8.5 (May 2014). Ed. by Charles E. Rupprecht, e2835. ISSN: 1935-2735. DOI: 10.1371/journal.pntd.0002835. URL: http://dx.plos.org/10.1371/journal.pntd.0002835 (visited on 02/04/2017).

[12] Rupprecht CE. "Rabies re-examined". In: *Lancet Infect Dis* 2 (2002), p. 327.

[13] William H Wunner and Karl-Klaus Conzelmann. "Rabies virus". In: *AC Jackson. Rabies, 3rd Edition. Oxford, UK: Acad Press/Elsevier* (2013), pp. 17–60.

[14] Anthony R Fooks et al. "Current status of rabies and prospects for elimination". en. In: *The Lancet* 384.9951 (Oct. 2014), pp. 1389–1399. ISSN: 01406736. DOI: 10.1016/S0140-6736(13)62707-5. URL: http://linkinghub.elsevier.com/retrieve/pii/S0140673613627075 (visited on 02/04/2017).

[15] Rajendra Singh et al. "Rabies – epidemiology, pathogenesis, public health concerns and advances in diagnosis and control: a comprehensive review". In: *Veterinary Quarterly* 37.1 (2017). PMID: 28643547, pp. 212–251. DOI: 10.1080/01652176.2017.1343516. eprint: http://dx.doi.org/10.1080/01652176.2017.1343516. URL: http://dx.doi.org/10.1080/01652176.2017.1343516.

[16] TJ Wiktor, A Flamand, and H Koprowski. "Use of monoclonal antibodies in diagnosis of rabies virus infection and differentiation of rabies and rabies-related viruses". In: *Journal of Virological Methods* 1.1 (1980), pp. 33–46.

[17] Noel Tordo, Anne Kouknetzoff, et al. "The rabies virus genome: an overview". In: (1993).

[18] Albertini AA. "Rabies virus transcription and replication". In: *Adv Virus Res* 79 (2011), p. 1.

[19] Aghahowa SE. "Incidence of dog bite and anti-rabies vaccine utilization in the, University of Benin Teaching Hospital, Benin City, Nigeria: a 12-year assessment". In: *Vaccine* 28 (2010), p. 4847.

[20] Hemachudha T. "Human rabies: neuropathogenesis, diagnosis, and management". In: *Lancet Neurol* 12 (2013), p. 498.

[21] Warrell MJ. "Rabies and other lyssavirus diseases". In: *Lancet* 363 (2004), p. 959.

[22] Baer GM. "Oral vaccination of foxes against rabies". In: *Am J Epidemiol* 93 (1971), p. 487.

[23] Winkler WG. "Airborne rabies transmission in a laboratory worker". In: *J Am Med Assoc* 226 (1973), p. 1219.

[24] Constantine DG. "Rabies transmission by non-bite route". In: *Public Health Rep* 77 (1962), p. 287.

[25] Gibbons RV. "Cryptogenic rabies, bats, and the question of aerosol transmission". In: *Ann Emerg Med* 39 (2002), p. 528.

[26] Srinivasan A. "Transmission of rabies virus from an organ donor to four transplant recipients". In: *N Engl J Med* 352 (2005), p. 1103.

[27] Hellenbrand W. "Cases of rabies in Germany following organ transplantation". In: *Eurosurveillance Weekly Release* 10 (2005), p. 050217.

[28] Dietzschold B. "Screening of organ and tissue donors for rabies". In: *Lancet* 365 (2005), p. 1305.

[29] Dutta JK. "Rabies transmission by oral and other non-bite routes". In: *J Indian Med Assoc* 96 (1998), p. 359.

[30] Tsiang H. "Infection of cultured rat myotubes and neurons from the spinal cord by rabies virus". In: *J Neuropathol Exp Neurol* 45 (1986), p. 28.

[31] Donald J. Dean, William M. Evans, and Robert C. McClure. "Pathogenesis of rabies". In: *Bull World Health Organ* 29.6 (1963), pp. 803–811. ISSN: 0042-9686. URL: http://www.ncbi.nlm.nih.gov/pmc/articles/PMC2555091/ (visited on 01/17/2017).

[32] Mazarakis ND. "Rabies virus glycoprotein pseudotyping of lentiviral vectors enables retrograde axonal transport and access to the nervous system after peripheral delivery". In: *Hum Mol Genet* 10 (2001), p. 2109.

[33] Makonnen Fekadu. "Pathogenesis of rabies virus infection in dogs". In: *Reviews of Infectious Diseases* 10.Supplement_4 (1988), S678–S683.

[34] CE Rupprecht, CA Hanlon, and D Slate. "Control and prevention of rabies in animals: paradigm shifts." In: *Developments in biologicals* 125 (2006), pp. 103–111.

[35] George M Baer and Garry L Bales. "Experimental rabies infection in the Mexican freetail bat". In: *The Journal of infectious diseases* (1967), pp. 82–90.

[36] Denny G Constantine, Richard W Emmons, and James D Woodie. "Rabies virus in nasal mucosa of naturally infected bats". In: *Science* 175.4027 (1972), pp. 1255–1256.

[37] Morimoto K. "Characterization of a unique variant of bat rabies virus responsible for newly emerging human cases in North America". In: *Proc Natl Acad Sci USA* 93 (1996), p. 5653.

[38] Hume Field, Brad McCall, and Janine Barrett. "Australian bat lyssavirus infection in a captive juvenile black flying fox." In: *Emerging infectious diseases* 5.3 (1999), p. 438.

[39] ML Baker, Tony Schountz, and L-F Wang. "Antiviral immune responses of bats: a review". In: *Zoonoses and public health* 60.1 (2013), pp. 104–116.

[40] KA McColl, N Tordo, and Setién AA Aguilar. "Bat lyssavirus infections." In: *Revue scientifique et technique (International Office of Epizootics)* 19.1 (2000), pp. 177–196.

[41] Juan L Pérez-Jordá et al. "Lyssavirus in Eptesicus serotinus (Chiroptera: Vespertilionidae)". In: *Journal of Wildlife Diseases* 31.3 (1995), pp. 372–377.

[42] Emmanuelle Robardet et al. "Longitudinal survey of two serotine bat (Eptesicus serotinus) maternity colonies exposed to EBLV-1 (European Bat Lyssavirus type 1): Assessment of survival and serological status variations using capture-recapture models". In: *PLOS Neglected Tropical Diseases* 11.11 (2017), e0006048.

[43] Jordi Serra-Cobo. "European Bat Lyssavirus Infection in Spanish Bat Populations". In: *Emerging Infectious Diseases* 8.4 (Apr. 2002), pp. 413–420. ISSN: 10806040. DOI: 10.3201/eid0804.010263. URL: http://www.cdc.gov/ncidod/EID/vol8no4/01-0263.htm (visited on 02/04/2017).

[44] GJ Wellenberg et al. "Presence of European bat lyssavirus RNAs in apparently healthy Rousettus aegyptiacus bats". In: *Archives of virology* 147.2 (2002), pp. 349–361.

[45] Andrew B Carey. "Multispecies rabies in the eastern United States". In: *Population dynamics of rabies in wildlife/edited by Philip J. Bacon* (1985).

[46] Jean S Smith. "Rabies virus epitopic variation: use in ecologic studies". In: *Advances in virus research* 36 (1989), pp. 215–253.

[47] Hervé Bourhy, Bachir Kissi, and Noél Tordo. "Molecular diversity of the Lyssavirus genus". In: *Virology* 194.1 (1993), pp. 70–81.

[48] Robert K Sikes. "Pathogenesis of rabies in wildlife. I. Comparative effect of varying doses of rabies virus inoculated into foxes and skunks." In: *American Journal of Veterinary Research* 23 (1962), pp. 1041–1047.

[49] R Keith Sikes. "Guidelines for the control of rabies." In: *American Journal of Public Health and the Nations Health* 60.6 (1970), pp. 1133–1138.

[50] Kuzmin IV. "Molecular inferences suggest multiple host shifts of rabies viruses from bats to mesocarnivores in Arizona during 2001–2009". In: *PLoS Pathog* 8 (2012), e1002786.

[51] Tenzin et al. "Dog Bites in Humans and Estimating Human Rabies Mortality in Rabies Endemic Areas of Bhutan". en. In: *PLoS Neglected Tropical Diseases* 5.11 (Nov. 2011). Ed. by Jakob Zinsstag, e1391. ISSN: 1935-2735. DOI: 10.1371/journal.pntd.0001391. URL: http://dx.plos.org/10.1371/journal.pntd.0001391 (visited on 06/20/2016).

[52] Salome Dürr et al. "Owner Valuation of Rabies Vaccination of Dogs, Chad". In: *Emerging Infectious Diseases* 14.10 (Oct. 2008), pp. 1650–1652. ISSN: 1080-6040, 1080-6059. DOI: 10.3201/eid1410.071490. URL: http://wwwnc.cdc.gov/eid/article/14/10/07-1490_article.htm (visited on 06/20/2016).

[53] J. Zinsstag et al. "Transmission dynamics and economics of rabies control in dogs and humans in an African city". en. In: *Proceedings of the National Academy of Sciences* 106.35 (Sept. 2009), pp. 14996–15001. ISSN: 0027-8424, 1091-6490. DOI: 10.1073/pnas.0904740106. URL: http://www.pnas.org/cgi/doi/10.1073/pnas.0904740106 (visited on 06/20/2016).

[54] WHO. *Data*. https://www.who-rabies-bulletin.org. 2017).

[55] J1 Schatz et al. "Bat rabies surveillance in Europe". In: *Zoonoses and public health* 60.1 (2013), pp. 22–34.

[56] P. L. Davis et al. "Phylogeography, Population Dynamics, and Molecular Evolution of European Bat Lyssaviruses". en. In: *Journal of Virology* 79.16 (Aug. 2005), pp. 10487–10497. ISSN: 0022-538X. DOI: 10.1128/JVI.79.16.10487-10497.2005. URL: http://jvi.asm.org/cgi/doi/10.1128/JVI.79.16.10487-10497.2005 (visited on 02/04/2017).

[57] Nidia Aréchiga Ceballos et al. "Novel Lyssavirus in Bat, Spain". In: *Emerging Infectious Diseases* 19.5 (May 2013), pp. 793–795. ISSN: 1080-6040, 1080-6059. DOI: 10.3201/eid1905.121071. URL: http://wwwnc.cdc.gov/eid/article/19/5/12-1071_article.htm (visited on 02/04/2017).

[58] Evelyne Picard-Meyer et al. "Isolation of Bokeloh bat lyssavirus in Myotis nattereri in France". en. In: *Archives of Virology* 158.11 (Nov. 2013), pp. 2333–2340. ISSN: 0304-8608, 1432-8798. DOI: 10.1007/s00705-013-1747-y. URL: http://link.springer.com/10.1007/s00705-013-1747-y (visited on 02/04/2017).

[59] Conrad M. Freuling et al. "Molecular diagnostics for the detection of Bokeloh bat lyssavirus in a bat from Bavaria, Germany". en. In: *Virus Research* 177.2 (Nov. 2013), pp. 201–204. ISSN: 01681702. DOI: 10.1016/j.virusres.2013.07.021. URL: http://linkinghub.elsevier.com/retrieve/pii/S0168170213002633 (visited on 02/04/2017).

[60] Ashley Banyard et al. "Lyssaviruses and Bats: Emergence and Zoonotic Threat". en. In: *Viruses* 6.8 (Aug. 2014), pp. 2974–2990. ISSN: 1999-4915. DOI: 10.3390/v6082974. URL: http://www.mdpi.com/1999-4915/6/8/2974/ (visited on 02/04/2017).

[61] Jordi Serra-Cobo et al. "Ecological Factors Associated with European Bat Lyssavirus Seroprevalence in Spanish Bats". en. In: *PLoS ONE* 8.5 (May 2013). Ed. by Michelle L. Baker, e64467. ISSN: 1932-6203. DOI: 10.1371/journal.pone.0064467. URL: http://dx.plos.org/10.1371/journal.pone.0064467 (visited on 02/04/2017).

[62] CE Rupprecht. "Bat rabies surveillance in the former Soviet Union". In: *Dev Biol (Basel)* 125 (2006), pp. 273–282.

[63] LG Schneider and JH Cox. "Bat lyssaviruses in Europe". In: *Current topics in microbiology and immunology* 187 (1994), pp. 207–218.

[64] B Amengual et al. "Evolution of European bat lyssaviruses." In: *Journal of General Virology* 78.9 (1997), pp. 2319–2328.

[65] MA Selimov et al. "New strains of rabies-related viruses isolated from bats in the Ukraine." In: *Acta virologica* 35.3 (1991), pp. 226–231.

[66] Wim H.M. Van der Poel et al. "European Bat Lyssaviruses, the Netherlands". In: *Emerging Infectious Diseases* 11.12 (Dec. 2005), pp. 1854–1859. ISSN: 1080-6040, 1080-6059. DOI: 10.3201/eid1112.041200. URL: http://wwwnc.cdc.gov/eid/article/11/12/04-1200_article.htm (visited on 02/04/2017).

[67] C. Freuling et al. "Experimental infection of serotine bats (Eptesicus serotinus) with European bat lyssavirus type 1a". en. In: *Journal of General Virology* 90.10 (Oct. 2009), pp. 2493–2502. ISSN: 0022-1317, 1465-2099. DOI: 10.1099/vir.0.011510-0. URL: http://jgv.microbiologyresearch.org/content/journal/jgv/10.1099/vir.0.011510-0 (visited on 02/04/2017).

[68] R. Franka et al. "Susceptibility of North American big brown bats (Eptesicus fuscus) to infection with European bat lyssavirus type 1". en. In: *Journal of General Virology* 89.8 (Aug. 2008), pp. 1998–2010. ISSN: 0022-1317, 1465-2099. DOI: 10.1099/vir.0.83688-0. URL: http://jgv.microbiologyresearch.org/content/journal/jgv/10.1099/vir.0.83688-0 (visited on 02/04/2017).

[69] Nicholas Johnson et al. "Experimental study of European bat lyssavirus type-2 infection in Daubenton's bats (Myotis daubentonii)". In: *Journal of General Virology* 89.11 (2008), pp. 2662–2672.

[70] Felix R. Jackson et al. "EXPERIMENTAL RABIES VIRUS INFECTION OF BIG BROWN BATS (EPTESICUS FUSCUS)". en. In: *Journal of Wildlife Diseases* 44.3 (July 2008), pp. 612–621. ISSN: 0090-3558. DOI: 10.7589/0090-3558-44.3.612. URL: http://www.jwildlifedis.org/doi/10.7589/0090-3558-44.3.612 (visited on 02/11/2017).

[71] AS Turmelle et al. "Host immunity to repeated rabies virus infection in big brown bats". In: *Journal of General Virology* 91.9 (2010), pp. 2360–2366.

[72] April D. Davis et al. "Rabies Virus Infection in Eptesicus fuscus Bats Born in Captivity (Naïve Bats)". en. In: *PLoS ONE* 8.5 (May 2013). Ed. by Bradley S. Schneider, e64808. ISSN: 1932-6203. DOI: 10.1371/journal.pone.0064808. URL: http://dx.plos.org/10.1371/journal.pone.0064808 (visited on 08/14/2017).

[73] Blanca Amengual et al. "Temporal Dynamics of European Bat Lyssavirus Type 1 and Survival of Myotis myotis Bats in Natural Colonies". en. In: *PLoS ONE* 2.6 (June 2007). Ed. by Etienne Joly, e566. ISSN: 1932-6203. DOI: 10.1371/journal.pone.0000566. URL: http://dx.plos.org/10.1371/journal.pone.0000566 (visited on 02/04/2017).

[74] Juan E Echevarria et al. "Screening of active lyssavirus infection in wild bat populations by viral RNA detection on oropharyngeal swabs". In: *Journal of clinical microbiology* 39.10 (2001), pp. 3678–3683.

[75] Charles E Rupprecht, Amy Turmelle, and Ivan V Kuzmin. "A perspective on lyssavirus emergence and perpetuation". In: *Current opinion in virology* 1.6 (2011), pp. 662–670.

[76] D. B. George et al. "Host and viral ecology determine bat rabies seasonality and maintenance". en. In: *Proceedings of the National Academy of Sciences* 108.25 (June 2011), pp. 10208–10213. ISSN: 0027-8424, 1091-6490. DOI: 10.1073/pnas.1010875108. URL: http://www.pnas.org/cgi/doi/10.1073/pnas.1010875108 (visited on 02/04/2017).

[77] J. C. Blackwood et al. "Resolving the roles of immunity, pathogenesis, and immigration for rabies persistence in vampire bats". en. In: *Proceedings of the National Academy of Sciences* 110.51 (Dec. 2013), pp. 20837–20842. ISSN: 0027-8424, 1091-6490. DOI: 10.1073/pnas.1308817110. URL: http://www.pnas.org/cgi/doi/10.1073/pnas.1308817110 (visited on 02/04/2017).

[78] Benoit De Thoisy et al. "Bioecological drivers of rabies virus circulation in a Neotropical bat community". In: *PLoS neglected tropical diseases* 10.1 (2016), e0004378.

[79] Louise C. Allen et al. "Roosting ecology and variation in adaptive and innate immune system function in the Brazilian free-tailed bat (Tadarida brasiliensis)". en. In: *Journal of Comparative Physiology B* 179.3 (Apr. 2009), pp. 315–323. ISSN: 0174-1578, 1432-136X. DOI: 10.1007/s00360-008-0315-3. URL: http://link.springer.com/10.1007/s00360-008-0315-3 (visited on 08/14/2017).

[80] Paul Elliott. *Bat Migrations in Europe–A Review of Banding Data and Literature, R. Hutterer, T. Ivanova, C. Meyer-Cords, L. Rodrigues. Federal Agency for Nature Conservation, Bonn (2005), 180 p.(pbk),£ 16.50, ISBN: 3-7843-3928-X*. 2006.

[81] Katie Hampson et al. "Transmission Dynamics and Prospects for the Elimination of Canine Rabies". en. In: *PLoS Biology* 7.3 (Mar. 2009). Ed. by Charles E Rupprecht, e1000053. ISSN: 1545-7885. DOI: 10.1371/journal.pbio.1000053. URL: http://dx.plos.org/10.1371/journal.pbio.1000053 (visited on 06/20/2016).

[82] H. Bourhy et al. "The origin and phylogeography of dog rabies virus". en. In: *Journal of General Virology* 89.11 (Nov. 2008), pp. 2673–2681. ISSN: 0022-1317, 1465-2099. DOI: 10.1099/vir.0.2008/003913-0. URL: http://jgv.microbiologyresearch.org/content/journal/jgv/10.1099/vir.0.2008/003913-0 (visited on 06/20/2016).

[83] D. David et al. "Identification of novel canine rabies virus clades in the Middle East and North Africa". en. In: *Journal of General Virology* 88.3 (Mar. 2007), pp. 967–980. ISSN: 0022-1317, 1465-2099. DOI: 10.1099/vir.0.82352-0. URL: http://jgv.microbiologyresearch.org/content/journal/jgv/10.1099/vir.0.82352-0 (visited on 06/20/2016).

[84] Bachir Kissi, Noël Tordo, and Hervé Bourhy. "Genetic Polymorphism in the Rabies Virus Nucleoprotein Gene". en. In: *Virology* 209.2 (June 1995), pp. 526–537. ISSN: 00426822. DOI: 10.1006/viro.1995.1285. URL: http://linkinghub.elsevier.com/retrieve/pii/S0042682285712858 (visited on 06/20/2016).

[85] B Maas et al. "Bat-eared fox behavioural ecology and the incidence of rabies in the Serengeti National Park". In: (1993).

[86] Andrew Alec McKenzie et al. "Biology of the black-backed jackal Canis mesomelas with reference to rabies". In: (1993).

[87] AJ Loveridge and DW Macdonald. "Seasonality in spatial organization and dispersal of sympatric jackals (Canis mesomelas and C. adustus): implications for rabies management". In: *Journal of Zoology* 253.1 (2001), pp. 101–111.

[88] Rosie Woodroffe and Christl A. Donnelly. "Risk of contact between endangered African wild dogs Lycaon pictus and domestic dogs: opportunities for pathogen transmission: Contact between domestic and wild dogs". en. In: *Journal of Applied Ecology* 48.6 (Dec. 2011), pp. 1345–1354. ISSN: 00218901. DOI: 10.1111/j.1365-2664.2011.02059.x. URL: http://doi.wiley.com/10.1111/j.1365-2664.2011.02059.x (visited on 06/20/2016).

[89] Deborah A. Randall et al. "Rabies in Endangered Ethiopian Wolves". In: *Emerging Infectious Diseases* 10.12 (Dec. 2004), pp. 2214–2217. ISSN: 1080-6040, 1080-6059. DOI: 10.3201/eid1012.040080. URL: http://wwwnc.cdc.gov/eid/article/10/12/04-0080_article.htm (visited on 06/20/2016).

[90] R Swanepoel et al. "Rabies in southern Africa." In: *The Onderstepoort journal of veterinary research* 60.4 (1993), pp. 325–346.

[91] Tiziana Lembo et al. "Exploring reservoir dynamics: a case study of rabies in the Serengeti ecosystem". en. In: *Journal of Applied Ecology* 45.4 (Aug. 2008), pp. 1246–1257. ISSN: 00218901, 13652664. DOI: 10.1111/j.1365-2664.2008.01468.x. URL: http://doi.wiley.com/10.1111/j.1365-2664.2008.01468.x (visited on 06/20/2016).

[92] S. Cleaveland and C. Dye. "Maintenance of a microparasite infecting several host species: rabies in the Serengeti". en. In: *Parasitology* 111.S1 (Jan. 1995), S33. ISSN: 0031-1820, 1469-8161. DOI: 10.1017/S0031182000075806. URL: http://www.journals.cambridge.org/abstract_S0031182000075806 (visited on 06/20/2016).

[93] T Lembo et al. "Molecular epidemiology identifies only a single rabies virus variant circulating in complex carnivore communities of the Serengeti". In: *Proceedings of the Royal Society of London B: Biological Sciences* 274.1622 (2007), pp. 2123–2130.

[94] Tiziana Lembo et al. "Exploring reservoir dynamics: a case study of rabies in the Serengeti ecosystem". In: *Journal of Applied Ecology* 45.4 (2008), pp. 1246–1257.

[95] AD El-Yuguda, AA Baba, and SSA Baba. "Dog population structure and cases of rabies among dog bite victims in urban and rural areas of Borno State, Nigeria". In: *Trop Vet* 25 (2007), pp. 34–40.

[96] Tiziana Lembo et al. "The Feasibility of Canine Rabies Elimination in Africa: Dispelling Doubts with Data". en. In: *PLoS Neglected Tropical Diseases* 4.2 (Feb. 2010). Ed. by Charles E. Rupprecht, e626. ISSN: 1935-2735. DOI: 10.1371/journal.pntd.0000626. URL: http://dx.plos.org/10.1371/journal.pntd.0000626 (visited on 06/20/2016).

[97] S Cleaveland. "A dog rabies vaccination campaign in rural Africa: impact on the incidence of dog rabies and human dog-bite injuries". en. In: *Vaccine* 21.17-18 (May 2003), pp. 1965–1973. ISSN: 0264410X. DOI: 10.1016/S0264-410X(02)00778-8. URL: http://linkinghub.elsevier.com/retrieve/pii/S0264410X02007788 (visited on 06/20/2016).

[98] M Kaare et al. "Rabies control in rural Africa: evaluating strategies for effective domestic dog vaccination". In: *Vaccine* 27.1 (2009), pp. 152–160.

[99] Alena S Gsell et al. "Domestic dog demographic structure and dynamics relevant to rabies control planning in urban areas in Africa: the case of Iringa, Tanzania". en. In: *BMC Veterinary Research* 8.1 (2012), p. 236. ISSN: 1746-6148. DOI: 10.1186/1746-6148-8-236. URL: http://bmcvetres.biomedcentral.com/articles/10.1186/1746-6148-8-236 (visited on 06/20/2016).

[100] KKIM De Balogh, Alexander I Wandeler, Francois-Xavier Meslin, et al. "A dog ecology study in an urban and a semi-rural area of Zambia". In: (1993).

[101] C. J. Rhodes et al. "Rabies in Zimbabwe: reservoir dogs and the implications for disease control". en. In: *Philosophical Transactions of the Royal Society B: Biological Sciences* 353.1371 (June 1998), pp. 999–1010. ISSN: 0962-8436, 1471-2970. DOI: 10.1098/rstb.1998.0263. URL: http://rstb.royalsocietypublishing.org/cgi/doi/10.1098/rstb.1998.0263 (visited on 06/20/2016).

[102] J. R. A. Butler and J. Bingham. "Demography and dog-human relationships of the dog population in Zimbabwean communal lands". en. In: *Veterinary Record* 147.16 (Oct. 2000), pp. 442–446. ISSN: 0042-4900, 2042-7670. DOI: 10.1136/vr.147.16.442. URL: http://veterinaryrecord.bmj.com/cgi/doi/10.1136/vr.147.16.442 (visited on 06/20/2016).

[103] Philip Kitala et al. "Dog ecology and demography information to support the planning of rabies control in Machakos District, Kenya". en. In: *Acta Tropica* 78.3 (Mar. 2001), pp. 217–230. ISSN: 0001706X. DOI: 10.1016/S0001-706X(01)00082-1. URL: http://linkinghub.elsevier.com/retrieve/pii/S0001706X01000821 (visited on 06/20/2016).

[104] P. M. Kitala et al. "Comparison of vaccination strategies for the control of dog rabies in Machakos District, Kenya". en. In: *Epidemiology and Infection* 129.01 (Aug. 2002). ISSN: 0950-2688, 1469-4409. DOI: 10.1017/S0950268802006957. URL: http://www.journals.cambridge.org/abstract_S0950268802006957 (visited on 07/27/2016).

[105] S Ben Youssef et al. "Field evaluation of a dog owner, participation-based, bait delivery system for the oral immunization of dogs against rabies in Tunisia." In: *The American journal of tropical medicine and hygiene* 58.6 (1998), pp. 835–845.

[106] Vianney Tricou et al. "Surveillance of Canine Rabies in the Central African Republic: Impact on Human Health and Molecular Epidemiology". en. In: *PLOS Neglected Tropical Diseases* 10.2 (Feb. 2016). Ed. by Jakob Zinsstag, e0004433. ISSN: 1935-2735. DOI: 10.1371/journal.pntd.0004433. URL: http://dx.plos.org/10.1371/journal.pntd.0004433 (visited on 06/20/2016).

[107] Hervé Bourhy et al. "Revealing the Micro-scale Signature of Endemic Zoonotic Disease Transmission in an African Urban Setting". en. In: *PLOS Pathogens* 12.4 (Apr. 2016). Ed. by Colin Parrish, e1005525. ISSN: 1553-7374. DOI: 10.1371/journal.ppat.1005525. URL: http://dx.plos.org/10.1371/journal.ppat.1005525 (visited on 06/20/2016).

[108] Darryn L Knobel et al. "A cross-sectional study of factors associated with dog ownership in Tanzania". en. In: *BMC Veterinary Research* 4.1 (2008), p. 5. ISSN: 1746-6148. DOI: 10.1186/1746-6148-4-5. URL: http://bmcvetres.biomedcentral.com/articles/10.1186/1746-6148-4-5 (visited on 06/20/2016).

[109] R Brooks. "Survey of the dog population of Zimbabwe and its level of rabies vaccination." In: *The Veterinary Record* 127.24 (1990), pp. 592–596.

[110] John Bingham. "Canine Rabies Ecology in Southern Africa". In: *Emerging Infectious Diseases* 11.9 (Sept. 2005), pp. 1337–1342. ISSN: 1080-6040, 1080-6059. DOI: 10.3201/eid1109.050172. URL: http://wwwnc.cdc.gov/eid/article/11/9/05-0172_article.htm (visited on 01/17/2017).

[111] K. Hampson et al. "Synchronous cycles of domestic dog rabies in sub-Saharan Africa and the impact of control efforts". en. In: *Proceedings of the National Academy of Sciences* 104.18 (May 2007), pp. 7717–7722. ISSN: 0027-8424, 1091-6490. DOI: 10.1073/pnas.0609122104. URL: http://www.pnas.org/cgi/doi/10.1073/pnas.0609122104 (visited on 06/20/2016).

[112] C. Talbi et al. "Evolutionary history and dynamics of dog rabies virus in western and central Africa". en. In: *Journal of General Virology* 90.4 (Mar. 2009), pp. 783–791. ISSN: 0022-1317, 1465-2099. DOI: 10.1099/vir.0.007765-0. URL: http://jgv.microbiologyresearch.org/content/journal/jgv/10.1099/vir.0.007765-0 (visited on 06/20/2016).

[113] Chiraz Talbi et al. "Phylodynamics and Human-Mediated Dispersal of a Zoonotic Virus". en. In: *PLoS Pathogens* 6.10 (Oct. 2010). Ed. by Michael Emerman, e1001166. ISSN: 1553-7374. DOI: 10.1371/journal.ppat.1001166. URL: http://dx.plos.org/10.1371/journal.ppat.1001166 (visited on 06/20/2016).

[114] Roy M. Anderson and Robert M. May. *Infectious Diseases of Humans: Dynamics and Control*. en. OUP Oxford, Aug. 1992. ISBN: 978-0-19-854040-3.

[115] K. Brunker et al. "Integrating the landscape epidemiology and genetics of RNA viruses: rabies in domestic dogs as a model". en. In: *Parasitology* 139.14 (Dec. 2012), pp. 1899–1913. ISSN: 0031-1820, 1469-8161. DOI: 10.1017/S003118201200090X. URL: http://www.journals.cambridge.org/abstract_S003118201200090X (visited on 06/20/2016).

[116] Andrew C. Breed et al. "Bats Without Borders: Long-Distance Movements and Implications for Disease Risk Management". en. In: *EcoHealth* 7.2 (June 2010), pp. 204–212. ISSN: 1612-9202, 1612-9210. DOI: 10.1007/s10393-010-0332-z. URL: http://link.springer.com/10.1007/s10393-010-0332-z (visited on 02/11/2017).

[117] Raina K. Plowright et al. "Transmission or Within-Host Dynamics Driving Pulses of Zoonotic Viruses in Reservoir–Host Populations". en. In: *PLOS Neglected Tropical Diseases* 10.8 (Aug. 2016). Ed. by Justin V. Remais, e0004796. ISSN: 1935-2735. DOI: 10.1371/journal.pntd.0004796. URL: http://dx.plos.org/10.1371/journal.pntd.0004796 (visited on 02/11/2017).

[118] Margarita Pons-Salort et al. "Insights into Persistence Mechanisms of a Zoonotic Virus in Bat Colonies Using a Multispecies Metapopulation Model". en. In: *PLoS ONE* 9.4 (Apr. 2014). Ed. by Caroline Colijn, e95610. ISSN: 1932-6203. DOI: 10.1371/journal.pone.0095610. URL: http://dx.plos.org/10.1371/journal.pone.0095610 (visited on 02/04/2017).

[119] Salome Dürr and Michael P Ward. "Roaming behaviour and home range estimation of domestic dogs in Aboriginal and Torres Strait Islander communities in northern Australia using four different methods". In: *Preventive veterinary medicine* 117.2 (2014), pp. 340–357.

[120] Emily G Hudson et al. "A Survey of Dog Owners in Remote Northern Australian Indigenous Communities to Inform Rabies Incursion Planning". In: *PLoS neglected tropical diseases* 10.4 (2016), e0004649.

[121] P. Lemey et al. "Phylogeography Takes a Relaxed Random Walk in Continuous Space and Time". en. In: *Molecular Biology and Evolution* 27.8 (Aug. 2010), pp. 1877–1885. ISSN: 0737-4038, 1537-1719. DOI: 10.1093/molbev/msq067. URL: http://mbe.oxfordjournals.org/cgi/doi/10.1093/molbev/msq067 (visited on 06/20/2016).

[122] Caecilia Windiyaningsih et al. "The rabies epidemic on Flores Island, Indonesia (1998-2003)." In: *Journal of the Medical Association of Thailand = Chotmaihet thangphaet* 87 11 (2004), pp. 1389–93.

[123] David TS Hayman et al. "Evolutionary history of rabies in Ghana". In: *PLoS neglected tropical diseases* 5.4 (2011), e1001.

[124] David L. Smith et al. "Predicting the spatial dynamics of rabies epidemics on heterogeneous landscapes". en. In: *Proceedings of the National Academy of Sciences* 99.6 (Mar. 2002), pp. 3668–3672. ISSN: 0027-8424, 1091-6490. DOI: 10.1073/pnas.042400799. URL: http://www.pnas.org/lookup/doi/10.1073/pnas.042400799 (visited on 01/17/2017).

[125] TJ Hagenaars, CA Donnelly, and NM Ferguson. "Spatial heterogeneity and the persistence of infectious diseases". In: *Journal of theoretical biology* 229.3 (2004), pp. 349–359.

[126] Paul C Cross et al. "Duelling timescales of host movement and disease recovery determine invasion of disease in structured populations". In: *Ecology Letters* 8.6 (2005), pp. 587–595.

[127] Ilkka Hanski and Michael Gilpin. "Metapopulation dynamics: brief history and conceptual domain". In: *Biological journal of the Linnean Society* 42.1-2 (1991), pp. 3–16.

[128] Mats Gyllenberg and Ilkka Hanski. "Habitat deterioration, habitat destruction, and metapopulation persistence in a heterogenous landscape". In: *Theoretical population biology* 52.3 (1997), pp. 198–215.

[129] Ilkka Hanski and Otso Ovaskainen. "Metapopulation theory for fragmented landscapes". In: *Theoretical population biology* 64.1 (2003), pp. 119–127.

[130] Ilkka Hanski and Oscar E Gaggiotti. *Ecology, genetics, and evolution of metapopulations*. Academic Press, 2004.

[131] Friederike Mayen. "Haematophagous bats in Brazil, their role in rabies transmission, impact on public health, livestock industry and alternatives to an indiscriminate reduction of bat population". In: *Zoonoses and Public Health* 50.10 (2003), pp. 469–472.

[132] Med Vet Net Working Group et al. "Passive and active surveillance of bat lyssavirus infections". In: *Rabies Bulletin Europe* 29.4 (2005), pp. 5–6.

[133] Stacy L Davlin and Helena M VonVille. "Canine rabies vaccination and domestic dog population characteristics in the developing world: a systematic review". In: *Vaccine* 30.24 (2012), pp. 3492–3502.

[134] Gyanendra Gongal and Alice E Wright. "Human rabies in the WHO Southeast Asia Region: forward steps for elimination". In: *Advances in preventive medicine* 2011 (2011).

[135] Songsri Kasempimolporn, Sutthichai Jitapunkul, and Visith SitprijaMD. "Moving towards the elimination of rabies in Thailand". In: *Journal of the Medical Association of Thailand* 91.3 (2011), p. 433.

[136] Maria Cristina Schneider et al. "Current status of human rabies transmitted by dogs in Latin America". In: *Cadernos de Saúde Pública* 23.9 (2007), pp. 2049–2063.

[137] Naohide Takayama. "Rabies control in Japan." In: *Japanese journal of infectious diseases* 53.3 (2000), pp. 93–97.

[138] Michelle K. Morters et al. "Evidence-based control of canine rabies: a critical review of population density reduction". en. In: *Journal of Animal Ecology* 82.1 (Jan. 2013). Ed. by Mike Boots, pp. 6–14. ISSN: 00218790. DOI: 10.1111/j.1365-2656.2012.02033.x. URL: http://doi.wiley.com/10.1111/j.1365-2656.2012.02033.x (visited on 06/20/2016).

[139] S Kasempimolporn et al. "Prevalence of rabies virus infection and rabies antibody in stray dogs: a survey in Bangkok, Thailand". In: *Preventive veterinary medicine* 78.3 (2007), pp. 325–332.

[140] L Touihri et al. "Evaluation of mass vaccination campaign coverage against rabies in dogs in Tunisia". In: *Zoonoses and public health* 58.2 (2011), pp. 110–118.

[141] Liisamaria Keates. "Rabies vaccines: WHO position paper—recommendations". In: *Vaccine* (2010).

[142] Sarah C Totton et al. "Stray dog population demographics in Jodhpur, India following a population control/rabies vaccination program". In: *Preventive veterinary medicine* 97.1 (2010), pp. 51–57.

[143] William J Fielding. "Changing Attitudes and Animal Welfare in Small Island Developing States: Dogs on New Providence, The Bahamas". In: *Journal of Applied Animal Welfare Science* 20.1 (2017), pp. 65–74.

[144] Jennifer Jackman and Andrew N Rowan. "Free-roaming dogs in developing countries: The benefits of capture, neuter, and return programs". In: (2007).

[145] Sunny E. Townsend et al. "Designing Programs for Eliminating Canine Rabies from Islands: Bali, Indonesia as a Case Study". en. In: *PLoS Neglected Tropical Diseases* 7.8 (Aug. 2013). Ed. by Charles E. Rupprecht, e2372. ISSN: 1935-2735. DOI: 10.1371/journal.pntd.0002372. URL: http://dx.plos.org/10.1371/journal.pntd.0002372 (visited on 06/20/2016).

[146] Elaine A. Ferguson et al. "Heterogeneity in the spread and control of infectious disease: consequences for the elimination of canine rabies". In: *Scientific Reports* 5 (Dec. 2015), p. 18232. ISSN: 2045-2322. DOI: 10.1038/srep18232. URL: http://www.nature.com/articles/srep18232 (visited on 06/21/2016).

[147] William Heaton Hamer. *The Milroy lectures on epidemic disease in England: the evidence of variability and of persistency of type*. Bedford Press, 1906.

[148] W. O. Kermack and A. G. McKendrick. "A Contribution to the Mathematical Theory of Epidemics". en. In: *Proceedings of the Royal Society A: Mathematical, Physical and Engineering Sciences* 115.772 (Aug. 1927), pp. 700–721. ISSN: 1364-5021, 1471-2946. DOI: 10.1098/rspa.1927.0118. URL: http://rspa.royalsocietypublishing.org/cgi/doi/10.1098/rspa.1927.0118 (visited on 06/20/2016).

[149] Matt J. Keeling and Pejman Rohani. *Modeling Infectious Diseases in Humans and Animals*. en. Princeton University Press, 2008. ISBN: 978-0-691-11617-4.

[150] JV Smith et al. "Population dynamics of fox rabies in Europe". In: *Nature* 289 (1981), p. 765.

[151] A Källen, P Arcuri, and JD Murray. "A simple model for the spatial spread and control of rabies". In: *Journal of theoretical biology* 116.3 (1985), pp. 377–393.

[152] JD Murray, EA Stanley, and DL Brown. "On the spatial spread of rabies among foxes". In: *Proceedings of the Royal Society of London. Series B, Biological Sciences* (1986), pp. 111–150.

[153] Bailey, Norman TJ, and others. *The mathematical theory of infectious diseases and its applications*. Charles Griffin & Company Ltd 5a Crendon Street High Wycombe Bucks HP13 6LE., 1975.

[154] O. Diekmann, J.A.P. Heesterbeek, and J.A.J. Metz. "On the definition and the computation of the basic reproduction ratio R 0 in models for infectious diseases in heterogeneous populations". en. In: *Journal of Mathematical Biology* 28.4 (June 1990). ISSN: 0303-6812, 1432-1416. DOI: 10.1007/BF00178324. URL: http://link.springer.com/10.1007/BF00178324 (visited on 06/20/2016).

[155] Odo Diekmann and Johan Andre Peter Heesterbeek. *Mathematical epidemiology of infectious diseases: model building, analysis and interpretation*. Vol. 5. John Wiley & Sons, 2000.

[156] O Diekmann, JAP Heesterbeek, and MG Roberts. "The construction of next-generation matrices for compartmental epidemic models". In: *Journal of the Royal Society Interface* (2009), rsif20090386.

[157] Roy M. Anderson et al. "Population dynamics of fox rabies in Europe". In: *Nature* 289.5800 (Feb. 1981), pp. 765–771. ISSN: 0028-0836. DOI: 10.1038/289765a0. URL: http://www.nature.com/doifinder/10.1038/289765a0 (visited on 06/20/2016).

[158] Kageaki Tojinbara et al. "Estimating the probability distribution of the incubation period for rabies using data from the 1948–1954 rabies epidemic in Tokyo". In: *Preventive veterinary medicine* 123 (2016), pp. 102–105.

[159] Philip E Sartwell and others. "The distribution of incubation periods of infectious disease." In: *American Journal of Hygiene* 51 (1950), pp. 310–318.

[160] RE Hope Simpson. "Infectiousness of communicable diseases in the household:(measles, chickenpox, and mumps)". In: *The Lancet* 260.6734 (1952), pp. 549–554.

[161] Dorothy Anderson and Ray Watson. "On the spread of a disease with gamma distributed latent and infectious periods". en. In: *Biometrika* 67.1 (1980), pp. 191–198. ISSN: 0006-3444, 1464-3510. DOI: 10.1093/biomet/67.1.191. URL: http://biomet.oxfordjournals.org/cgi/doi/10.1093/biomet/67.1.191 (visited on 06/20/2016).

[162] Alun L Lloyd and Robert M May. "Spatial heterogeneity in epidemic models". In: *Journal of theoretical biology* 179.1 (1996), pp. 1–11.

[163] Matthew J Keeling and BT Grenfell. "Disease extinction and community size: modeling the persistence of measles". In: *Science* 275.5296 (1997), pp. 65–67.

[164] Håkan Andersson and Tom Britton. "Stochastic epidemics in dynamic populations: quasi-stationarity and extinction". In: *Journal of mathematical biology* 41.6 (2000), pp. 559–580.

[165] A. L. Lloyd. "Destabilization of epidemic models with the inclusion of realistic distributions of infectious periods". en. In: *Proceedings of the Royal Society B: Biological Sciences* 268.1470 (May 2001), pp. 985–993. ISSN: 0962-8452, 1471-2954. DOI: 10.1098/rspb.2001.1599. URL: http://rspb.royalsocietypublishing.org/cgi/doi/10.1098/rspb.2001.1599 (visited on 06/20/2016).

[166] Helen J Wearing, Pejman Rohani, and Matt J Keeling. "Appropriate Models for the Management of Infectious Diseases". en. In: *PLoS Medicine* 2.7 (July 2005). Ed. by Stephen P. Ellner, e174. ISSN: 1549-1676. DOI: 10.1371/journal.pmed.0020174. URL: http://dx.plos.org/10.1371/journal.pmed.0020174 (visited on 06/20/2016).

[167] Herbert W Hethcote and David W Tudor. "Integral equation models for endemic infectious diseases". In: *Journal of mathematical biology* 9.1 (1980), pp. 37–47.

[168] David Roxbee Cox. *The theory of stochastic processes*. Routledge, 2017.

[169] O. Krylova and D. J. D. Earn. "Effects of the infectious period distribution on predicted transitions in childhood disease dynamics". en. In: *Journal of The Royal Society Interface* 10.84 (May 2013), pp. 20130098–20130098. ISSN: 1742-5689, 1742-5662. DOI: 10.1098/rsif.2013.0098. URL: http://rsif.royalsocietypublishing.org/cgi/doi/10.1098/rsif.2013.0098 (visited on 06/15/2017).

[170] Zhilan Feng, Dashun Xu, and Haiyun Zhao. "Epidemiological Models with Non-Exponentially Distributed Disease Stages and Applications to Disease Control". en. In: *Bulletin of Mathematical Biology* 69.5 (June 2007), pp. 1511–1536. ISSN: 0092-8240, 1522-9602. DOI: 10.1007/s11538-006-9174-9. URL: http://link.springer.com/10.1007/s11538-006-9174-9 (visited on 06/20/2016).

[171] Steven Riley. "Large-scale spatial-transmission models of infectious disease". In: *Science* 316.5829 (2007), pp. 1298–1301.

[172] Vittoria Colizza and Alessandro Vespignani. "Epidemic modeling in metapopulation systems with heterogeneous coupling pattern: Theory and simulations". In: *Journal of theoretical biology* 251.3 (2008), pp. 450–467.

[173] Joaquín Marro and Ronald Dickman. *Nonequilibrium phase transitions in lattice models*. Cambridge University Press, 2005.

[174] Nicolaas Godfried Van Kampen. *Stochastic processes in physics and chemistry*. Vol. 1. Elsevier, 1992.

[175] Andrea Baronchelli, Michele Catanzaro, and Romualdo Pastor-Satorras. "Bosonic reaction-diffusion processes on scale-free networks". In: *Physical Review E* 78.1 (2008), p. 016111.

[176] Robert M May and Roy M Anderson. "Spatial heterogeneity and the design of immunization programs". In: *Mathematical Biosciences* 72.1 (1984), pp. 83–111.

[177] Lisa Sattenspiel and Klaus Dietz. "A structured epidemic model incorporating geographic mobility among regions". In: *Mathematical biosciences* 128.1-2 (1995), pp. 71–91.

[178] Matt J Keeling and Pejman Rohani. "Estimating spatial coupling in epidemiological systems: a mechanistic approach". In: *Ecology Letters* 5.1 (2002), pp. 20–29.

[179] Duncan J Watts et al. "Multiscale, resurgent epidemics in a hierarchical metapopulation model". In: *Proceedings of the National Academy of Sciences of the United States of America* 102.32 (2005), pp. 11157–11162.

[180] Anatol Rapoport. "Spread of information through a population with socio-structural bias: I. Assumption of transitivity". In: *Bulletin of Mathematical Biology* 15.4 (1953), pp. 523–533.

[181] William Goffman and Vaun A Newill. "Generalization of epidemic theory: An application to the transmission of ideas". In: *Nature* 204.4955 (1964), pp. 225–228.

[182] William Goffman. "Mathematical approach to the spread of scientific ideas—the history of mast cell research". In: *Nature* 212.5061 (1966), pp. 449–452.

[183] Klaus Dietz. "Epidemics and rumours: A survey". In: *Journal of the Royal Statistical Society. Series A (General)* (1967), pp. 505–528.

[184] JV Noble. "Geographic and temporal development of plagues". In: *Nature* 250.5469 (1974), pp. 726–729.

[185] James D. Murray. *Mathematical Biology I. An Introduction*. 3rd ed. Vol. 17. Interdisciplinary Applied Mathematics. New York: Springer, 2002. DOI: 10.1007/b98868.

[186] B. Bolker and B. Grenfell. "Space, Persistence and Dynamics of Measles Epidemics". en. In: *Philosophical Transactions of the Royal Society B: Biological Sciences* 348.1325 (May 1995), pp. 309–320. ISSN: 0962-8436, 1471-2970. DOI: 10.1098/rstb.1995.0070. URL: http://rstb.royalsocietypublishing.org/cgi/doi/10.1098/rstb.1995.0070 (visited on 06/20/2016).

[187] D. J. D. Earn, P. Rohani, and B. T. Grenfell. "Persistence, chaos and synchrony in ecology and epidemiology". en. In: *Proceedings of the Royal Society B: Biological Sciences* 265.1390 (Jan. 1998), pp. 7–10. ISSN: 0962-8452, 1471-2954. DOI: 10.1098/rspb.1998.0256. URL: http://rspb.royalsocietypublishing.org/cgi/doi/10.1098/rspb.1998.0256 (visited on 06/20/2016).

[188] Matt J. Keeling. "Metapopulation moments: coupling, stochasticity and persistence". en. In: *Journal of Animal Ecology* 69.5 (Sept. 2000), pp. 725–736. ISSN: 0021-8790, 1365-2656. DOI: 10.1046/j.1365-2656.2000.00430.x. URL: http://doi.wiley.com/10.1046/j.1365-2656.2000.00430.x (visited on 06/20/2016).

[189] Andrew W Park, Simon Gubbins, and Christopher A Gilligan. "Extinction times for closed epidemics: the effects of host spatial structure". In: *Ecology Letters* 5.6 (2002), pp. 747–755.

[190] Janet E Foley, Patrick Foley, and Niels C Pedersen. "The persistence of a SIS disease in a metapopulation". In: *Journal of Applied Ecology* 36.4 (1999), pp. 555–563.

[191] Jim D Broadfoot, Richard C Rosatte, and David T O'Leary. "Raccoon and skunk population models for urban disease control planning in Ontario, Canada". In: *Ecological Applications* 11.1 (2001), pp. 295–303.

[192] GR Fulford, MG Roberts, and JAP Heesterbeek. "The metapopulation dynamics of an infectious disease: tuberculosis in possums". In: *Theoretical population biology* 61.1 (2002), pp. 15–29.

[193] I Gudelj and KAJ White. "Spatial heterogeneity, social structure and disease dynamics of animal populations". In: *Theoretical population biology* 66.2 (2004), pp. 139–149.

[194] Hawthorne L. Beyer et al. "The implications of metapopulation dynamics on the design of vaccination campaigns". en. In: *Vaccine* 30.6 (Feb. 2012), pp. 1014–1022. ISSN: 0264410X. DOI: 10.1016/j.vaccine.2011.12.052. URL: http://linkinghub.elsevier.com/retrieve/pii/S0264410X11019876 (visited on 06/20/2016).

[195] H. L. Beyer et al. "Metapopulation dynamics of rabies and the efficacy of vaccination". en. In: *Proceedings of the Royal Society B: Biological Sciences* 278.1715 (July 2011), pp. 2182–2190. ISSN: 0962-8452, 1471-2954. DOI: 10.1098/rspb.2010.2312. URL: http://rspb.royalsocietypublishing.org/cgi/doi/10.1098/rspb.2010.2312 (visited on 06/20/2016).

[196] Jordi Serra-Cobo, Victor Sanz-Trullén, and Juan Pablo Martinez-Rica. "Migratory movements of Miniopterus schreibersii in the north-east of Spain". In: *Acta Theriologica* 43 (Sept. 1998), pp. 271–283. ISSN: 00017051, 21903743. DOI: 10.4098/AT.arch.98-22. URL: http://rcin.org.pl/ibs/dlibra/docmetadata?id=12771&from=publication (visited on 02/04/2017).

[197] Serra-Cobo, J., López-Roig, M., Bayer, X., Amengual, B. i Guasch, C. "Bats. Science and myth." Universitat de Barcelona, 2009.

[198] WorldPop. *Data*. www.worldpop.org.uk/data. 2014).

[199] Catherine Linard and Andrew J Tatem. "Large-scale spatial population databases in infectious disease research". en. In: *International Journal of Health Geographics* 11.1 (2012), p. 7. ISSN: 1476-072X. DOI: 10.1186/1476-072X-11-7. URL: http://ij-healthgeographics.biomedcentral.com/articles/10.1186/1476-072X-11-7 (visited on 01/17/2017).

[200] Philippe Lemey et al. "Bayesian Phylogeography Finds Its Roots". en. In: *PLoS Computational Biology* 5.9 (Sept. 2009). Ed. by Christophe Fraser, e1000520. ISSN: 1553-7358. DOI: 10.1371/journal.pcbi.1000520. URL: http://dx.plos.org/10.1371/journal.pcbi.1000520 (visited on 06/20/2016).

[201] C. H. Calisher et al. "Bats: Important Reservoir Hosts of Emerging Viruses". en. In: *Clinical Microbiology Reviews* 19.3 (July 2006), pp. 531–545. ISSN: 0893-8512. DOI: 10.1128/CMR.00017-06. URL: http://cmr.asm.org/cgi/doi/10.1128/CMR.00017-06 (visited on 02/04/2017).

[202] D. T. S. Hayman et al. "Ecology of Zoonotic Infectious Diseases in Bats: Current Knowledge and Future Directions: Ecology of Zoonotic Infectious Diseases in Bats". en. In: *Zoonoses and Public Health* 60.1 (Feb. 2013), pp. 2–21. ISSN: 18631959. DOI: 10.1111/zph.12000. URL: http://doi.wiley.com/10.1111/zph.12000 (visited on 02/04/2017).

[203] Ashley C Banyard and Anthony R Fooks. "The impact of novel lyssavirus discovery". In: *Microbiology Australia* 38.1 (2017), pp. 17–21.

[204] Olivier Delmas et al. "Genomic Diversity and Evolution of the Lyssaviruses". en. In: *PLoS ONE* 3.4 (Apr. 2008). Ed. by Oliver G. Pybus, e2057. ISSN: 1932-6203. DOI: 10.1371/journal.pone.0002057. URL: http://dx.plos.org/10.1371/journal.pone.0002057 (visited on 06/20/2016).

[205] Florence Cliquet et al. "Eliminating Rabies in Estonia". en. In: *PLoS Neglected Tropical Diseases* 6.2 (Feb. 2012). Ed. by James E. Childs, e1535. ISSN: 1935-2735. DOI: 10.1371/journal.pntd.0001535. URL: http://dx.plos.org/10.1371/journal.pntd.0001535 (visited on 01/17/2017).

[206] "FLI. Rabies Bulletin Europe. Rabies Information System of the WHO Collaboration Centre for Rabies Surveillance and Research. [Internet]. Available from: http://www.who-rabies-bulletin.org".

[207] Florence Cliquet et al. "Experimental infection of Foxes with European bat Lyssaviruses type-1 and 2". en. In: *BMC Veterinary Research* 5.1 (2009), p. 19. ISSN: 1746-6148. DOI: 10.1186/1746-6148-5-19. URL: http://bmcvetres.biomedcentral.com/articles/10.1186/1746-6148-5-19 (visited on 02/04/2017).

[208] Gaël D Maganga et al. "Bat distribution size or shape as determinant of viral richness in african bats". In: *PLoS One* 9.6 (2014), e100172.

[209] Raina K Plowright et al. "Urban habituation, ecological connectivity and epidemic dampening: the emergence of Hendra virus from flying foxes (Pteropus spp.)" In: *Proceedings of the Royal Society of London B: Biological Sciences* 278.1725 (2011), pp. 3703–3712.

[210] Dobromir T Dimitrov and Thomas G Hallam. "Effects of immune system diversity and physical variation ofimmunotypic mixing on the dynamics of rabies in bats". In: *Journal of biological dynamics* 3.2-3 (2009), pp. 164–179.

[211] Angela D. Luis et al. "Network analysis of host-virus communities in bats and rodents reveals determinants of cross-species transmission". en. In: *Ecology Letters* 18.11 (Nov. 2015). Ed. by José Marìa Gomez, pp. 1153–1162. ISSN: 1461023X. DOI: 10.1111/ele.12491. URL: http://doi.wiley.com/10.1111/ele.12491 (visited on 08/14/2017).

[212] M. C. M. DeJong, O. Dieckmann, and J. A. P. Heesterbeek. "How does transmission of infection depend on population size?" In: *Epidemic models: their structure and relation to data models.* Ed. by D. Mollison. Cambridge: Cambridge University Press, 1995, pp. 84–94.

[213] Marc López-Roig et al. "Seroprevalence Dynamics of European Bat Lyssavirus Type 1 in a Multispecies Bat Colony". en. In: *Viruses* 6.9 (Sept. 2014), pp. 3386–3399. ISSN: 1999-4915. DOI: 10.3390/v6093386. URL: http://www.mdpi.com/1999-4915/6/9/3386/ (visited on 02/04/2017).

[214] Thomas J. O'Shea et al. "Variability in Seroprevalence of Rabies Virus Neutralizing Antibodies and Associated Factors in a Colorado Population of Big Brown Bats (Eptesicus fuscus)". en. In: *PLoS ONE* 9.1 (Jan. 2014). Ed. by Michelle L. Baker, e86261. ISSN: 1932-6203. DOI: 10.1371/journal.pone.0086261. URL: http://dx.plos.org/10.1371/journal.pone.0086261 (visited on 08/14/2017).

[215] Alberto Aleta et al. "Human mobility networks and persistence of rapidly mutating pathogens". In: *Royal Society Open Science* 4.3 (2017), p. 160914.

[216] Jordi Serra-Cobo and Marc Lopez-Roig. "Bats and emerging infections: an ecological and virological puzzle". In: (2016).

[217] Thomas J. O'Shea et al. "Bat Flight and Zoonotic Viruses". In: *Emerging Infectious Diseases* 20.5 (May 2014), pp. 741–745. ISSN: 1080-6040, 1080-6059. DOI: 10.3201/eid2005.130539. URL: http://wwwnc.cdc.gov/eid/article/20/5/13-0539_article.htm (visited on 02/11/2017).

[218] Peng Zhou et al. "Contraction of the type I IFN locus and unusual constitutive expression of *IFN* in bats". en. In: *Proceedings of the National Academy of Sciences* 113.10 (Mar. 2016), pp. 2696–2701. ISSN: 0027-8424, 1091-6490. DOI: 10.1073/pnas.1518240113. URL: http://www.pnas.org/lookup/doi/10.1073/pnas.1518240113 (visited on 08/14/2017).

[219] Isabelle M Cote and Robert Poulinb. "Parasitism and group size in social animals: a meta-analysis". In: *Behavioral Ecology* 6.2 (1995), pp. 159–165.

[220] Per Arneberg. "Host population density and body mass as determinants of species richness in parasite communities: comparative analyses of directly transmitted nematodes of mammals". In: *Ecography* 25.1 (2002), pp. 88–94.

[221] Michael Begon et al. "Rodents, cowpox virus and islands: densities, numbers and thresholds". In: *Journal of Animal Ecology* 72.2 (2003), pp. 343–355.

[222] Hamish McCallum, Nigel Barlow, and Jim Hone. "How should pathogen transmission be modelled?" In: *Trends in ecology & evolution* 16.6 (2001), pp. 295–300.

[223] Gerald Kerth. "Causes and consequences of sociality in bats". In: *AIBS Bulletin* 58.8 (2008), pp. 737–746.

[224] Gerald Kerth, Nicolas Perony, and Frank Schweitzer. "Bats are able to maintain long-term social relationships despite the high fission–fusion dynamics of their groups". In: *Proceedings of the Royal Society of London B: Biological Sciences* 278.1719 (2011), pp. 2761–2767.

[225] HV Richter and GS Cumming. "First application of satellite telemetry to track African straw-coloured fruit bat migration". In: *Journal of Zoology* 275.2 (2008), pp. 172–176.

[226] Cécile Troupin et al. "Large-Scale Phylogenomic Analysis Reveals the Complex Evolutionary History of Rabies Virus in Multiple Carnivore Hosts". en. In: *PLOS Pathogens* 12.12 (Dec. 2016). Ed. by Colin Parrish, e1006041. ISSN: 1553-7374. DOI: 10.1371/journal.ppat.1006041. URL: http://dx.plos.org/10.1371/journal.ppat.1006041 (visited on 07/28/2017).

[227] Betty Dodet et al. "Human rabies deaths in Africa: breaking the cycle of indifference". en. In: *International Health* 7.1 (Jan. 2015), pp. 4–6. ISSN: 1876-3413, 1876-3405. DOI: 10.1093/inthealth/ihu071. URL: https://academic.oup.com/inthealth/inthealth/article/2964839/Human (visited on 07/28/2017).

[228] Bernadette Abela-Ridder et al. "2016: the beginning of the end of rabies?" en. In: *The Lancet Global Health* 4.11 (Nov. 2016), e780–e781. ISSN: 2214109X. DOI: 10.1016/S2214-109X(16)30245-5. URL: http://linkinghub.elsevier.com/retrieve/pii/S2214109X16302455 (visited on 07/28/2017).

[229] E. Nakouné et al. "New introduction and spread of rabies among dog population in Bangui". en. In: *Acta Tropica* 123.2 (Aug. 2012), pp. 107–110. ISSN: 0001706X. DOI: 10.1016/j.actatropica.2012.04.005. URL: http://linkinghub.elsevier.com/retrieve/pii/S0001706X12001829 (visited on 06/20/2016).

[230] V F Nettles et al. "Rabies in translocated raccoons." en. In: *American Journal of Public Health* 69.6 (June 1979), pp. 601–602. ISSN: 0090-0036, 1541-0048. DOI: 10.2105/AJPH.69.6.601. URL: http://ajph.aphapublications.org/doi/abs/10.2105/AJPH.69.6.601 (visited on 06/20/2016).

[231] M. L. Wilson et al. "Emergence of raccoon rabies in Connecticut, 1991-1994: spatial and temporal characteristics of animal infection and human contact". eng. In: *Am. J. Trop. Med. Hyg.* 57.4 (Oct. 1997), pp. 457–463. ISSN: 0002-9637.

[232] P. Bajardi et al. "Optimizing surveillance for livestock disease spreading through animal movements". en. In: *Journal of The Royal Society Interface* 9.76 (Nov. 2012), pp. 2814–2825. ISSN: 1742-5689, 1742-5662. DOI: 10.1098/rsif.2012.0289. URL: http://rsif.royalsocietypublishing.org/cgi/doi/10.1098/rsif.2012.0289 (visited on 05/29/2017).

[233] Katariina Kulonen et al. "Ecology and evolution of rabies virus in Europe". en. In: *Journal of General Virology* 80.10 (Oct. 1999), pp. 2545–2557. ISSN: 0022-1317, 1465-2099. DOI: 10.1099/0022-1317-80-10-2545. URL: http://jgv.microbiologyresearch.org/content/journal/jgv/10.1099/0022-1317-80-10-2545 (visited on 01/17/2017).

[234] Tenzin et al. "Reemergence of Rabies in Chhukha District, Bhutan, 2008". In: *Emerging Infectious Diseases* 16.12 (Dec. 2010), pp. 1925–1930. ISSN: 1080-6040, 1080-6059. DOI: 10.3201/eid1612.100958. URL: http://wwwnc.cdc.gov/eid/article/16/12/10-0958_article.htm (visited on 01/17/2017).

[235] Simon Dellicour et al. "Using Viral Gene Sequences to Compare and Explain the Heterogeneous Spatial Dynamics of Virus Epidemics". en. In: *Molecular Biology and Evolution* (June 2017). ISSN: 0737-4038, 1537-1719. DOI: 10.1093/molbev/msx176. URL: https://academic.oup.com/mbe/article-lookup/doi/10.1093/molbev/msx176 (visited on 07/28/2017).

[236] Alyssa M. Bilinski et al. "Optimal frequency of rabies vaccination campaigns in Sub-Saharan Africa". en. In: *Proceedings of the Royal Society B: Biological Sciences* 283.1842 (Nov. 2016), p. 20161211. ISSN: 0962-8452, 1471-2954. DOI: 10.1098/rspb.2016.1211. URL: http://rspb.royalsocietypublishing.org/lookup/doi/10.1098/rspb.2016.1211 (visited on 01/17/2017).

[237] Salome Dürr and Michael P. Ward. "Development of a Novel Rabies Simulation Model for Application in a Non-endemic Environment". en. In: *PLOS Neglected Tropical Diseases* 9.6 (June 2015). Ed. by Jakob Zinsstag, e0003876. ISSN: 1935-2735. DOI: 10.1371/journal.pntd.0003876. URL: http://dx.plos.org/10.1371/journal.pntd.0003876 (visited on 01/17/2017).

[238] Christopher Torrence and Gilbert P. Compo. "A Practical Guide to Wavelet Analysis". en. In: *Bulletin of the American Meteorological Society* 79.1 (Jan. 1998), pp. 61–78. ISSN: 0003-0007, 1520-0477. DOI: 10.1175/1520-0477(1998)079<0061:APGTWA>2.0.CO;2. URL: http://journals.ametsoc.org/doi/abs/10.1175/1520-0477%281998%29079%3C0061%3AAPGTWA%3E2.0.CO%3B2 (visited on 06/20/2016).

[239] Catherine Linard et al. "Population Distribution, Settlement Patterns and Accessibility across Africa in 2010". en. In: *PLoS ONE* 7.2 (Feb. 2012). Ed. by Guy J-P. Schumann, e31743. ISSN: 1932-6203. DOI: 10.1371/journal.pone.0031743. URL: http://dx.plos.org/10.1371/journal.pone.0031743 (visited on 06/20/2016).

[240] Forrest R. Stevens et al. "Disaggregating Census Data for Population Mapping Using Random Forests with Remotely-Sensed and Ancillary Data". en. In: *PLOS ONE* 10.2 (Feb. 2015). Ed. by Luís A. Nunes Amaral, e0107042. ISSN: 1932-6203. DOI: 10.1371/journal.pone.0107042. URL: http://dx.plos.org/10.1371/journal.pone.0107042 (visited on 06/20/2016).

[241] V. A. Alegana et al. "Fine resolution mapping of population age-structures for health and development applications". en. In: *Journal of The Royal Society Interface* 12.105 (Mar. 2015), pp. 20150073–20150073. ISSN: 1742-5689, 1742-5662. DOI: 10.1098/rsif.2015.0073. URL: http://rsif.royalsocietypublishing.org/cgi/doi/10.1098/rsif.2015.0073 (visited on 06/20/2016).

[242] A. J. K. Conlan et al. "Resolving the impact of waiting time distributions on the persistence of measles". en. In: *Journal of The Royal Society Interface* 7.45 (Apr. 2010), pp. 623–640. ISSN: 1742-5689, 1742-5662. DOI: 10.1098/rsif.2009.0284. URL: http://rsif.royalsocietypublishing.org/cgi/doi/10.1098/rsif.2009.0284 (visited on 06/20/2016).

[243] Alun L. Lloyd. "Realistic Distributions of Infectious Periods in Epidemic Models: Changing Patterns of Persistence and Dynamics". en. In: *Theoretical Population Biology* 60.1 (Aug. 2001), pp. 59–71. ISSN: 00405809. DOI: 10.1006/tpbi.2001.1525. URL: http://linkinghub.elsevier.com/retrieve/pii/S0040580901915254 (visited on 06/20/2016).

[244] M.J. Keeling and B.T. Grenfell. "Effect of variability in infection period on the persistence and spatial spread of infectious diseases". en. In: *Mathematical Biosciences* 147.2 (Jan. 1998), pp. 207–226. ISSN: 00255564. DOI: 10.1016/S0025-5564(97)00101-6. URL: http://linkinghub.elsevier.com/retrieve/pii/S0025556497001016 (visited on 06/20/2016).

[245] Florence Ribadeau-Dumas et al. "Travel-Associated Rabies in Pets and Residual Rabies Risk, Western Europe". In: *Emerging Infectious Diseases* 22.7 (July 2016), pp. 1268–1271. ISSN: 1080-6040, 1080-6059. DOI: 10.3201/eid2207.151733. URL: http://wwwnc.cdc.gov/eid/article/22/7/15-1733_article.htm (visited on 07/28/2017).

[246] Tiffany Leung and Stephen A Davis. "Rabies Vaccination Targets for Stray Dog Populations". In: *Frontiers in Veterinary Science* 4 (2017).

[247] Betty Dodet et al. "Fighting rabies in Africa: the Africa rabies expert bureau (AfroREB)". In: *Vaccine* 26.50 (2008), pp. 6295–6298.

[248] Terence Peter Scott et al. "The Pan-African rabies control network (PARACON): a unified approach to eliminating canine rabies in Africa". In: *Antiviral research* 124 (2015), pp. 93–100.

[249] T. R. Eng et al. "Urban epizootic of rabies in Mexico: epidemiology and impact of animal bite injuries." en. In: *Bulletin of the World Health Organization* 71.5 (1993), p. 615. URL: http://www.ncbi.nlm.nih.gov/pmc/articles/PMC2393488/ (visited on 06/20/2016).

[250] Michelle K. Morters et al. "The demography of free-roaming dog populations and applications to disease and population control". en. In: *Journal of Applied Ecology* 51.4 (Aug. 2014). Ed. by Hamish McCallum, pp. 1096–1106. ISSN: 00218901. DOI: 10.1111/1365-2664.12279. URL: http://doi.wiley.com/10.1111/1365-2664.12279 (visited on 06/20/2016).

[251] Anne Conan et al. "Population Dynamics of Owned, Free-Roaming Dogs: Implications for Rabies Control". en. In: *PLOS Neglected Tropical Diseases* 9.11 (Nov. 2015). Ed. by Charles E Rupprecht, e0004177. ISSN: 1935-2735. DOI: 10.1371/journal.pntd.0004177. URL: http://dx.plos.org/10.1371/journal.pntd.0004177 (visited on 06/20/2016).

[252] J. C. Jr New et al. "Birth and death rate estimates of cats and dogs in U.S. households and related factors". English. In: *Journal of applied animal welfare science : JAAWS* (2004). ISSN: 1088-8705. URL: http://agris.fao.org/agris-search/search.do?recordID=US201301007213 (visited on 06/20/2016).

[253] Brian J Coburn, Justin T Okano, and Sally Blower. "Using geospatial mapping to design HIV elimination strategies for sub-Saharan Africa". In: *Science translational medicine* 9.383 (2017), eaag0019.

[254] Vittoria Colizza et al. "Modeling the worldwide spread of pandemic influenza: baseline case and containment interventions". In: *PLoS medicine* 4.1 (2007), e13.

[255] Duygu Balcan et al. "Seasonal transmission potential and activity peaks of the new influenza A (H1N1): a Monte Carlo likelihood analysis based on human mobility". In: *BMC medicine* 7.1 (2009), p. 45.

[256] Vittoria Colizza et al. "Predictability and epidemic pathways in global outbreaks of infectious diseases: the SARS case study". In: *BMC medicine* 5.1 (2007), p. 34.

[257] C Poletto et al. "Assessment of the Middle East respiratory syndrome coronavirus (MERS-CoV) epidemic in the Middle East and risk of international spread using a novel maximum likelihood analysis approach". In: *Eurosurveillance* 19.23 (2014), p. 3.